Photochemistry and structural aspects of the Photosystem II reaction centre

Promotor: dr. T.J. Schaafsma, hoogleraar in de moleculaire fysica

Co-promotor: dr. A.W. Rutherford, directeur de recherche CNRS, Gif-sur-Yvette

Frans van Mieghem

Photochemistry and structural aspects of the Photosystem II reaction centre

Proefschrift

ter verkrijging van de graad van doctor
in de landbouw- en milieuwetenschappen
op gezag van de rector magnificus,
dr. C.M. Karssen,
in het openbaar te verdedigen
op dinsdag 11 januari 1994
des namiddags te vier uur in de Aula
van de Landbouwuniversiteit te Wageningen.

CIP-GEGEVENS KONINKLIJKE BIBLIOTHEEK, DEN HAAG

ISBN 90-5485-206-2

Stellingen

1 The double reduction of Q_A probably is an intermediate step during photoinhibition (this Thesis, Chapter 3).

2 The proposal of Vass *et al.* that the Photosystem II reaction centre triplet can be detected in samples with Q_A singly reduced using standard EPR, following strong illumination under anaerobic conditions, is not sufficiently supported by their data (Vass, I., Styring, S., Hundal, T., Koivuniemi, A., Aro, E.-M. and Andersson, B. (1992) Proc. Natl. Acad. Sci. USA 89, 1408-1412; Vass, I. and Styring, S. (1993) Biochemistry 32, 3334-3341).

3 The hypothesis of Proskuryakov *et al.* that in *Rhodobacter sphaeroides* R26 mutants significant thermo-activated triplet energy transfer occurs from the primary donor to a monomeric bacteriochlorophyll, can be ruled out (Proskuryakov, I.I. and Manikowski, Kh. (1987) Dokl. Acad. Nauk SSSR (Biophys.) 297, 1250-1252).

4 Conclusions concerning the structure of P680, obtained from the presently available D_1D_2 preparations, are not straightforwardly applicable to intact Photosystem II (this Thesis, Chapter 8).

5 The statement made by Crystall *et al.* that these authors detect a 20 times higher amount of a 25-35 ns fluorescence decay component in D_1D_2 preparations than Seibert *et al.*, is exaggerated (Crystall, B., Booth, P.J., Klug, D.R., Barber, J. and Porter, G. (1989) FEBS Lett. 249, 75-78; Seibert, M., Picorel, P., Rubin, A.B. and Conolly, J.S. (1988) Plant. Physiol. 87, 303-306).

6 There is a candidate for a Photosystem II analogue of the bacteriochlorophyll monomer-binding histidine in the L-subunit of the purple bacterial reaction centre: asparagine-181 in the D_1 protein of Photosystem II.

7 The spatial organisation of organic cofactors of the electron transfer chain in Photosystem I, proposed by Witt *et al.*, is rather arbitrary in view of the available X-ray data (Witt, H.T., Krauss, N., Hinrichs, W., Witt, I., Fromme, P. and Saenger, W. (1992) in Research in Photosynthesis (Murata, N., ed.) Vol I, pp. 521-528).

8 The absolute amount of Ca^{2+} taken up by isolated nerve terminals upon KCl depolarisation, measured using $^{45}Ca^{2+}$, is at least three orders of magnitude higher than the increase in free intracellular Ca^{2+}, measured under the same conditions using fluoresecent Ca^{2+} indicators. Presently known intracellular Ca^{2+} buffers cannot explain this difference.

Stellingen behorend bij het proefschrift "Photochemistry and structural aspects of the photosystem II reaction centre", Frans van Mieghem, 11 januari 1994.

Preface

I would like to thank all the people who have contributed to the work described in this Thesis. Their help and advice were essential. In particular I thank Bill Rutherford for his continuous support and enthusiasm and the always stimulating discussions of my experiments. Also many thanks to Tjeerd Schaafsma for his support and the stimulating and instructive discussions we have had, especially at the stage of writing up. Alain Boussac has contributed to this Thesis in many different ways, varying from teaching me how to make BBYs to explaining how to use certain computer programs. I have been very happy to work in the Section de Bioénergétique in Saclay during the last four years and I thank Paul Mathis for his hospitality and his interest in my work. Apart from visits for discussions I was also several times in the Department of Molecular Physics in Wageningen in order to do experiments and I thank Arie van Hoek and Geoff Searle for their cooperation. I also thank Dietmar Stehlik and Christian Bock, in whose laboratory (Fachbereich Physik, Freie Universität Berlin) I had the opportunity to do time-resolved EPR measurements. Furthermore, I thank Bill Coleman, Diana Kirilovsky and Tony Mattioli for their cooperation and useful discussions. The experiments described in Chapter 8 would not have been possible without Klaus Brettel. I also thank him for his good advice during the writing up. The curve fittings in Chapter 8 were done with a computer program provided by Pierre Sétif for which many thanks. Also thanks to Stefan Franzen, Bettina Hillman, Andreas Kamlowski and Eberhard Schlodder who communicated results prior to publication. Finally, I gratefully acknowledge financial support by the CEA and the EEC.

Frans van Mieghem, 30 september 1993

Contents

Chapters 3, 4 and 6 are reproduced with kind permission of Elsevier Science Publishers B.V.

Abbreviations

BPh	the primary electron acceptor in purple bacteria
Chl	chlorophyll
EDTA	ethylenediaminetetraacetate
Mes	morpholineethanesulphonic acid
Mops	4-morpholinepropanesulphonic acid
P	primary electron donor
P680	the primary electron donor in photosystem II
Ph	the primary electron acceptor in photosystem II
PPBQ	phenyl-*p*-benzoquinone
PSI	photosystem I
PSII	photosystem II
Q_A	the first quinone electron acceptor
Q_B	the second quinone electron acceptor
S_2	redox state of the oxygen evolving enzyme
T-S	triplet-minus-singlet
Tyr D	secondary electron donor in photosystem II

Chapter 1

Introduction

Photosystem II (PSII) is a photosynthetic enzyme complex found in green plants and cyanobacteria, which catalyses the reaction in which oxygen is produced from water. It spans the photosynthetic thylakoid membrane. The oxidation of water producing oxygen and protons occurs only at one side of the thylakoid membrane. On the opposite side plastoquinone is reduced to plastoquinol. As a result of this spatial separation of the two reactions, the enzyme also contributes to the proton gradient over the thylakoid membrane. The energy needed for these redox reactions to take place is furnished by light. For a general review on the light reactions in photosynthesis in green plants and cyanobacteria, see Ref. [1]; for more specific reviews on PSII see Refs. [2-6].

Other known types of photosynthetic systems are: Photosystem I (PSI), which, like PSII, is found in green plants and cyanobacteria, and those from purple bacteria, green sulphur bacteria and heliobacteria. These are reviewed in Refs. [3,7-13].

The common features of these photosynthetic systems are the following. All have light-harvesting components (the antenna) containing pigments, absorbing incident light and rapidly transferring the excitation energy within that antenna and also to reaction centres, which are closely connected to the antenna. In these reaction centres, the absorption of excitation energy results in charge separation, i.e. the creation of positively and negatively charged ions. Such oppositely charged ions are initially formed at a short distance from each other, following photoinduced electron transfer from a photoexcited electron donor to a nearby electron acceptor. The charges then move away from each other via further electron transfer steps until they reach positions at opposite sides of the membrane, where they can subsequently take part in chemical (redox) reactions. Apart from these common features, the enzymes differ in many aspects which are related to their specific function.

An example of a relatively simple photosynthetic system which has been extensively characterised is that from purple bacteria. In this system, spectroscopic studies have profited from the fact that it is possible to isolate the reaction centre from the antenna, without changing its properties to a large extent (see [7] for a review). This allowed the identification of a number of electron carriers involved in the electron transfer: the photoexcitable primary electron donor (P) was found to consist of a pair of bacteriochlorophylls, a bacteriopheophytin was found to be the primary acceptor (BPh) and subsequent acceptors Q_A and Q_B have been identified as quinone molecules (see [7]). The role of a non-heme iron ion located on the acceptor side is still unclear. Also, when Q_A was prereduced or absent, a transient state could be formed, which was identified with the first excited triplet state of P, being formed via charge recombination from the primary radical pair P^+BPh^- (see [14] for a review).

A major advance was made in the understanding of the purple bacterial reaction centre when its structure was resolved using X-ray crystallography and

the exact location of the components discussed above became known [15] (see also [16,17]). Knowledge of this structure has been of great use for more detailed spectroscopic studies (reviewed in [9,10]), theoretical work (see [10] for a review) and also studies of genetically modified reaction centres using site-directed mutagenesis (reviewed in [18]).

Focusing now on the reaction centre of PSII, the theme of this Thesis, one has to state that it is less well understood than that of purple bacteria. The first reason for this is that crystals which can be analysed using X-ray diffraction are still lacking for PSII. Furthermore, a PSII reaction centre preparation comparable to that of purple bacteria is not yet available (for example, the present PSII reaction centre preparation is damaged at the acceptor side, see [6] for a review). In addition, optical spectroscopy is more difficult to do due to the fact that the different reaction centre pigments in PSII have more spectral overlap than those in purple bacteria. Finally, site-directed mutagenesis studies of PSII are hampered compared to those in purple bacteria due to a greater delicacy of PSII in response to genetic modifications, which is related to the greater complexity of PSII. Nevertheless, considerable progress has been made over the past few years in the study of PSII (see [2-6]).

An important factor in this progress has been the consideration that the reaction centres of PSII and purple bacteria are analogous to each other (see the Introduction to Chapter 6 [19] for a review). This analogy comprises at least the several identical acceptor side components (the primary acceptor in PSII is a pheophytin *a*; there are two quinone acceptors Q_A and Q_B as well as a non-heme iron ion) and some of their mechanistic and spectroscopic properties. In the present work, the comparison with purple bacteria is therefore often made.

The first set of experiments of this Thesis, described in Chapter 3 [20], deals with observations in the literature which were related to the topic of the analogy between the reaction centres of purple bacteria and PSII. It had been reported that in PSII, the reaction centre triplet state (detected by EPR under continuous illumination at cryogenic temperatures) was only seen at redox potentials much lower than the midpoint potential of the Q_A/Q_A^- redox couple [21,22]. This was different from purple bacteria where the reaction centre triplet and the reduction of Q_A have the same redox dependence (see above and [7]).

To explain the observations in PSII, an extra electron acceptor had been proposed to be located in between the primary acceptor (Ph, a pheophytin *a*) and Q_A [21,22]. However, the experiments in Chapter 3 [20] show that the redox event matching the induction of the EPR-detected reaction centre triplet is in fact the double reduction of Q_A. Thus, there was no longer a need to propose the additional electron acceptor in PSII, a proposal for which other evidence was lacking and which was in fact very difficult to reconcile with the analogy between the reaction centres of purple bacteria and PSII.

As explanations for the marked influence of the double reduction of Q_A on the reaction centre triplet state, a number of possibilities were given (see Chapter 3 [20]). In one of them, the double reduction of QA was thought to increase the EPR triplet signal due to an increased yield or an increased

lifetime of the primary radical pair. The low yield or short lifetime of the primary radical pair in the presence of singly reduced Q_A was explained by an electrostatic influence of Q_A^- on the energy level of the radical pair state P^+Ph^-. Upon double reduction, the negative charge on Q_A would disappear due to protonation. The occurrence of such an electrostatic influence had already been proposed earlier to explain differences in the yield of the primary radical pair in samples with Q_A oxidised and singly reduced [23,24].

The idea that the yield of the primary radical pair might be different in samples with Q_A singly and doubly reduced, led to the series of experiments described in Chapter 4 [25]. Fluorescence decay measurements at ambient temperature were used to compare the rate of charge separation in samples with Q_A singly reduced to that in samples with Q_A doubly reduced. On the assumption that the fluorescence is trap-limited, such measurements give information on the rate of charge separation: if the fluorescence is trap-limited, the excited state is, on the timescale of the experiment, rapidly equilibrated over the antenna system including the primary donor and the overall decay rate of this equilibrated excited state is limited by the rate of charge separation; the fastest detectable fluorescence decay is thus dependent on the rate of charge separation (see Ref. [23] for a kinetic model and a mathematical description). Using then the model of trap-limited fluorescence decay, the data in Chapter 4 [25] indicated that charge separation was faster in samples with Q_A doubly reduced as compared to those with singly reduced Q_A.

These results thus indicated that the yield of the primary radical pair at ambient temperature increases upon double reduction of Q_A, as had been proposed to be the case at the cryogenic temperatures used in the EPR work (chapter 3 [20]). However, there were doubts to what extent the results obtained at ambient temperature could be extrapolated to lower temperatures. In fact, an indication came from flash absorbance measurements that at 77 K the primary radical pair yield was high in samples with Q_A singly reduced [26]. Therefore, flash absorbance spectroscopy was carried out at a temperature close to that in the EPR work and samples with Q_A singly reduced and doubly reduced were compared in detail. These measurements are described in Chapter 8. For the interpretation of the results, the value for the risetime of the reaction centre triplet as measured by time-resolved EPR (Chapter 7), played an important role. Thus, it was found that the yield of the primary radical pair was similar in samples with Q_A singly and doubly reduced. The same was found for the reaction centre triplet yield: it was similar in both types of sample. It then became clear that the hypothesis of a significantly increased primary radical pair yield upon double reduction of Q_A, was not valid at low temperature and could not explain the increase in the triplet EPR amplitude upon double reduction of Q_A. Nevertheless, the experiments did provide an (unexpected) explanation for the observation that the triplet was not detectable by EPR under continuous illumination when Q_A was singly reduced: the triplet lifetime was found to be very short, too short in fact to give a detectable signal in a standard EPR experiment.

Apart from comparative experiments on samples with Q_A singly and doubly reduced, this Thesis deals with a number of other aspects, being directly or indirectly related to the double reduction of Q_A.

a) The reversibility of the Q_A double reduction was studied (see Chapters 4 [25] and 5). Only a small degree of reversibility was found and it was suggested that this is due to an irreversible modification of the immediate environment of the non-heme iron (possibly its loss).

b) Structural studies (see Chapters 6 [19] and 8). The orientation dependence of the reaction centre triplet EPR signal in PSII had already been measured [27,28] a few years after the signal had been detected for the first time in 1980 [29]. These early measurements had given approximate values for the angles between the magnetic triplet axes and the photosynthetic membrane plane. In this way, direct structural information on the reaction centre of PSII was obtained. The results indicated that the reaction centre triplet was localised on a chlorophyll oriented approximately parallel to the membrane [27,28]. However, the accuracy of the measurements was rather low.

The discovery that the triplet is in fact only detectable (using conventional EPR) after double reduction of Q_A and the establishment of procedures (see Chapter 3 [20]) of preparing samples with close to 100 % doubly reduced Q_A, triggered a renewed study of the triplet orientation (see Chapter 6 [19]). From this study it was concluded that the triplet is localised on a chlorophyll which is oriented at an angle of 30° to the membrane. This was in agreement with the approximately parallel orientation found in the earlier work [27,28] and completely different from the orientation found in purple bacteria (see e.g. [30,31]). In reaction centres of the latter (and also in other types of photosynthetic reaction centres [32-34]), the triplet had been found to be localised on (bacterio)chlorophyll(s) which are oriented *perpendicular* to the membrane. Notwithstanding these results, there is a considerable weight of evidence for a significant degree of analogy between the reaction centres of purple bacteria and that of PSII (see above). The discussion of this topic, which dates back from the time of the first EPR orientation measurements on PSII [27,28], has resulted in several proposals trying to reconcile the triplet orientation data with models in which the reaction centre structures of PSII and purple bacteria are similar. These models are reviewed in more detail in the Introduction to Chapter 6 [19]. The refined measurement of the reaction centre triplet orientation (Chapter 6 [19]) as well as optical difference spectra obtained from the low temperature flash absorbance data in Chapter 8 have added new ideas to the discussion on the analogy between the reaction centres of PSII and purple bacteria (see Chapters 6 [19] and 8). Nevertheless, a definitive choice for an unambiguous structural model for the PSII reaction centre cannot yet be made.

c) The intactness of the D_1D_2 reaction centre preparation of PSII. The optical difference spectra of relatively intact PSII membrane preparations (chapter 8) turned out to be quite different from equivalent spectra obtained from D_1D_2 preparations [35]. It is suggested in Chapter 8 that apart from modifications on the acceptor side (see above), the D_1D_2 preparation is also considerably modified at the donor side.

d) There are several discrepancies in the literature with respect to the kinetics and the yield of the primary radical pair in dithionite reduced PSII samples (compare e.g. refs [23,36-39]). In Chapters 3 [20] and 4 [25], these discrepancies are suggested to be due to the presence of varying amounts of doubly reduced Q_A, depending on the conditions of sample preparation.

e) Photoinhibition. PSII is thought to be the main target for inhibition of photosynthesis in green plants and cyanobacteria due to high amounts of light (see [40] for a recent review). In Chapter 3 [20], double reduction of Q_A was shown to be light-inducible and it was suggested that this reaction, with the associated high yield of a long-lived chlorophyll triplet state, would occur during certain photoinhibitory conditions and possibly in vivo. Several of the suggestions in Chapter 3 [20], have been followed up by others, in studies specifically addressed at understanding photoinhibition (see e.g. [41,42]).

The chlorophyll triplet state (which is present for milliseconds if Q_A is doubly reduced, Chapter 3 [20]) has been suggested to be responsible for the light-dependent degradation of the D_1 reaction centre protein because it may give rise to reactive oxygen radicals [43].

Also in chapter 5, the relevance of the data to photoinhibition is briefly discussed.

References

1 Forti, G. (1987) in New Comprehensive Biochemistry: Photosynthesis (Amesz, J., ed.), pp. 1-17, Elsevier, Amsterdam.
2 Van Gorkom H.J. (1985) Photosynth. Res 6 97-112.
3 Mathis, P. and Rutherford, A.W. (1987) in "New Comprehensive Biochemistry: Photosynthesis" (J.Amesz ed), pp. 63-96, Elsevier, Amsterdam.
4 Rutherford, A.W. (1989) Trends Biochem. Sci. 14, 227-232.
5 Hansson, Ö. and Wydrzynski, T. (1990) Photosynth. Res. 23, 131-162.
6 Renger, G. (1992) in Topics in Photosynthesis Vol 11 (Barber, J., ed.), pp. 45-100, Elsevier, Amsterdam.
7 Parson, W.W. and Ke, B. (1982) in "Photosynthesis: energy conversion by plants and bacteria" (Govindjee ed) pp 331-385 Academic press, New York.
8 Golbeck, J.H. (1987) Biochim. Biophys. Acta 895, 167-204.
9 Kirmaier, C. and Holten,D. (1987) Photosynth. Res. 13, 225-260.
10 Friesner, R.A. and Won, Y. (1989) Biochim. Biophys. Acta 977, 99-122.
11 Nitschke, W. and Rutherford (1991) Trends Biochem. Sci. 16, 241-245.
12 Setif, P. (1992) in Topics in Photosynthesis Vol 11 (Barber, J., ed.), pp. 471-500, Elsevier, Amsterdam.
13 Feiler, U. and Hauska, G. (1994) in Anoxygenic Photosynthetic Bacteria (Blankenship, R.E., Madigan, M.T. and Bauer, C.E., eds.), in press.
14 Budil, D.E. and Thurnauer, M.C. (1991) Biochim. Biophys. Acta 1057, 1-41.
15 Deisenhofer, J., Epp, O., Miki, K., Huber, R. and Michel, H. (1985) Nature (London) 318, 618-624.
16 Allen, J.P., Feher, J., Yeates, T.O., Komiya, H. and Rees, D.C. (1987) Proc. Natl. Acad. Sci. USA 84, 5730-5734.
17 Ermler, U., Fritzsch, G., Buchanan, S. and Michel, H. (1992) in Research in Photosynthesis Vol I (Murata, N., ed.), pp. 341-347, Kluwer, Dordrecht.
18 Coleman, W.J. and Youvan, D.C. (1990) Annu. Rev. Biophys. Biophys. Chem. 19, 333-367.
19 Van Mieghem, F.J.E., Satoh, K. and Rutherford, A.W. (1991) Biochim. Biophys. Acta 1058, 379-385.

20 Van Mieghem, F.J.E., Nitschke, W., Mathis, P. and Rutherford, A.W. (1989) Biochim. Biophys. Acta 977, 207-214.
21 Atkinson, Y.E. and Evans, M.C.W. (1983) FEBS lett. 159, 141-144.
22 Evans, M.C.W., Atkinson, Y.E. and Ford, R.C. (1985) Biochim. Biophys. Acta 806, 247-254.
23 Schatz, G.H., Brock, H. and Holzwarth, A.R. (1987) Proc. Natl. Acad. Sci. USA 84, 8414-8418.
24 Schatz, G.H., Brock, H. and Holzwarth, A.R. (1988) Biophys. J. 54, 397-405.
25 Van Mieghem, F.J.E., Searle, G.F.W., Rutherford, A.W. and Schaafsma, T.J. (1992) Biochim. Biophys. Acta 1100, 198-206.
26 Schlodder, E. and Hillmann, B. (1992) in Research in Photosynthesis (Murata, N., ed.), pp. 45-48, Kluwer, Dordrecht.
27 Rutherford, A.W. (1985) Biochim. Biophys. Acta 807, 189-201.
28 Rutherford, A.W. and Acker, S. (1986) Biophys. J. 49, 101-102.
29 Rutherford, A.W., Paterson, D.R. and Mullet, J.E. (1981) Biochim Biophys Acta 635, 205-214.
30 Hales, B.J. and Gupta, A.D. (1979) Biochim. Biophys. Acta 548, 276-286.
31 Tiede, D.M. and Dutton, P.L. (1981) Biochim. Biophys. Acta 637, 278-290.
32 Rutherford, A.W. and Sétif, P. (1990) Biochim. Biophys. Acta 1019, 128-132.
33 Nitschke, W., Feiler, U. and Rutherford, A.W. (1990) Biochemistry 29, 3834-3842.
34 Nitschke, W., Sétif, P., Liebl, U., Feiler, U. and Rutherford, A.W. (1990) Biochemistry 29, 11079-11088.
35 Van Kan, P.J.M., Otte, S.C.M., Kleinherenbrink, F.A.M., Nieveen, M.C., Aartsma, T.J. and Van Gorkom, H.J. (1990) Biochim. Biophys. Acta 1020, 146-152.
36 Eckert, H.J., Renger, G., Bernarding, J., Faust, P., Eichler, H.J. and Salk, J. (1987) Biochim Biophys Acta 893, 208-218.
37 Hansson, Ö., Duranton, J. and Mathis P. (1988) Biochim Biophys Acta 932, 91-96.
38 Schlodder, E. and Brettel, K. (1988) Biochim. Biophys. Acta 933, 22-34.
39 Leibl, W., Breton, J., Deprez, J. and Trissl, H.-W. (1989) Photosynth. Res. 22, 257-275.
40 Prásil, O, Adir, N. and Ohad, I. (1992) in Topics in Photosynthesis Vol 11 (Barber, J., ed.), pp. 295-348, Elsevier, Amsterdam.
41 Vass, I., Styring, S., Hundal, T., Koivuniemi, A., Aro, E.-M. and Andersson, B. (1992) Proc. Natl. Acad. Sci. USA 89, 1408-1412.
42 Vass, I. and Styring, S. (1993) Biochemistry 32, 3334-3341.
43 Durrant, J.R., Giorgi, L.B., Barber, J., Klug, D.R. and Porter, G. (1990) Biochim. Biophys. Acta 1017, 167-175.

Chapter 2

General overview of methods and techniques used

Biochemical methods

The following types of PSII preparations (from spinach) were used.

1) PSII-enriched membranes (Chapters 3-8). The PSII containing stacked regions of chloroplast thylakoid membranes were separated from PSI containing non-stacked regions by solubilisation of the latter using the detergent Triton X-100, as described in Ref. [1] (initially described in Ref. [2]).

2) PSII-core complexes (Chapter 4). PSII-enriched membranes were treated with the detergent octylglucopyranoside to partly remove the antenna, as described in Ref. [3].

3) D_1D_2 reaction centre preparations (Chapter 6). This preparation is devoid of all antenna and contains only the reaction centre proteins D_1 and D_2 together with small associated proteins such as cytochrome *b*-559. The preparation used in this work [4] was a kind gift from K. Satoh. More recent preparation procedures are described in Refs. [5-7].

Double reduction of Q_A (Chapters 3-8) was achieved by room temperature illumination or prolonged dark incubation of PSII samples in the presence of dithionite (see Chapter 3). The dark incubation was often carried out in the presence of benzyl viologen, which accelerated the reaction. Additional possible procedures for doubly reducing Q_A have been discovered by us: low temperature photoaccumulation of Ph^- in the presence of Q_A^- followed by thawing (the electron on Ph^- then goes to Q_A^-); prolonged illumination under aerobic conditions; illumination under anaerobic conditions (see also [8,9]). In all cases the double reduction reaction was evidenced by decreasing $Q_A^-Fe^{2+}$ and increasing triplet EPR signals (see Chapter 3).

For preparative use, the dark-incubation method (in the presence of dithionite and benzyl viologen) for the double reduction of Q_A was preferred, because in this way a close to 100 % yield in double reduction could be achieved and because secondary, light-induced, effects are avoided. The completeness of the reaction was checked by monitoring $Q_A^-Fe^{2+}$ and triplet EPR signals. For detailed descriptions of the procedures used, see Chapters 3, 4 and 6.

Procedures for bringing samples back into the original state, after Q_A had been doubly reduced (preparation of "reversed samples", see Chapter 4 and 5) involved incubation with ferricyanide and sometimes $FeCl_2$. These procedures are described in more detail in Chapters 4 and 5 respectively.

Preparation of oriented samples (Chapters 6 and 7) was carried out by drying samples in very dilute buffer slowly on mylar strips. More details are given in Chapter 6 and Ref. [10].

For a detailed description of the procedures involved in redox titrations (Chapter 3) see Ref. [11].

Measuring techniques

Conventional EPR measurements (Chapters 3-8) were performed using a standard X-band EPR machine from Bruker (Bruker 200) fitted with an Oxford Instruments cryostat and temperature control system. Time-resolved EPR measurements (Chapter 7) were carried out with an (X-band) experimental set-up which is described in detail in Ref. [12].

Picosecond time-resolved fluorescence measurements (Chapter 4) were performed using the technique of single photon counting. More details of the experimental set-up and the analysis of the data are given in Chapter 4 and Ref. [13].

Technical details of the flash-induced absorbance difference spectroscopy used in Chapters 3 and 8 and the data analysis in the latter are given in Refs. [14,15] and Chapter 8 respectively.

References

1 Ford, R.C. and Evans, M.C.W. (1983) FEBS Lett 160, 159-164.
2 Berthold, D.A., Babcock, G.T. and Yocum, C.F. (1981) FEBS Lett. 134, 231-234.
3 Ghanotakis, D.F., Demetriou, D.M. and Yocum, C.F. (1987) Biochim. Biophys. Acta, 891, 15-21.
4 Nanba, O. and Satoh, K. (1987) Proc. Natl Acad Sci USA 84, 109-112.
5 Chapman, D.J., Gounaris, K. and Barber, J. (1988) Biochim. Biophys. Acta 933, 423-431.
6 Ghanotakis, D.F., de Paula, J.C., Demetriou, D.M., Bowlby, N.R., Petersen, J., Babcock, G.T. and Yocum, C.F. (1989) Biochim. Biophys. Acta 974, 44-53.
7 Van Leeuwen, P.J., Nieveen, M.C., Van de Meent, E.J., Dekker, J.P. and Van Gorkom, H.J. (1991) Photosynth. Res. 28, 149-153.
8 Vass, I., Styring, S., Hundal, T., Koivuniemi, A., Aro, E.-M. and Andersson, B. (1992) Proc. Natl. Acad. Sci. USA 89, 1408-1412.
9 Vass, I. and Styring, S. (1993) Biochemistry 32, 3334-3341.
10 Blasie, J.K., Erecinska, M., Samuels, S. and Leigh, J.S. (1978) Biochim. Biophys. Acta 501, 33-52.
11 Dutton, P.L. (1971) Biochim Biophys Acta 226, 63-80.
12 Stehlik, D., Bock, C.H. and Thurnauer, M.C. (1990) in Advanced EPR in Biology and Biochemistry (Hoff, A.J., ed.) pp.371-404, Elsevier, Amsterdam.
13 Searle, G.F.W., Tamkivi, R., Van Hoek, A. and Schaafsma, T.J. (1988) J. Chem. Faraday Trans. 2 84, 315-327.
14 Kramer H. and Mathis P. (1980). Biochim Biophys Acta 593, 319-329.
15 Takahashi, Y., Hansson, Ö., Mathis, P. and Satoh, K. (1987) Biochim Biophys Acta 893, 49-59.

Chapter 3

The influence of the quinone-iron electron acceptor complex on the reaction centre photochemistry of Photosystem II

F.J.E. van Mieghem *, W. Nitschke, P. Mathis and A.W. Rutherford

Service de Biophysique, Département de Biologie, Centre d'Etudes Nucléaires de Saclay, Gif sur Yvette (France)

(Received 14 April 1989)

Key words: Semiquinone iron; Triplet state; Radical pair state; Photoinhibition; Plastoquinone; Photosynthesis

A correlation is demonstrated between the loss of the $Q_A^-Fe^{2+}$ EPR signal and the ability to photoinduce the radical-pair-recombination triplet state in Photosystem II. The $Q_A^-Fe^{2+}$ signal is diminished by procedures which are thought to reduce the semiquinone by a further electron: (1) low quantum yield photoreduction in the presence of sodium dithionite at room temperature; (2) chemical reduction in the dark by sodium dithionite at pH 7.0. The chemical reduction process is extremely slow ($t_{1/2} \approx 5$ h) but can be accelerated ($t_{1/2} \approx 1.5$ h) by the presence of the redox mediator, benzyl viologen. In redox titrations at pH 7.0 the $Q_A^-Fe^{2+}$ signal disappears with an irreversible transition at potentials lower than −350 mV. The ability to observe the triplet signal shows a corresponding potential dependence. The variations in the amplitude of the triplet EPR signal match variations in triplet yield measured by flash absorption spectroscopy at low temperature. From these observations the following conclusions are drawn: (1) The redox titration data that led to the suggestion that an extra component functions between pheophytin and $Q_A^-Fe^{2+}$ (Evans, M.C.W., Atkinson, Y.E. and Ford, R.C. (1985) Biochim. Biophys. Acta 806, 247–254) can probably be explained instead by the second reduction of $Q_A^-Fe^{2+}$. (2) The variable yield of triplet and of $P680^+Ph^-$, and possibly the lifetime of the latter, which have been reported in the literature probably reflect, at least in part, different amounts of native $Q_A^-Fe^{2+}$ remaining in the various preparations used. From considerations of the literature, an increase in quantum yield of charge separation is thought to occur upon the second reduction of $Q_A^-Fe^{2+}$. The most likely explanation for this is the disappearance of an electrostatic interaction between $Q_A^-Fe^{2+}$ and $P680^+Ph^-$ as $Q_A^-Fe^{2+}$ becomes further reduced. Other factors which may influence or be responsible for these phenomena and comparisons with the primary photochemistry in purple bacteria are discussed. In addition the relevance of these observations to the lesions involved in photoinhibition is pointed out.

Introduction

In the reaction centre of purple photosynthetic bacteria the first detectable radical pair formed after excitation by light is P^+BPh^-. P, the primary electron donor, is a special pair of bacteriochlorophyll molecules and BPh, the primary electron acceptor, is a bacteriopheophytin molecule (reviewed in Refs. 1, 2). If further forward electron transfer is blocked by removal or reduction of the subsequent electron acceptor, a quinone molecule (Q_A), spin dephasing followed by charge recombination takes place resulting in the formation of a triplet state of P. The yield of formation of the triplet state of P is close to 100% at liquid helium temperature [3]. At ambient temperature other recombination pathways occur and the triplet yield is only approx. 15% [1].

In Photosystem II (PS II), similar photochemistry is thought to take place [4] (reviewed in Ref. 5). However, a number of observations have led to suggestions that PS II differs significantly from purple bacteria with regard to the number and nature of the electron acceptors (e.g., Ref. 6). In a detailed study of the triplet EPR signal it was shown that the triplet signal was very small until the potential was decreased to below −350 mV [6]. In the same work it was shown that Q_A^-, measured as the $Q_A^-Fe^{2-}$ signal at $g \approx 1.85$ [7], was fully formed

* On leave from the Department of Molecular Physics, Agricultural University, Wageningen, The Netherlands.

Abbreviations: BPh, bacteriopheophytin; Mes, 4-morpholineethanesulphonic acid; P, the primary electron donor in purple bacterial reaction centres; P680, the primary electron donor in Photosystem II; Ph, pheophytin; PS II Photosystem II; Q_A, the first quinone electron acceptor; Q_B, the second quinone electron acceptor.

Correspondence: A.W. Rutherford, Département de Biologie, Centre d'Etudes Nucléaires de Saclay, 91191 Gif-sur-Yvette, France.

at much higher potentials [6]. The non-correlation of triplet formation with the Q_A/Q_A^- transition led to the suggestion that an extra component, U, was present which functioned as an electron acceptor in PS II between Ph and Q_A [6,8].

There is plenty of precedence for 'extra acceptors' in this photosystem (reviewed in Ref. 9), yet the weight of evidence, both spectroscopic [5,9] and biochemical [10,11], pointing to a close analogy with the bacterial reaction centre led us to look for other explanations for this effect.

The quinone in the Q_A site in the reaction centres of PS II and purple bacteria shows redox chemistry which is very different from that of quinones in solution. The quinone is tightly bound to the protein and under normal circumstances undergoes a single electron reduction forming the semiquinone. In purple bacteria it was shown that, in the presence of reducing conditions and an efficient electron donor, illumination at room temperature resulted in the low quantum yield reduction of Q_A to form the fully reduced quinol [12,13]. This second reduction of Q_A can be achieved by chemical reductants in the dark in a slow, quasi-irreversible reaction [14]. Normal Q_A function could be reestablished only after the system was fully reoxidized [14]. This behaviour may be rationalized as follows: upon double reduction, QH_2 is lost from the site; upon raising the potential, QH_2 in solution undergoes a two-electron oxidation forming the fully oxidized quinone which can then rebind in the Q_A site.

In PS II, a similar light-driven double reduction of Q_A has been reported [15,16]. In this work we tested the idea that double reduction of Q_A could influence the yield of PS II reaction centre triplet formation.

A preliminary report of these results has appeared elsewhere [17].

Materials and Methods

PS II-enriched thylakoid membrane fragments were prepared from spinach as described earlier [18] using the modifications in Ref. 19. In some experiments, the membranes were washed with Tris before use. Membranes (0.5 mg chlorophyll/ml) were exposed to room light for 30 min at 0 °C in the presence of 0.8 M Tris (pH 8.2)/1 mM EDTA/1 mM EGTA. The Tris-treated membranes were pelleted and washed once in a buffer containing 50 mM Mops (pH 7.0)/10 mM NaCl/5 mM $MgCl_2$ and resuspended in the buffer used for redox titrations (50 mM Mops (pH 7.0)/10 mM NaCl/5 mM $MgCl_2$/30% ethylene glycol/1 mM EDTA). EPR samples (about 250 μl) were in calibrated quartz tubes (3 mm internal diameter). For time-course experiments, incubations were done in the EPR tube at room temperature in darkness. At a given time, the incubation was stopped by freezing the samples, the spectra were recorded, the sample thawed and the incubation allowed to continue at room temperature. It was demonstrated that multiple freeze–thaw cycles under these conditions had no noticeable effect on the EPR signals monitored.

Redox titrations of Tris-washed samples (about 5 mg chlorophyll/ml) were performed in near darkness at 20 °C essentially as described by Dutton [20]. The following redox mediators were used: phenyl-*p*-benzoquinone, indigo tetrasulphonate, indigo disulphonate, 2,6-dichlorophenol indophenol, Methylene blue, anthroquinone 2-sulphonate, anthroquinone 2,6-disulphonate, Saphranine T and Neutral red, all at 50 μM; in addition, benzyl viologen and methyl viologen were present at 20 μM.

Samples for flash absorption kinetic studies were transfered from EPR tube to the optical cuvette under argon. Except for the chlorophyll concentration (2.9 mg chlorophyll/ml for EPR and 50 or 100 μg chlorophyll/ml for absorption measurements) and the benzyl viologen concentration (34 μM for EPR and 0.7 μM or 1.4 μM for absorption) the other conditions (buffer, cryoprotectant, temperature) were identical for both kinds of measurement (see legends).

White light from an 800 W tungsten projector was used for illuminating samples after passing through 2 cm of water and two calflex heat filters (Balzers). For room temperature illuminations ($\approx 7000\ \mu E \cdot m^{-2} \cdot s^{-1}$) samples were maintained at 20 °C in a water-bath. When illuminated in the EPR cavity the intensity was $\approx 16000\ \mu E \cdot m^{-2} \cdot s^{-1}$ at the cavity window. EPR spectra were recorded using a Bruker 200 X-band spectrometer fitted with an Oxford Instruments cryostat and temperature control system.

Absorption measurements were made using a flash kinetic spectrophotometer described earlier [21], except that the detector was a PIN 10 photo-diode equipped with a 1 MHz bandwidth amplifier. Some measurements were also made using a different spectrophotometer as described previously [22]. Samples were cooled to close to liquid N_2 or liquid He temperature using S.M.C. cryostats.

Results

To obtain reproducible conditions for low-temperature illumination experiments, relatively dilute samples (3 mg Chl/ml) were used frozen in 30% ethylene glycol. To obtain measureable EPR signals from $Q_A^-Fe^{2+}$ under these conditions sodium formate was added, since this results in a greater than 10-fold increase in the EPR signal at $g = 1.85$ [23] probably due to binding of this chemical directly to the iron [5]. When such samples were reduced by sodium dithionite they exhibited easily detectable EPR signals at $g = 1.85$ typical of the formate-modified $Q_A^-Fe^{2+}$ (Fig. 1c). No detectable triplet EPR signal could be observed in these samples when

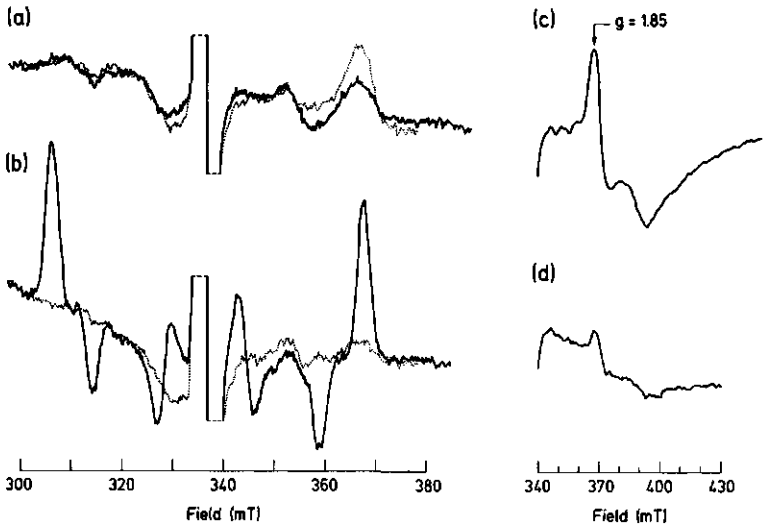

Fig. 1. The influence of room temperature illumination on dithionite-reduced PS-II-enriched thylakoid membranes monitored by EPR. The samples (3 mg chlorophyll/ml) were in 25 mM Mes (pH 6.5)/0.3 M sucrose/10 mM NaCl/5 mM $CaCl_2$/30% ethylene glycol/1 mM EDTA/40 mM dithionite. Spectra a and c were recorded in a sample incubated in the dark for 20 min after dithionite addition. Spectra b and d were recorded in the same sample but after thawing and a total of 12 min (i.e., six periods of 2 min to avoid sample heating) illumination at 20 °C followed by dark adaptation for 25 min. Triplet spectra (a and b) were recorded under illumination (solid lines), dotted lines show dark spectra. EPR conditions: temperature, 4.2 K; microwave power, 35 dB (63 μW); microwave frequency, 9.44 GHz; modulation amplitude, 22 G; gain $2 \cdot 10^5$. $Q_A^- Fe^{2+}$ (c and d) were recorded in the dark with EPR instrument settings as for the triplet except that the temperature was 4.7 K, microwave power, 8 dB (32 mW) and the gain $2 \cdot 10^4$.

continuous illumination was provided at liquid helium temperature (Fig. 1a). Room temperature illumination of dithionite reduced PS II results in the trapping of Ph^- [24] and the loss of the $Q_A^- Fe^{2+}$ signal [15,16] presumably due to its double reduction. The trapped Ph^- exhibits a 13 G wide free radical EPR signal at $g = 2.0033$ [24]. Dark adaptation of such a sample results in the slow detrapping of the Ph^- radical, as this highly reducing species ($E_m \approx -600$ mV [25,26]) equilibrates with the environment (not shown). The $Q_A^- Fe^{2+}$ EPR signal is not regenerated by this treatment (Fig. 1d). Illumination at 4 K of PS II pretreated in this way results in the formation on an easily detectable triplet EPR signal (Fig. 1b) with the polarization pattern typical of its formation by radical-pair recombination (see [27]).

Fig. 1 shows that when the $Q_A^- Fe^{2+}$ signal is diminished, the triplet signal greatly increases. To determine whether these two effects are linked or whether one or both are due to non-specific photodamage, other methods of double reducing the quinone were looked for. Experiments were performed in which PS II membranes were incubated with sodium dithionite in darkness at room temperature. At various times during the incubation, samples were frozen to 4 K and the photoinduced triplet and $Q_A^- Fe^{2+}$ signals were recorded. A decrease occurred in the $Q_A^- Fe^{2+}$ signal by approx. 50% in 5.5 h; the photoinduced triplet signal increased with a similar time dependence (not shown). Due to the very long incubation times required, we looked for a redox mediator that would accelerate the reduction process. Fig. 2a shows that, in the presence of benzyl viologen, the $Q_A^- Fe^{2+}$ disappeared upon dark incubation with dithionite with a $t_{1/2}$ of approx. 1 h 20 min. The triplet signal amplitude increased with a similar time dependence. The close correlation between the loss of the $Q_A^- Fe^{2+}$ signal and the appearance of the photoinduced triplet is clearly shown in Fig. 2b.

The behaviour of the $Q_A^- Fe^{2+}$ signal and of the photoinduced triplet signal were investigated under the controlled conditions of redox titrations. Decreasing the ambient redox potential inevitably results in the chemical reduction and consequent release of the Mn ions associated with the oxygen evolving activity of PS II. The material used in the redox titrations was Tris-washed to remove the Mn and prevent any slow evolution of the state of the electron donor side of PS II during the course of the experiments.

Fig. 3 shows that the first reduction of $Q_A Fe^{2+}$ forming $Q_A^- Fe^{2+}$ (measured in the presence of sodium formate as the signal at $g = 1.85$ [23]) occurs with an $E_m \approx -16$ mV (obtained by fitting with an $n = 1$ Nernst curve). The signal from $Q_A^- Fe^{2+}$ disappears at redox potentials lower than approx. -350 mV. The ap-

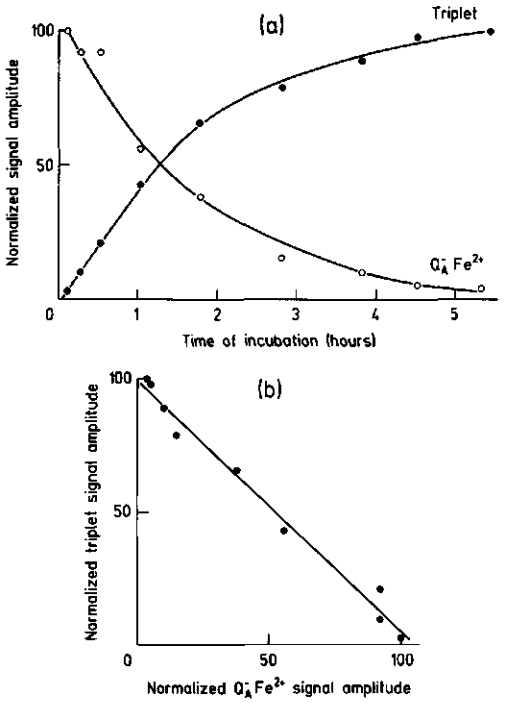

Fig. 2. Dark incubation under reducing conditions in the presence of benzyl viologen. Sample conditions were the same as in Fig. 1 except that no $CaCl_2$ was present, the EDTA concentration was 0.5 mM and 34 μM benzyl viologen was also present. (a) The amplitude of the triplet EPR signal (●) and the $Q_A^- Fe^{2+}$ signal (○) as a function of dark incubation time. (b) The amplitude of the triplet signal plotted as a function of the amplitude of the $Q_A^- Fe^{2+}$ signal in the same experiment as (a). The signal amplitudes were measured as follows: $Q_A^- Fe^{2+}$, the height of the signal measured between the peak maximum at $g \approx 1.85$ and the trough at $g \approx 1.7$; triplet, as the height of the lowest field line. EPR conditions were as described in Fig. 1 except that the gain was $8 \cdot 10^4$ and the modulation amplitude was 25 G.

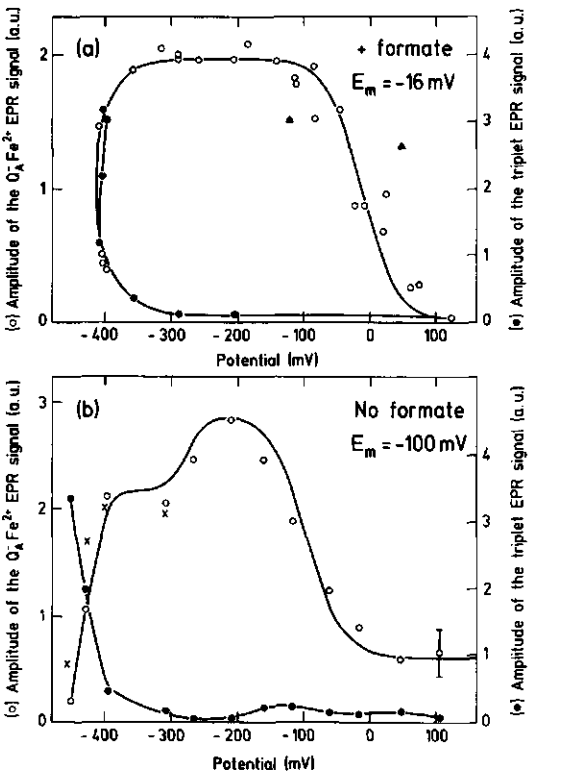

Fig. 3. Redox titrations at pH 7.0 of Tris-washed PS II enriched thylakoid membranes. The amplitude of the triplet (●) and $Q_A^- Fe^{2+}$ (○) spectra are plotted versus ambient potential. The amplitude of the triplet when reduced samples were reoxidized (▲) are also shown. (a) redox titrations in the presence of 200 mM formate. (b) redox titrations without addition of formate. EPR conditions were as in Fig. 1, except that $Q_A^- Fe^{2+}$ in the absence of formate was recorded using 32 G modulation amplitude and 6 dB (40 μW). An estimate of the error in recording $Q_A^- Fe^{2+}$ arising from the poor signal to noise in the absence of formate is shown by the error bars for a point in (b). The amplitude of the split Ph^- EPR signal (×) induced by a period of illumination at 200 K monitored during the redox titrations is also shown in (b) EPR conditions were as for $Q_A^- Fe^{2+}$ in Fig. 1 except that the modulation amplitude was 16 G.

pearance of the photoinduced triplet corresponds closely with the loss of the $Q_A^- Fe^{2+}$ signal. Once this redox transition had occurred, titrations in the oxidizing direction resulted in no reappearance of the $Q_A^- Fe^{2+}$ signal and only a minor (approx. 30%) decrease in the triplet signal amplitude (Fig. 3a, solid triangles). This redox transition does not follow a Nernst curve, the curve drawn is hand-fitted to the points, the position of which varied with the sampling frequency.

As a control for the possible involvement of formate in the redox characteristics of $Q_A Fe^{2+}$, experiments were performed in the absence of formate (Fig. 3b). As expected, the $Q_A^- Fe^{2+}$ signal is much smaller [23] and it is dominated by a signal centered at $g = 1.9$ at this pH [16]. Due to the decrease in signal amplitude the data are noisier. However, it seems that the first reduction step of $Q_A Fe^{2+}$ reduction occurs with an E_m value (−100 mV) lower than that in the presence of formate *. In addition, a slight decrease in $Q_A^- Fe^{2+}$ signal am-

* The difference in the $E_{m,7.0}$ for $Q_A Fe^{2+}/Q_A^- Fe^{2+}$ in Fig. 3a and b may indicate a formate-induced negative shift. Vermaas and Govindjee [42], however, reported that addition of bicarbonate to a formate-treated thylakoid did not induce a shift in the E_m ($E_{m,6.5}$, −145 mV). This apparent discrepancy may be due to the different comparisons made (i.e., untreated vs. formate-treated here, formate-treated vs. formate-treated plus addition of bicarbonate [42]), but also might by due to other differences in experimental conditions (pH, material, etc.).

plitude occurs between −200 mV and −300 mV. The origin of this slight decrease is not clear; however, it does not seem to be associated with an increase in the triplet signal. Despite these minor differences, the major decrease in the $Q_A^- Fe^{2+}$ occurs at low potential and this corresponds to the appearance of the photoinduced triplet signal, just as observed in the presence of formate.

In response to a reviewer's comment, in Fig. 3b we also show the amplitude of the split Ph^- signal (crosses) over the potential range in which the $Q_A^- Fe^{2+}$ signal disappears. The signal is generated by illumination at 200 K and arises from an interaction between Ph^+ and $Q_A^- Fe^{2+}$ [24]. The signal is lost with the same potential dependence shown for the loss of $Q_A^- Fe^{2+}$ and the appearance of the triplet. This result is in apparent contrast to the report that the split Ph^- signal decreases at potentials lower than those required for appearance of the triplet signal [6]. We suggest that the observations in Ref. 6 might be due to the fact that the data for the triplet and the split Ph^- were recorded in different titration experiments. Variations in the apparent redox dependencies for this transition are likely to be obtained from titration to titration because the redox event being monitored is slow and irreversible. Under such conditions, the form of the 'redox curve' is more dependent on time (i.e., sampling frequency) than on the ambient redox potential.

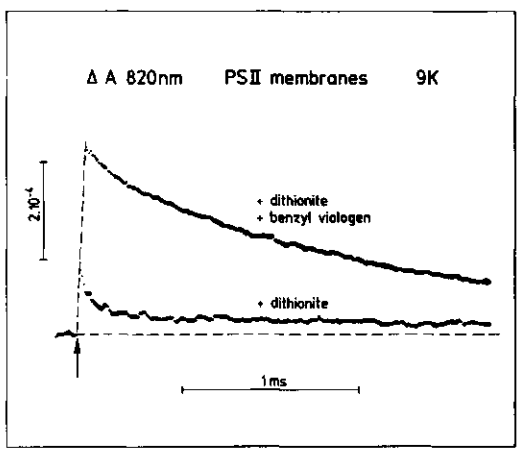

Fig. 4. Flash-induced absorption changes at 820 nm at 9 K in sodium dithionite-reduced PS II membranes incubated in the presence and absence of benzyl viologen (34 μM). The chlorophyll concentration was 110 μg per ml in a buffer comprising 50% ethylene glycol/40 mM sodium dithionite/200 mM sodium formate/82 mM Mops (pH 7.0)/8.4 mM NaCl/4.2 mM $MgCl_2$/1 mM EDTA. The sample incubated (about 3 h) in benzyl viologen contained 1.4 μM of this mediator in the cuvette. The sample in the absence of benzyl viologen was incubated for about 1 h. The cuvette thickness was 1.1 mm. The traces are the average of 32 flashes.

To verify that the amplitude changes of the EPR triplet signal are a direct reflection of the triplet yield, experiments were performed using flash absorption kinetic spectrophotometry. The reaction-centre triplet yield was measured by its absorption increase at 820 nm which decays with a $t_{1/2}$ of approx. 0.9 ms at liquid helium temperature [28,29]. Samples were treated with sodium dithionite in the presence or absence of benzyl viologen for different times of incubation in darkness. The EPR properties of the samples were monitored prior to their dilution and use in the absorption experiments. Fig. 4 shows the results of such an experiment. A small change is seen at 820 nm in the sample incubated in dithionite alone. Most of this small change decays rapidly ($t_{1/2} \approx 50$ μs). The origin of this phase is unknown. A smaller longer-lived phase may represent a small amount triplet formation as predicted from the EPR measurement (yield < 20%). In the sample treated with benzyl viologen, a much bigger absorption change is seen. This decays with a $t_{1/2}$ of approx. 1.1 ms and is attributed to the reaction centre triplet. Using the approximate absorption coefficient for the triplet of 3800 $M^{-1} \cdot cm^{-1}$ [21], it can be calculated that the triplet yield in the sample treated with benzyl viologen is close to 100%, while that with dithionite alone is less than 20%.

Although these yields are rather uncertain due to the large uncertainty in the P680 triplet absorption coefficient, their relative values correspond well with the amplitude of the triplet signal observed by EPR using the same samples.

Discussion

The earlier observation that the reduction of a component at low potential (about −350 mV) must occur before the triplet can be generated [6] is verified by the current work. Here, however, we show that the ability to photoinduce the triplet correlates with the loss of the $Q_A^- Fe^{2+}$ signal. Thus, there is no need to invoke the presence of a new redox component between Ph and Q_A. Instead, the redox transition responsible is presumed to be the second reduction of the quinone, forming the fully reduced quinol.

Direct evidence for formation of the quinol is lacking; the argument relies heavily on precedence in the bacterial reaction centre [12–14] and on reasonable expectations of quinone chemistry under photochemical and chemical reduction conditions. In the bacterial system the quasi-reversibility of the loss of $Q_A^- Fe^{2+}$ provided confidence in this explanation. In PS II, however, at least in the titration work reported here, we were unable to see such reversibility. The suggested loss of the QH_2 from the site (see Introduction) could be followed in PS II by an irreversible change in the Q_A site which prevents rebinding of PQ. This scenario is

not unreasonable, since it is known that the Q_A site is labile in the absence of the quinone [30] (see also Ref. 31). It is of note that a small degree of reversibility of $Q_A^-Fe^{2+}$ double-reduction in PS II was reported earlier in photoreduced samples which were rapidly reoxidized [15].

The nature of the effect by which $Q_A^-Fe^{2+}$ prevents triplet formation (or by which its double reduction induces triplet formation) is not clear. However, some of the possible explanations are considered below. (1) A direct effect of $Q_A^-Fe^{2+}$ on the P^+Ph^- radical pair could occur via an electrostatic interaction between Q_A^- and Ph^-. This would make the $P680^+Ph^-$ radical pair a higher energy state, displacing the equilibrium, $^*P680Ph \leftrightarrow P680^+Ph^-$, to the left. These effects could result in the radical pair having a smaller yield and possibly a shorter lifetime, hence the triplet yield would be greatly diminished. (2) A direct magnetic effect of $Q_A^-Fe^{2+}$ on the radical pair could influence spin dephasing, favouring singlet radical-pair recombination. Both of these direct effects would be removed by the second reduction of Q_A. The electrostatic effect could be lost due to the protonation of the fully reduced form and its probable simultaneous detachment from the Q_A site. The magnetic effect would be lost because the quinol is diamagnetic. (3) Indirect effects, due to secondary events associated with the second reduction of Q_A, could influence $P680^+Ph^-$ radical pair yield, lifetime and back-reaction pathway. Such secondary events include, for example, protonations, conformational changes perhaps associated with debinding of the quinol from the Q_A site.

From considerations of the literature we favour the first of these explanations. A direct electrostatic effect of Q_A^- on the $P680^+Ph^-$ radical pair has been invoked recently to explain ps/ns fluorescence and absorption data [32,33] (see also Ref. 34). A lower yield of $P680^+Ph^-$ radical-pair formation was observed in closed PS II reaction centres (i.e., when Q_A^- is present) compared to open PS II reaction centres (i.e., when Q_A is present). An interaction between Q_A^- and $P680^+Ph^-$ was estimated to increase the free energy of the radical pair by 50 mV [32]. It is reasonable to propose that when Q_A is double-reduced or absent, the free energy of the $P680^+Ph^-$ radical pair could resemble that in open centres. Fig. 5 shows a simplified schematic representation of the influence of the redox state of Q_A on the free energy level of $P680^+Ph^-$ and is an extension of the model of Schatz et al. [32].

It is also worth pointing out that the 'jammed' state is likely to be a lower fluorescent state that the closed state. Experiments correlating the EPR changes with fluorescence changes are required before the extent of the quenching can be estimated.

The kinetics of $P680^+Ph^-$ radical pair formation in PS II membranes have already been studied under

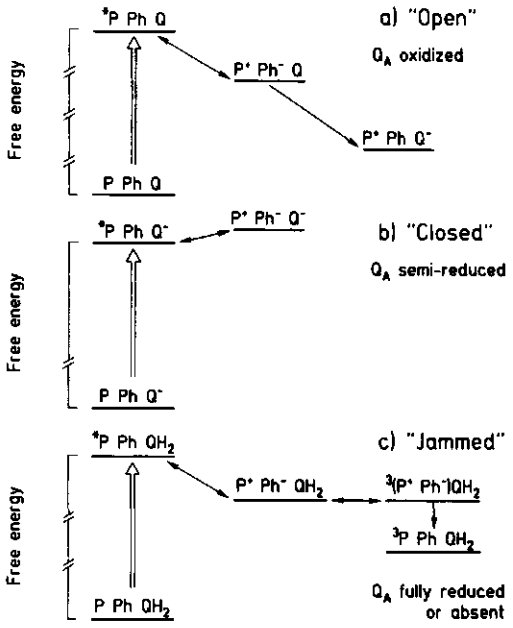

Fig. 5. Simplified schemes of the free energy levels of the states involved in the primary photochemistry of PS II with different redox states of Q_A (Q). The three states (a) open, (b) closed and (c) 'jammed', correspond to Q_A being oxidized, semireduced and fully reduced (or absent), respectively. Absorption of a photon of light in the (a) open and (c) 'jammed' conditions results in a high quantum yield of charge separation. In case (a) this leads to charge stabilization by electron transfer from Ph^+ to Q_A. In case (c) this leads to triplet formation. Absorption of light in the (b) closed condition gives rise to a very low yield of charge separation and the energy is wasted as prompt fluorescence. In addition, the antenna size is thought to influence the yield of charge separation [32,35,36]. See the text for further details.

conditions which correspond to those of Fig. 1, i.e., the closed and 'jammed' states in Fig. 5 [34]. The phenomena observed could be interpreted in two ways: either the radical pair lifetime increased from less than 500 ps to 3 ns or the quantum yield of charge separation greatly increased upon preillumination and dark adaptation, a treatment now known to result in the loss of $Q_A^-Fe^{2+}$. Both of these explanations would be consistent with our observation of the appearance of the photoinduced triplet in the preilluminated sample. The explanation involving an increase in the quantum yield fits better with the scheme in Fig. 5 and with the models of Schatz et al. [32] and Schlodder and Brettel [33].

In purple bacteria, schemes similar to those in Fig. 5 can be drawn; however, in all three states the free energy level of P^+BPh^- would be low enough to result in a 100% quantum yield of charge separation. What then could be the origin of the difference in the energet-

ics (and thus the photochemistry) seen when comparing PS II and purple bacteria under conditions where Q_A is present?

The first factor to be considered is the postulated electrostatic interaction between Q_A^- and $P680^+Ph^-$. Even if it is assumed that the chromophores occupy identical relative positions in both reaction centres, differences in amino acid residues in the region of the Ph and Q_A could result in a local dielectric that favours the electrostatic interactions between the two negatively charged species in PS II. Very recently, exactly such a diminished dielectric in PS II was postulated from photovoltage measurements [37].

Secondly, the intrinsic redox potentials of the components in PS II could make the free energy difference between $^*P$ and $P680^+Ph^-$ in the open state smaller than the corresponding value in the purple bacteria reaction centre. Thus the influence of Q^- on $P680^+Ph^-$ could be more marked in PS II, even if the electrostatic interaction in both kinds of reaction centre were the same.

Thirdly, the presence of a large number of antenna chlorophylls in PS II, many of which have long-wavelength maxima close in energy to P680, makes P680 a very 'shallow trap' [32,35,36]. An equilibrium distribution towards the excited state rather than the radical pair is favoured by increasing the size of the antenna: $^*[Chl]_n$ $P680Ph \leftrightarrow [Chl]_n$ $^*P680Ph \leftrightarrow [Chl]_nP680^+Ph^-$.

A combination of a larger electrostatic effect of Q_A^- on $P680^+Ph^-$ in PS II and the influence of the antenna on the yield of charge separation may best describe the situation observed in PS II. Studies of the $P680^+Ph^-$ yield and lifetime have been performed using a range of PS II preparations with varying antenna sizes. Increases in the radical-pair lifetime and yield were observed as the antenna size decreased [38], in accordance with the shallow trap theory [35]. However, the correlation was far from perfect and it was concluded that antenna size was not the only factor influencing the equilibrium. It now seems likely that the additional factor is the presence of $Q_A^-Fe^{2+}$. It is also clear that, at least under our conditions, this is the dominant factor influencing the energetics of the radical pair.

It was reported earlier that harsh detergent treatments result in marked increases in the amplitude of the triplet EPR signal [28]. It now seems likely that this is due to a detergent-induced loss of the $Q_A^-Fe^{2+}$ complex and also perhaps to the diminution of the functional antenna size. A survey of several different PS II preparations seems to confirm the existence of an inverse relationship between the triplet state and the $Q_A^-Fe^{2+}$ signal. PS II-enriched membranes show little or no triplet under conditions in which a large $Q_A^-Fe^{2+}$ signal is observable (e.g., Fig. 1). In the smallest PS II preparations, $Q_A^-Fe^{2+}$ is lacking and the triplet is easily seen [39]. A range of different core preparations, which can be classed between these two extremes, show intermediate properties, i.e., variable amounts of triplet [4,8] and $Q_A^-Fe^{2+}$ (e.g., Ref. 8 and A.W.R., unpublished data). According to the current work and the literature discussed above, the presence of the triplet in such preparations could reflect two additive effects: the degree of $Q_A^-Fe^{2+}$ destroyed by the detergent treatment and the size of the functional antenna. The relative influence of each one of these effects is difficult to judge. In this regard, it will be extremely useful to look at the triplet yield in D1/D2 preparations which still maintain Q_A when (if) such a preparation is isolated.

It has been recently reported that the dithionite-reducable $Q_A^-Fe^{2+}$ signal is lost simultaneously with PS II electron transfer during photoinhibition of PS II with strong light [40]. Since Ph^- photoaccumulation has been demonstrated under strong light in the absence of chemical reductants [41], it was predictable that Q_AFe^{2+} double-reduction should occur under these conditions. We can now propose that the changes in primary photochemistry due to $Q_A^-Fe^{2+}$ double-reduction which are reported here (i.e., increased triplet yield, probably increased $P680^+Ph^-$ yield and possibly lifetime) are likely to be found in photoinhibited material. In addition, since we have observed that the double-reduction of Q_A is an irreversible process, we suggest that this event could be the primary lesion which results in an irreversible electron transfer block in PS II during photoinhibition.

Acknowledgements

We would like to thank Dr G. Renger for useful discussion. A.W.R. is supported by the CNRS. W.N. is supported by the Deutsche Forschungsgemeinschaft.

References

1 Parson, W.W. and Ke, B. (1982) in Photosynthesis: Energy Conversion by Plants and Bacteria (Govindjee, ed.), pp. 331–385, Academic Press, New York.

2 Okamura, M.Y., Feher, G. and Nelson, N. (1982) in Photosynthesis: Energy Conversion by Plants and Bacteria (Govindjee, ed.), pp. 195–272, Academic Press, New York.

3 Wraight, C.A. and Clayton, R.K. (1977) Biochim. Biophys. Acta 333, 246–260.

4 Rutherford, A.W., Paterson, D.R. and Mullet, J.E. (1981) Biochim. Biophys. Acta 635, 205–214.

5 Rutherford, A.W. (1987) in Progress in Photosynthesis Research (Biggins, J., ed.), Vol. 1, pp. 277–283, Martinus Nijhoff, Dordrecht.

6 Evans, M.C.W., Atkinson, Y.E. and Ford, R.C. (1985) Biochim. Biophys. Acta 806, 247–254.

7 Nugent, J.H.A., Diner, B.A. and Evans, M.C.W. (1981) FEBS Lett. 124, 241–244.

8 Atkinson, Y.E. and Evans, M.C.W. (1983) FEBS Lett. 159, 141–144.

9 Mathis, P. and Rutherford, A.W. (1987) in New Comprehensive Biochemistry: Photosynthesis (Amesz, J., ed.), pp. 63–96, Elsevier, Amsterdam.

10 Trebst, A. (1986) Z. Naturforsch. 41c, 240–245.
11 Michel, H. and Deisenhofer, J. (1988) Biochemistry 27, 1–7.
12 Okamura, M.Y., Isaacson, R.A. and Feher, G. (1977) Biophys. J. 17, 49a.
13 Okamura, M.Y., Isaacson, R.A. and Feher, G. (1979) Biochim. Biophys. Acta 546, 394–417.
14 Rutherford, A.W., Heathcote, P. and Evans, M.C.W. (1979) Biochem. J. 182, 515–523.
15 Rutherford, A.W., Zimmermann, J.L. and Mathis, P. (1984) Advances in Photosynthesis Research (Sybesma, C. ed.), Vol. 1, pp. 445–448, Martinus Nijhoff, Dordrecht.
16 Rutherford, A.W. and Zimmermann, J.L. (1984) Biochim. Biophys. Acta 767, 168–175.
17 Rutherford, A.W., Mathis, P. and Van Mieghem, F. (1988) Table ronde Roussel-Uclaf No 63: Structure, function and molecular mechanisms in photosystem II, p. 22, Inst. Scientifique Roussel, Paris.
18 Berthold, D.A., Babcock, G.T. and Yocum, C.F. (1981) FEBS Lett. 134, 231–234.
19 Ford, R.C. and Evans, M.C.W. (1983) FEBS Lett. 160, 159–164.
20 Dutton, P.L. (1971) Biochim. Biophys. Acta 226, 63–80.
21 Takahashi, Y., Hansson, O., Mathis, P. and Satoh, K. (1987) Biochim. Biophys. Acta 793, 49–59.
22 Kramer, H. and Mathis, P. (1980) Biochim. Biophys. Acta 593, 319–329.
23 Vermaas, W.F.J. and Rutherford, A.W. (1984) FEBS Lett. 175, 243–248.
24 Klimov, V.V., Dolan, E. and Ke, B. (1980) FEBS Lett. 112, 97–100.
25 Klimov, V.-V., Allakherdiev, S.I., Demeter, S. and Krasnovskii (1980) Dokl. Akad. Nauk. 249, 227–230.
26 Rutherford, A.W., Mullet, J.E. and Crofts, A.R. (1981) FEBS Lett. 123, 235–237.
27 Thurnauer, M.C., Katz, J.J. and Norris, J.R. (1975) Proc. Natl. Acad. Sci. USA 72, 3270–3274.
28 Rutherford, A.W., Satoh, K. and Mathis, P. (1983) Biophys. J. 41, 40a.
29 Den Blanken, H.J., Hoff, A.J., Jongenelis, A.P.J.M. and Diner, B.A. (1983) FEBS Lett. 157, 21–27.
30 Diner, B.A., De Vitry, C. and Popot, J.L. (1988) Biochim. Biophys. Acta 934, 47–54.
31 Nanba, O. and Satoh, K. (1987) Proc. Natl. Acad. Sci. USA 84, 109–112.
32 Schatz, G.H., Brock, H. and Holzwarth, A.R. (1988) Biophys. J. 54, 397–405.
33 Schlodder, E. and Brettel, K. (1988) Biochim. Biophys. Acta 933, 22–34.
34 Eckert, H.J., Renger, G., Bernarding, J., Faust, P., Eichler, H.J. and Salk, J. (1987) Biochim. Biophys. Acta 893, 208–218.
35 Schatz, G.H. and Holzwarth, A.R. (1986) Photosynth. Res. 10, 309–318.
36 Van Gorkom, H.J. (1985) Photosynth. Res. 6, 97–112.
37 Trissl, H.-W. and Leibl, W. (1989) FEBS Lett. 244, 85–88.
38 Hansson, O., Duranton, J. and Mathis, P. (1988) Biochim. Biophys. Acta 932, 91–96.
39 Okamura, M.Y., Satoh, K., Isaacson, R.A. and Feher, G. (1987) in Progress in Photosynthesis Research (Biggins, J., ed.), Vol. 1, pp. 379–381, Martinus Nijhoff, Dordrecht.
40 Andersson, B., Virgin, I. and Styring, S. (1989) in Highlights of Modern Biochemistry (Kotyk, A., Skoda, J., Taces, V. and Kostka, V., eds.), pp. 923–932, V.S.P. International Science Publishers, Zeist.
41 Klimov, V.V., Shuvalov, V.A. and Heber, U. (1985) Biochim. Biophys. Acta 809, 345–350.
42 Vermaas, W.F.J. and Govindjee (1982) Biochim. Biophys. Acta 680, 202–209.

Chapter 4

The influence of the double reduction of Q_A on the fluorescence decay kinetics of Photosystem II

F.J.E. van Mieghem [a,b], G.F.W. Searle [b], A.W. Rutherford [a] and T.J. Schaafsma [b]

[a] *Section de Bioénergétique, Département de Biologie Cellulaire et Moléculaire, CE Saclay, Gif-sur-Yvette (France) and* [b] *Department of Molecular Physics, Agricultural University, Wageningen (Netherlands)*

(Received 30 October 1991)

Key words: EPR; Radical pair state; Plastoquinone; Photosynthesis; Photosystem II preparation; Chlorophyll

The acceptor Q_A of PS II was doubly reduced by treatment of PS II-enriched membranes (200–300 chlorophylls per PS II-reaction centre) with dithionite and benzyl viologen. After double reduction of Q_A, two major differences appeared in the fluorescence decay kinetics (at 4°C), as compared to the situation with all Q_A singly reduced: (1) a dominant fast phase (lifetime approx. 200 ps) was observed, similar to that in samples with Q_A oxidised; (2) a slow phase with a lifetime of approx. 7 ns was observed, which disappeared upon reoxidation of the sample. The fluorescence yield was approximately half of that of samples with singly reduced Q_A. The fast phase is interpreted as being indicative of a high efficiency of charge separation due to the absence of a negatively charged Q_A. This is explained by the double protonation of doubly reduced Q_A giving rise to the electrically neutral quinol. Similar observations were made in a core complex preparation (60–80 chlorophylls per reaction centre). This preparation involves a detergent solubilisation step and data from both EPR and fluorescence indicated that it was more susceptible to double reduction of Q_A by dithionite (as compared to PS II membranes). The possibility that this is a general phenomenon in detergent solubilised PS II preparations is discussed.

Introduction

The reaction centre of PS II is generally considered to be similar in all green plants, algae and cyanobacteria and also to be closely related to the reaction centre of photosynthetic purple bacteria (see Ref. 1 for a review). It is connected to an antenna system that captures the light and transfers the energy to the primary electron donor P, which is located in the reaction centre and consists of one or more chlorophyll *a* molecules. Electron transfer can then occur from P to a nearby pheophytin *a*, the primary acceptor Phe. Thus, the primary radical pair is formed. This charge separation is subsequently stabilised by electron transfer to Q_A, a plastoquinone (see Refs. 2 and 3 for reviews on electron transfer processes in PS II).

It is now generally accepted that prereducing Q_A to its singly reduced semiquinone form decreases the yield of charge separation (see e.g. Refs. 4–9). However, there is some disagreement with regard to what extent this occurs. The lower yield of charge separation in reaction centres with Q_A^- present, compared to that of reaction centres with Q_A oxidised, has been explained by a net repulsive electrostatic interaction between Q_A^- and the primary radical pair [6,10].

When the primary radical pair P^+Phe^- is formed, and if it lives long enough to allow dephasing of the electron spins, charge recombination to the molecular triplet state of P can occur [11]. These conditions can be reached when Q_A is absent [12] or doubly reduced [9]. When Q_A is singly reduced, no triplet state can be detected [9]. As the most straightforward explanation for this observation, it was suggested in Ref. 9 that the yield of the primary radical pair in PS II reaction centres with Q_A^- present, is very low, due to the electrostatic effect, as proposed in Refs. 6 and 10. Double reduction of Q_A, followed by a double protonation neutralises the negative charge at the site of Q_A and the formation of the primary radical pair is no longer electrostatically inhibited [9]. The triplet yield is high, because the lifetime of the primary radical pair is sufficiently long for triplet formation.

Abbreviations: Chl, chlorophyll; EDTA, ethylenediaminetetraacetate; Mes, morpholineethanesulphonic acid; Mops, 4-morpholinepropanesulphonic acid; P, the primary electron donor in Photosystem II; Phe, pheophytin; PS II, Photosystem II; Q_A, the first quinone electron acceptor.

Correspondence: F.J.E. van Mieghem, Section de Bioénergétique, Département de Biologie Cellulaire et Moléculaire, CE Saclay, 91191 Gif-sur-Yvette Cedex, France.

In this work we test the hypothesis that the double reduction of Q_A modulates the yield of the primary radical pair and hence the yield of the triplet. For this, we looked at the rate of charge separation, using picosecond fluorescence measurements. It was suggested earlier that the double reduction of Q_A may be responsible for fluorescence quenching in PS II [9,13].

We used two types of PS II preparations from spinach, differing in their antenna size. The reduction of the antenna size is usually achieved by detergent treatment, which may affect the intactness of the acceptor side [9].

A preliminary report of these results has appeared elsewhere [14].

Materials and Methods

PS II-enriched thylakoid membrane fragments were prepared from spinach as described earlier [15] using the modifications in Ref. 16. PS II core complexes were prepared according to Ref. 17. In order to obtain reaction centres with Q_A doubly reduced, membrane fragments were maintained in the dark for several hours in the presence of approximately 40 mM sodium dithionite and 100 μM benzyl viologen (sodium dithionite was added from a 10-fold concentrated stock solution, also containing 400 mM Mops at pH 7.0) [9]. In addition, 50 mM Mops (pH 7.0), 300 mM sucrose, 200 mM sodium formate, 10 mM NaCl, 5 mM $MgCl_2$ and 1 mM EDTA were present during the incubation. In experiments in which Q_A was reoxidised, the membranes were washed with buffer in order to remove dithionite and benzyl viologen and the sample was then suspended in a buffer containing 5 mM ferricyanide which was subsequently removed by washing.

Core complexes were also treated with sodium dithionite and benzyl viologen, but this was done in a buffer containing 50 mM Mes (pH 6.0), 400 mM sucrose, 200 mM sodium formate, 10 mM NaCl, 5 mM $CaCl_2$ and 1 mM EDTA.

Incubations with dithionite and benzyl viologen were done in EPR tubes in order to enable the monitoring of the triplet [11] and formate enhanced $Q_A^- Fe^{2+}$ [18] EPR signals during the treatment (see also Ref. 9). The incubations were ended after all Q_A had been doubly reduced (i.e., the triplet EPR signal had reached its maximal level and the $Q_A^- Fe^{2+}$ signal had decreased beyond detection [9]). The samples were stored under argon and at 77 K in the dark until use.

EPR spectra were recorded using a Bruker 200 X-band spectrometer fitted with an Oxford Instruments cryostat and temperature control system. In order to record spectra during illumination, an 800 W tungsten projector was used. The light was filtered through 2 cm water and three Calflex (Balzers) heat filters.

For fluorescence kinetics measurements, samples were diluted in near darkness into fluorescence cuvettes in an argon flushed buffer (4°C), containing 50 mM Mes (pH 6.0), 400 mM sucrose, 10 mM NaCl and 5 mM $CaCl_2$. After dilution, the cuvettes were sealed and kept in the dark until use. Samples with Q_A doubly reduced were diluted in buffer, to which 4 mM sodium dithionite had already been added. Thus, a possible partial reoxidation of doubly reduced Q_A was avoided. Q_A was singly reduced by the addition of 4 mM dithionite to a sample that had not been treated with dithionite and benzyl viologen. The addition was made shortly before the measurement. For measurements under conditions of oxidised Q_A, the sample was in the presence of 0.05 mM ferricyanide and the light intensity of the exciting light was diminished to a level at which the contributions of decay components longer than one nanosecond were minimal. In particularly in the case of oxidised core complexes, the lifetimes of the decay components increased considerably with the intensity of the excitation light.

Fluorescence kinetic measurements were performed in 10×10 mm anaerobic cuvettes at a concentration of 1–10 μg Chl/ml. During the measurements, the samples were stirred and maintained at 4°C. The experimental conditions were as described previously [19]. The excitation source was a mode locked Ar ion laser, wavelength 457.8 nm, the pulse frequency was 596 kHz and the pulse energy was approximately 2 pJ/cm^2. The time resolution of the multi-channel analyser was 10.2 ps/channel. The pulse width after detection was 200 ps full width at half maximum. To check for a wavelength dependence of the fluorescence decay kinetics, the detection wavelength was set at 679, 693 or 707 nm using Balzers B-40 interference filters. No significant wavelength dependence was observed. Therefore, subsequent measurements were carried out using a broadband (Balzers K70) filter.

The fluorescence decay of a reference compound (Rose Bengal in methanol, lifetime 0.55 ns) fluorescing at the same wavelengths as chlorophyll was determined before and after the measurement of the fluorescence decay in a PS II sample. The averaged reference was then used to generate a laser pulse shape using a deconvolution programme employing Fourier transformation. The deconvolution parameters were varied and were considered optimal when the resulting pulse shape showed minimal oscillations.

The fluorescence decay kinetics were analysed with the Global Analysis programme of Beechem, Gratton and Mantulin (Globals Unlimited, Urbana, USA, 1990). The input file for this programme consisted of the sample data file and the associated deconvoluted pulse file. The data was weighted with the square root of the number of counts per channel and fitted to a sum of up to 6 discrete components. The criterion for the good-

TABLE I

Analysis of the fluorescence decay data (summary from several experiments) of PS II membranes, before and after dithionite / benzyl viologen treatment of membranes and of reoxidised membranes

Fluorescence decay components are given in ns and the relative amplitude is given as a percentage in brackets; estimated errors are given. Values for the relative fluorescence yields are given in arbitrary units (see Materials and Methods for procedure).

Sample	Additions	Fluorescence decay components				Rel. yield
Before dithionite/benzyl viologen treatment	A 0.05 mM ferricyanide	0.14 ± 0.03 (73 ± 10)	0.33 ± 0.04 (27 ± 5)	3.2 ± 1 (0.04 ± 0.02)		19
	B 4 mM dithionite	0.60 + 0.1 (25 ± 10)	1.4 + 0.3 (68 ± 10)	3.3 + 1 (7 ± 3)		133
Dithionite/benzyl viologen treated	C 4 mM dithionite	0.22 ± 0.04 (69 ± 10)	0.60 ± 0.1 (18 ± 4)	2.0 ± 0.5 (8 ± 2)	7.1 ± 2 (5 ± 1)	77
Reoxidised after dithionite/benzyl viologen treatment	D 0.05 mM ferricyanide	0.11 ± 0.03 (64 ± 10)	0.35 ± 0.05 (35 ± 7)	1.1 ± 0.3 (1 ± 0.3)	5.6 ± 2 (0.03 ± 0.01)	21

ness of the fit was the χ^2 value. The quality of the fits was also judged from a plot of the distribution of weighted residuals (experimental minus calculated counts per channel). In some cases, short components (0.1–40 ps) were found, with lifetimes and relative amplitudes that were not reproducible. The relative amplitudes and lifetimes of the remaining components were reproducible within the errors given in Tables I and II. Therefore, only the latter components are considered in our discussion of the fluorescence decay kinetics. Values for the relative fluorescence yield were calculated by $\Sigma\alpha_i\tau_i$ (α_i is the relative amplitude of component i in percent and τ_i its lifetime in ns). The values for the relative fluorescence yield (Tables I and II), corresponded with those obtained from fluorescence measurements under continuous illumination (Table III). Thus, the values for the relative yield, calculated from the decay kinetics can be taken as being proportional to the fluorescence yield.

For fluorescence measurements under continuous illumination, a home-built apparatus was used. The onset of the exciting light (expanded He-Ne laserlight, 633 nm) was accomplished by the opening of an electrical shutter (opening time faster than 1 ms). Detection was around 687 nm (monochromator) using a photomultiplier (S20) and an analogue-to-digital conversion card.

Results

PS II-enriched membranes

PS II membranes were pretreated with dithionite and benzyl viologen as described in Materials and Methods, in order to obtain reaction centres with Q_A doubly reduced [9]. This was checked by EPR at liquid helium temperature by measuring the decrease of the $Q_A^-Fe^{2+}$ signal and the increase of the light-inducible reaction centre triplet signal. The triplet signal was small at the start of the treatment and a large $Q_A^-Fe^{2+}$ signal was observed (Fig. 1a). The incubations were ended after the triplet EPR signal had reached its maximal level and the $Q_A^-Fe^{2+}$ signal had decreased

TABLE II

Analysis of the fluorescence decay data (summary from several experiments) of PS II core complexes, before and after dithionite / benzyl viologen treatment

Fluorescence decay components are given in ns and the relative amplitude is given as a percentage in brackets; estimated errors are given. Values for the relative fluorescence yield are given in arbitrary units (see Materials and Methods for procedure).

Sample	Additions	Fluorescence decay components				Rel. yield
Before dithionite/benzyl viologen treatment	A 0.05 mM ferricyanide	0.06 ± 0.02 (75 ± 10)	0.25 ± 0.04 (22 ± 5)	0.68 ± 0.1 (3 ± 1)	3.1 ± 1 (0.2 ± 0.1)	13
	B 4 mM *dithionite*	0.1 ± 0.03 (32 ± 6)	0.51 ± 0.1 (36 ± 7)	1.5 ± 0.4 (26 ± 5)	4.9 ± 1 (6 ± 2)	90
Dithionite/benzyl viologen treated	C 4 mM dithionite	0.075 ± 0.02 (50 ± 10)	0.32 ± 0.04 (32 ± 6)	1.3 ± 0.3 (13 ± 3)	7.1 ± 2 (5 ± 1)	66
	D 0.05 mM ferricyanide	*0.1 ± 0.03* (65 ± 10)	*0.37 ± 0.05* (30 ± 6)	1.2 ± 0.3 (4 ± 1)	5.9 ± 2 (1 ± 0.3)	28

TABLE III

Values for the fluorescence yield, measured under continuous illumination in PS II membranes and PS II core complexes

The sample conditions were similar to those used in the fluorescence decay measurements. The fluorescence yield is given in arbitrary units.

Sample	Additions	Fluorescence yield	
		membranes	core complexes
Before dithionite/ benzyl viologen treatment	A[a] 0.05 mM ferricyanide	18	26
	B 4 mM dithionite	149	146
Dithionite/benzyl viologen treated	C 4 mM dithionite	73	72
	D[a] 0.05 mM ferricyanide	27	46

[a] Values are those measured at the onset of the illumination.

beyond detection (Fig 1b, see also Ref 9). Samples pretreated in this way are referred to as 'dithionite/benzyl viologen-treated samples' throughout the text. They were kept under reducing conditions unless otherwise mentioned. For the fluorescence decay measurements, we also prepared PS II membranes in the two other redox states of Q_A: with Q_A oxidised and

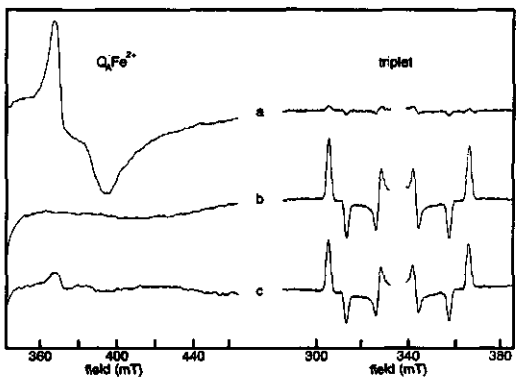

Fig. 1. $Q_A^- Fe^{2+}$ and reaction centre triplet signals from PS II-enriched membranes (4 mg Chl/ml) after different redox treatments; average of two experiments. (a) Spectra recorded 15 min after the addition of 40 mM dithionite; (b) after approximately 4 h incubation in the presence of 40 mM dithionite and 0.1 mM benzyl viologen in the dark at 20°C; (c) after subsequentially washing the sample in buffer, 5 mM ferricyanide, buffer(2×); 15 min before freezing the sample, 40 mM dithionite was added. EPR conditions for the $Q_A^- Fe^{2+}$ spectra: temperature, 4.7 K; microwave power, 32 mW; microwave frequency, 9.44 GHz; modulation amplitude, 25 G. The triplet spectra are difference spectra (light on minus light off); the EPR conditions are the same as for $Q_A^- Fe^{2+}$ except that the microwave power was 63 μW.

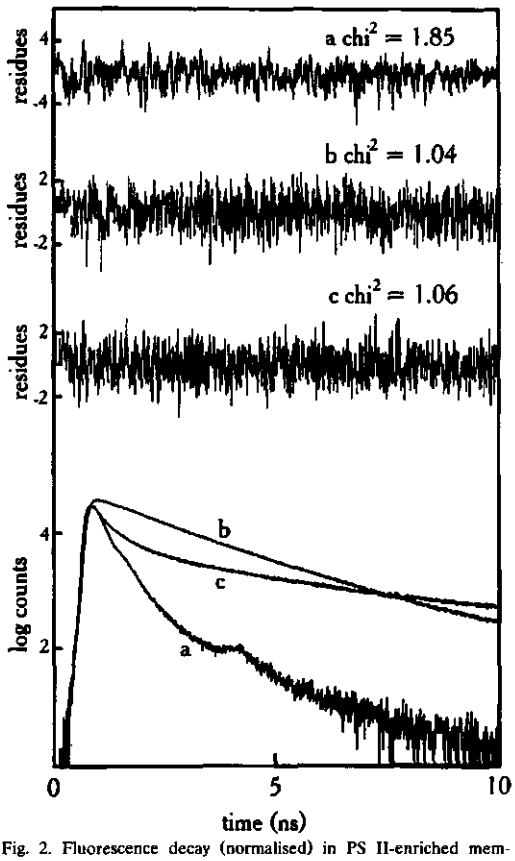

Fig. 2. Fluorescence decay (normalised) in PS II-enriched membranes. Weighted residual plots are also shown (upper traces). (a) 0.05 mM ferricyanide present in the measuring cuvette; (b) 4 mM dithionite present; (c) sample, treated as described in the legend to Fig. 1b; the dithionite concentration in the cuvette was 4 mM. The number of counts in the peak channel was: (a) 29 000; (b) 41 000; (c) 22 000.

with Q_A singly reduced (see Materials and Methods for details on the experimental conditions).

Typical fluorescence decay curves for the three types of samples are shown in Fig. 2 for PS II membranes. Comparing traces A (Q_A oxidised) and B (Q_A singly reduced) reveals that upon reducing Q_A with one electron, the fluorescence lifetime increases drastically. This is characteristic for PS II (see Refs. 20 and 21 for reviews on fluorescence of PS II). When Q_A is doubly reduced (trace C), there is an initial fast decay, similar to that in oxidised samples. However, there is also a very slow component present, slower than that of samples with singly reduced Q_A.

To obtain more quantitative information on the fluorescence decay kinetics, we fitted the decay curves to a multi-exponential decay function (see Materials

and Methods for details on the fitting procedure). The results are shown in Table I (A, B and C). Fitting of the curves yielded three (Q_A oxidised and singly reduced) or four (Q_A doubly reduced) components. As shown in the weighted residual plots of Fig 2, the fitted curves agree well with the experimental curves. In samples with oxidised Q_A, relatively high values for χ^2 were found, due to a lower signal to noise ratio. The lower signal to noise ratio was caused by the relatively low fluorescence yield and also the low excitation intensity used for samples with oxidised Q_A (see Materials and Methods). The results of the analyses of the decay kinetics were reproducable within the errors given in Table I.

The data of Table IA, B, C confirm the qualitative impressions from Fig. 2. When Q_A is oxidised, the kinetics are dominated by a fast component of approx. 140 ps. Singly reducing Q_A results in an increased fluorescence yield. This is caused by the lengthening of the fluorescence lifetime of the components and a shift in the distibution to slower components, of which a component with a lifetime of approx. 1.4 ns is dominant. These observations are in agreement with reports in the literature on similar preparations [4,8,22].

In samples with Q_A doubly reduced, the fluorescence yield is also higher than that in samples with Q_A oxidised, but it is only half that of samples with Q_A singly reduced (see also Table IIIB, C). There is a short component of 220 ps with high relative amplitude, which is similar to the 140 ps component found when Q_A is oxidised. A similar component with high relative amplitude together with an irreversible decrease in fluorescence yield has been observed previously after strong illumination in the presence of dithionite [4] (see also Ref. 23). It has been shown recently that such conditions indeed generate reaction centres with Q_A doubly reduced [9]. Finally, there is an unusually long component of 7.1 ns present when Q_A is doubly reduced, which is absent when Q_A is in the semiquinone form. Since the time window used was 10 ns, the value for the slow component is an approximate value. However, it is clearly slower than that in samples with singly reduced Q_A (see Fig. 2a,b). Slow (25–35 ns) fluorescence decay components, similar to the lifetime of the primary radical pair, have been observed before, in D1/D2/cyt *b*-559 particles which contain no Q_A [24–26].

In order to check whether the appearance of the 7.1 ns component was reversible, dithionite/benzyl viologen-treated samples were reoxidised by washing with ferricyanide (see Materials and Methods). Table ID summarises the fluorescence decay kinetics of the reoxidised samples. The decay kinetics and the relative fluorescence yield were similar to those of samples that had not been treated with dithionite and benzyl viologen (Table IA). The amplitudes of decay components of 1 ns or longer were small (approx. 1%). Generally, the kinetics were more similar to those of oxidised samples not treated with dithionite and benzyl viologen (Table IA). This indicates that the double reduction of Q_A is reversible when the sample is reoxidised and that slow components, observed in samples with dithionite present are not due to the presence of disconnected antenna.

EPR measurements were also carried out on reoxidised samples, in order to test whether the state $Q_A^- Fe^{2+}$ could be made again in its normal form [18] by re-adding dithionite. We found that only in a small proportion of the sample could this state be formed (in approximately 10%, comparing Fig. 1a and c). At the same time, there was a significant reaction-centre triplet signal detectable (Fig. 1c), although it was smaller than in samples with all the Q_A doubly reduced. This indicates that in most of the reaction centres in this preparation, Q_A is immediately doubly reduced upon dithionite addition. This is probably due to an irreversible conformational change that in turn results in a destabilised Q_A^- state.

PS II core complexes

The experiments described above were repeated with a different type of PS II preparation, which is designated 'core complex'. In this preparation there is a solubilisation step involved, for which the detergent octylglucopyranoside was used [17]. The core complexes are devoid of the major PS II light-harvesting protein, LHC II, and have approx. 70 chlorophylls per reaction centre [17]. The dithionite/benzyl viologen treatment for the double reduction of Q_A was similar to that described for PS II membranes. However, we noted that in this preparation, the yield of the reaction centre triplet was already significant at the beginning of the treatment (approx. 30% of the maximum obtainable level, data not shown). This suggests that in part of the reaction centres double reduction is essentially instantaneous when dithionite is added.

The results of the fluorescence lifetime measurements on the PS II core complexes are shown in Fig. 3. The traces show a number of features which are similar to those indicated for PS II membranes (Fig. 2): trace C (Q_A doubly reduced) shows a fast initial decay, as does trace A (Q_A oxidised) and there is a slow component in trace C that seems slower than that in trace B (Q_A singly reduced). However, the difference between the traces before and after dithionite/benzyl viologen treatment (Fig. 3b,c) is less pronounced than for the case of membranes (Fig. 2b,c).

The decay curves of core complexes were fitted using the same procedure as for membranes (Table IIA,B,C). The results for samples with Q_A oxidised and Q_A singly reduced agree with recent data obtained from a similar preparation [27]. A more quantitative

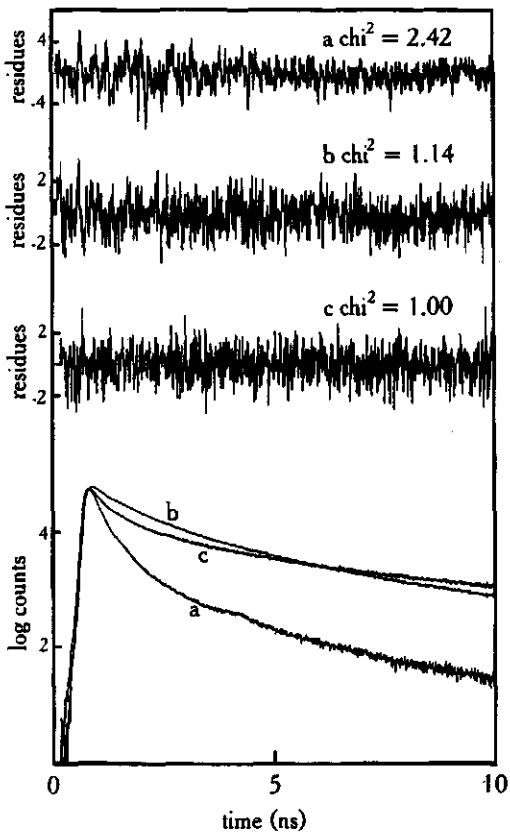

Fig. 3. Fluorescence decay (normalised) in PS II core complexes. Weighted residual plots are also shown (upper traces). Sample conditions were as described in the legend to Fig. 2. The number of counts in the peak channel was: (a) 61 000; (b) 50 000; (c) 16 000.

comparison between the results from membranes and core complexes can be made when Table I (A,B,C) and Table II (A,B,C) are compared. This reveals one major difference: the presence of a fast component (100 ps) in core complexes with dithionite added in order to singly reduce Q_A (Table IIB), compared to membranes, in which the fastest component has a lifetime of 600 ps under these conditions (Table IB). In core complexes, fast components (of the order of 100 ps) are present both before (Table IIB) and after (Table IIC) dithionite/benzyl viologen treatment. This accounts for the fact that in core complexes, the traces before (Fig. 3b) and after (Fig. 3c) dithionite/benzyl viologen treatment are more alike than they are in membrane samples.

Dithionite/benzyl viologen-treated core complex samples were tested for the reversibility of the presence of slow components by measuring them also in the presence of 0.05 mM ferricyanide. The slow components (1.3 ns and 7.1 ns) observed under reducing conditions decreased considerably in relative amplitude in the presence of ferricyanide.

Discussion

PS-II membranes

Fluorescence measurements with short time resolution have been used extensively to study the primary photochemical reactions in PS II. A large variety of preparations has been used and the fluorescence kinetics have been found to be significantly dependent on the type of preparation and the organism used and probably also on the measuring system used (see Refs. 20 and 21 for recent reviews). Our results on samples with Q_A singly reduced and Q_A oxidised are in agreement with previous work on similar preparations (e.g. Refs. 4, 8 and 22. They are also in agreement with results from intact chloroplasts and green algae (see Refs. 20 and 21), except that we did not have contributions from PS I. We will focus in the following on the doubly reduced redox state of Q_A, which has not been investigated before using picosecond fluorescence measurements, and compare its fluorescence decay kinetics with those of the oxidised and singly reduced states of Q_A.

We will analyse our results, assuming that the fluorescence decay kinetics of PS II are trap-limited (see e.g. Refs. 6 and 28, also Ref. 29, and Refs. 20 and 21 for comparisons with other concepts). In line with those studies, we assume that the excitation energy equilibrates over the antenna system, including P-680, within a few picoseconds (faster than the time resolution of our measuring system). The lifetime and amplitude of the fastest decay component thus reflect the trapping of the equilibrated excited state into the primary radical pair state. The lifetime and the amplitude of the fastest decay component are to a large extent responsible for the initial part of the fluorescence decay curve. Therefore, we assume that the initial decay observed in the fluorescence decay curve (Fig. 2), reflects the formation of the primary radical pair.

Comparing different redox states of Q_A in the same kind of PS II preparation will reveal influences of the Q_A state on primary photochemistry. When the traces A (Q_A oxidised) and B (Q_A singly reduced) of Fig. 2 are compared, a much faster initial decay is observed in the oxidised situation. Similar observations have been explained previously by a decreased yield of charge separation when Q_A is reduced, assuming trap-limited fluorescence decay kinetics [6,28]. A net repulsive electrostatic interaction between Q_A^- and the radical pair was thought responsible for this reduced yield [6,10].

Comparing traces B and C of Fig. 1 reveals that the initial decay in trace C (Q_A doubly reduced) is faster than that in trace B (Q_A singly reduced). Assuming trap-limited decay kinetics, this indicates a higher rate of charge separation (resulting in a higher yield) when Q_A is doubly reduced, compared to reaction centres with Q_A singly reduced. This was proposed before in a study on the triplet yield in relation to the redox state of Q_A [9]. In the latter study, a negligible triplet yield was found in reaction centres with Q_A singly reduced at liquid helium temperature and a drastic increase in triplet yield (close to 100%) was observed when Q_A was subsequently doubly reduced [9]. In a purely electrostatic model in which charges at the Q_A site directly influence the yield of the primary radical pair [6,10], the high rate of charge separation in the doubly reduced state implies that the negative charge at the Q_A site is neutralised. To explain this, we suggest that Q_A undergoes protonation upon double reduction forming the quinol, as was suggested before [9].

If double reduction of Q_A involves a protonation resulting in the electrically neutral quinol, the electrostatic repulsion between Q_A and the radical pair is absent and the yield of charge separation is probably similar to that of reaction centres with Q_A oxidised. This seems indeed the case from Table I: the lifetime and the relative amplitude of the fastest decay component are similar when comparing samples with Q_A oxidised (140 ps, 73%, Table IA) and Q_A doubly reduced (220 ps, 69% Table IC).

It should be pointed out that the data might also be explained by conformational changes triggered by the Q_A redox state [9]. The electrostatic model discussed above and models invoking conformational changes are not necessarily mutually exclusive.

Apart from the similarities in the fastest decay component of oxidised and doubly reduced reaction centres mentioned above, the other decay components are different from each other. The most obvious difference is the presence of a component of approx. 7 ns with significant amplitude in samples with Q_A doubly reduced, whereas components longer than 1 ns are negligible in samples with Q_A oxidised. We stress that decay components in the range of 1–10 ns always disappeared upon reoxidation of samples (see Tables ID and IID). Thus, they are not the result of disconnected antenna. It is more likely that the presence of the 7 ns component in samples with doubly reduced Q_A is related to the longer lived radical pair in these samples. In the oxidised state, the second component observed has a lifetime of 330 ps, which is in the range of values reported for the lifetime of the primary radical pair under those conditions [10,30–32].

Comparing samples with Q_A singly and doubly reduced (Table IB,C), it is seen that in samples with Q_A doubly reduced (dithionite/benzyl viologen-treated), four components were found. In the case of singly reduced Q_A, three components were found which is in agreement with earlier work (see Refs. 20 and 21 for reviews). It is possible that the 2 ns component (8%) in dithionite/benzyl viologen-treated samples (Table IC) is due to a small fraction of reaction centres with Q_A still singly reduced but not detectable by EPR, in which case the doubly reduced state may also be characterised by three decay components. The presence of a 7 ns component when Q_A is doubly reduced, compared to 3 ns for the singly reduced state, indicates that the lifetime of the radical pair is longer in the doubly reduced state. However, the relation between the fluorescence decay kinetics and the lifetime of the primary radical pair is complex, and it is not straightforward to determine it from the fluorescence decay. For a homogenous sample, neglecting singlet-triplet mixing, the kinetics of the radical pair are described by an expression in which all of the exponential fluorescence decay components and their relative amplitudes appear (see Refs. 6, 8 and 19, for example). In the most simple model, in which there are forward and reverse reactions between two states (the excited state and the singlet primary radical pair state), only two decay components are present [6]. Here (see also Ref. 22), the situation is more complex because there are at least three decay components in samples with Q_A singly or doubly reduced. The presence of three or more PS II fluorescence decay components in green algae has been described assuming PS II-α/β heterogeneity [33]. Although we used PS II membranes [15] that were prepared from the grana which consist only of PS II-α, we can not rule out that our samples are heterogenous as regards the primary photochemical reactions. Thus, heterogeneity may explain the fact that three or more components are found in PS II membranes. However, in the case of doubly reduced Q_A, the fluorescence decay kinetics are probably influenced by the singlet-triplet mixing of the primary radical pair, the decay of which is then described by a Stochastic Liouville Equation [34]. Therefore, analysing the fluorescence decay kinetics as a sum of discrete, exponential, decay components is probably approximate and a rigorous mathematical analysis is hampered. Also, sample heterogeneity may give rise to a distribution of lifetimes, rather than discrete decay components. This is the case if the values for the rate constants of the primary reactions are gradually distributed around some average value. Nevertheless, there are some other indications, from flash absorption measurements, that the radical pair lives longer when Q_A is doubly reduced, compared to the singly reduced state. (1) Strong illumination in the presence of dithionite (now known to result in double reduction of Q_A [9]), gave an increase in the lifetime of the radical pair up to 15 ns [4]. (2) Comparison of different PS II preparations led to the suggestion that

the the yield of charge separation and also the lifetime of the primary radical pair increase when Q_A is doubly reduced [5,9].

PS II core complexes

Above, using the fluorescence decay curves of PS II membranes (Fig. 2), we have compared the yields of charge separation in samples with different states of the Q_A acceptor system, assuming trap-limited fluorescence decay. The same features as seen in PS II membranes (Fig. 2) are, to a somewhat lesser extent, present in PS II core complexes (Fig. 3): the initial decay of samples with Q_A oxidised and doubly reduced is faster than that of samples with Q_A singly reduced. We will now in some more detail compare the results from PS II membranes and PS II core complexes as shown in the Tables IA,B,C and IIA,B,C.

The core complexes were obtained from the membranes by a detergent solubilisation step, which results in a smaller antenna size (approximately 70 chlorophylls per reaction centre [17]). For trap-limited fluorescence decay, the rate of trapping is dependent on the antenna size [6]: decreasing the antenna size increases the free energy of the excited state relative to the primary radical pair state and hence the rate of trapping increases. This is illustrated for example under oxidised conditions: the fast component in core complexes is shorter (60 ps, Table IIA) compared to membranes (140 ps, Table IA).

There is a more striking difference between core complexes and membranes obvious in samples with Q_A singly reduced by addition of dithionite (Tables IB and IIB). In core complexes there is an additional 100 ps component present which is absent in PS II membranes. Such a component was also found in samples with Q_A doubly reduced (Table IIC). It is thus likely that the 100 ps component found in core complexes in the presence of dithionite reflects a significant percentage of reaction centres in the doubly reduced state. This corresponds to the observation made by EPR, that double reduction of Q_A in core complexes occurs immediately upon dithionite addition in a fraction (approx. 30%) of the reaction centres. The data thus suggest that in core complexes the Q_A site has been modified to the extent that double reduction of Q_A can occur rapidly when dithionite is added. Thus, a sample with part of the Q_A population in the singly reduced state and part in the doubly reduced state is obtained. Accordingly, the primary photochemistry and the fluorescence kinetics are heterogenous.

It was suggested before [9] that the intactness of the Q_A site decreases gradually with the severity of detergent treatments applied (usually in order to purify the reaction centre). This could be the factor (apart from antenna size effects) that was responsible for the differences in the yield of charge separation and the radical pair lifetime, reported for different preparations [5]. In particular, the stability of Q_A^- may decrease, going from intact membrane preparations towards small reaction centre preparations. The Q_A^- state may be less stabilised in these preparations due to detergent-induced conformational changes (see the situation in purple bacteria after removal of Fe^{2+} [35,36]) and an increased accessibility to dithionite. Therefore, we propose that dithionite, added with the aim of singly reducing Q_A, will at least partly doubly reduce Q_A in these preparations. This would give rise to a higher yield of charge separation and probably a longer radical pair lifetime than expected for a sample with all its Q_A singly reduced. Double reduction of Q_A can also occur in membrane preparations, if the sample is illuminated or incubated in the presence of dithionite [9]. The amount of double reduced Q_A is thus dependent on several factors, which are often not well controlled. It may also depend on the type of organism used.

The presence of different amounts of doubly reduced Q_A may explain part of the controversy in the literature on the yield of charge separation and the lifetime of the primary radical pair in reaction centres with Q_A thought to be singly reduced (see e.g. Refs. 5–7 and 10 for measurements on PS II samples with antenna sizes of 60–100 chlorophylls). In fact, in some cases, two phases were resolved in the radical pair decay [5,7]; the slow phase found (10 or more nanoseconds) probably reflects the radical pair lifetime in the fraction of reaction centres with Q_A doubly reduced.

Acknowledgments

We would like to thank A. van Hoek for technical assistance with the time-resolved fluorescence measurements and J.-M. Ducruet for his help with the fluorescence measurements under continuous illumination. We also thank P.J. Booth, K. Brettel, H.J. van Gorkom and W. Leibl for useful discussions and T.A. Roelofs for sending a preprint of unpublished work. F.v.M. is supported by the EEC (SCIENCE Programme) and A.W.R. is supported by the CNRS (URA 1290).

References

1 Rutherford, A.W. (1988) in Light-Energy Transduction in Photosynthesis: Higher Plant and Bacterial Models (Stevens, S.E. and Bryant, D.A., eds.), pp. 163–177, The American Society of Plant Physiologists, Rockville.
2 Van Gorkom, H.J. (1985) Photosynth. Res. 6, 97–112.
3 Hansson, Ö. and Wydrzynski, T. (1990) Photosynth. Res. 23, 131–162.
4 Eckert, H.J., Renger, G., Bernarding, J., Faust, P., Eichler, H.J. and Salk, J. (1987) Biochim. Biophys. Acta 893, 208–218.
5 Hansson, Ö., Duranton, J. and Mathis, P. (1988) Biochim. Biophys. Acta 932, 91–96.

6 Schatz, G.H., Brock, H. and Holzwarth, A.R. (1988) Biophys. J. 54, 397–405.
7 Schlodder, E. and Brettel, K. (1988) Biochim. Biophys. Acta 933, 22–34.
8 Leibl, W., Breton, J., Deprez, J. and Trissl, H.-W. (1989) Photosynth. Res. 22, 257–275.
9 Van Mieghem, F.J.E., Nitschke, W., Mathis, P. and Rutherford, A.W. (1989) Biochim. Biophys. Acta 977, 207–214.
10 Schatz, G.H., Brock, H. and Holzwarth, A.R. (1987) Proc. Natl. Acad. Sci. USA 84, 8414–8418.
11 Rutherford, A.W., Paterson, D.R. and Mullet, J.E. (1981) Biochim. Biophys. Acta 635, 205–214.
12 Okamura, M.Y., Satoh, K., Isaacson, M.A. and Feher, G. (1987) in Progress in Photosynthesis Research (Biggins, J., ed.), Vol. 1, pp. 379–381, Martinus Nijhoff, Dordrecht.
13 Rutherford, A.W., Zimmermann, J.L. and Mathis, P. (1984) Advances of Photosynthesis Research (Sybesma C., ed.), Vol 1, pp. 445–448, Martinus Nijhoff, Dordrecht.
14 Van Mieghem, F.J.E., Searle, G.F.W., Rutherford, A.W. and Schaafsma, T.J. (1991) 37th Harden Conference: The Molecular and Structural Basis of Regulation in Photosynthesis, p. 52, The Biochemical Society, London.
15 Berthold, D.A., Babcock, G.T. and Yocum, C.F. (1981) FEBS Lett. 134, 231–234.
16 Ford, R.C. and Evans, M.C.W. (1983) FEBS Lett. 160, 159–164.
17 Ghanotakis, D.F., Demetriou, D.M. and Yocum, C.F. (1987) Biochim. Biophys. Acta 891, 15–21.
18 Vermaas, W.F.J. and Rutherford, A.W. (1984) FEBS Lett. 175, 243–248.
19 Searle, G.F.W., Tamkivi, R., Van Hoek, A. and Schaafsma, T.J. (1988) J. Chem. Soc. Faraday Trans. 2 84, 315–327.
20 Geacintov, N.E. and Breton, J. (1987) CRC Crit. Rev. Plant Sci. 5, 1–44.
21 Holzwarth, A.R. (1991) in The Chlorophylls (Scheer, H., ed.), pp. 1125–1151, CRC Press, Boca Raton.
22 Hodges, M. and Moya, I. (1986) Biochim. Biophys. Acta 849, 193–202.
23 Renger, G., Koike, N., Yuasa, M. and Inoue, Y. (1983) FEBS Lett. 163, 89–93.
24 Mimuro, M., Yamazaki, I., Itoh, S., Tamai, N. and Satoh, K. (1988) Biochim. Biophys. Acta 933, 478–486.
25 Seibert, M., Picorel, R., Rubin, A.B. and Connolly, J.S. (1988) Plant Physiol. 87, 303–306.
26 Crystall, B., Booth, P.J., Klug, D.R., Barber, J. and Porter, G. (1989) FEBS Lett. 249, 75–78.
27 Hodges, M. and Moya, I. (1988) Biochim. Biophys. Acta 935, 41–52.
28 Schatz, G.H. and Holzwarth, A.R. (1986) Photosynth. Res. 10, 309–318.
29 Van Gorkom, H.J. (1986) Bioelectrochemistry and Bioenergetics 16, 77–87.
30 Nuijs, A.M., Van Gorkom, H.J., Plijter, J.J. and Duysens, L.N.M. (1986) Biochim. Biophys. Acta 848, 167–175.
31 Eckert, H.-J., Wiese, N., Bernarding, J., Eichler, H.-J. and Renger, G. (1988) FEBS Lett. 240, 153–158.
32 Trissl, H-W. and Leibl, W. (1989) FEBS Lett. 244, 85–88.
33 Lee, C.-H., Roelofs, T.A. and Holzwarth, A.R. (1990) in Current Research in Photosynthesis (Baltscheffsky, M., ed.), Vol I, pp. 387–390, Kluwer Academic Publishers, Dordrecht.
34 Hoff, A.J. (1981) Q. Rev. Biophys. 14, 599–665.
35 Dutton, P.L., Prince, R.C. and Tiede, D.M. (1978) Photochem. Photobiol. 28, 939–949.
36 Debus, R.J., Feher, G. and Okamura, M.Y. (1986) Biochemistry 25, 2276–2287.

Chapter 5

The influence of the non-heme iron on the reversibility of the Q_A double reduction in Photosystem II

The reversibility of the double reduction of Q_A in the reaction centre of Photosystem II was investigated in detail, using low-temperature EPR spectroscopy. It was found that in a fraction of reaction centres the properties of the semiquinone-iron acceptor complex (Q_AFe^{2+}) were modified irreversibly after double reduction of Q_A: 1) this fraction was found to be more susceptible to double reduction of its Q_A by dithionite or ascorbate; 2) it did not form the $Q_A^-Fe^{2+}$ state upon low temperature illumination; 3) its (non-heme) Fe^{2+} could not be oxidised, using ferricyanide, to give the usual (EPR detectable) Fe^{3+} state. From these observations, it is suggested that a loss of Fe^{2+} from the Q_AFe^{2+} site is at the origin of the irreversibility. Preliminary iron-reconstitution experiments showed a somewhat increased degree of reversibility.

Introduction

In previous work, the double reduction of the quinone electron acceptor Q_A in the Photosystem II (PSII) reaction centre has been shown to significantly influence primary reaction centre photochemistry [1-3] (see Refs. [4-6] for reviews on the primary reaction centre photochemistry of PSII).

In Ref. [1], such an influence was reported on the properties of the reaction centre triplet state, a state which can be formed after the primary charge separation reaction (see [7] for a review on the reaction centre triplet state). A dramatic increase of the amplitude of the reaction centre triplet EPR signal was observed at cryogenic temperatures, upon double reduction of Q_A [1]. Recent low temperature flash absorbance measurements [3] have indicated that this is due to an increase in the lifetime of the triplet, from microseconds if Q_A is singly reduced to milliseconds if Q_A is doubly reduced.

In the low-temperature optical work an influence of the double reduction of Q_A was also found on the lifetime of the pair of radicals which is formed after the primary charge separation (the primary radical pair, see [4-6]). In addition, time-resolved fluorescence measurements at ambient temperature [2] indicated that the rate of charge separation as well as the lifetime of the primary radical pair increase upon double reduction of Q_A. This is supported by flash absorption measurements at ambient temperature [8,9].

The exact mechanism(s) relating the redox state of Q_A to the radical pair and triplet kinetics is (are) not clear at present. The primary radical pair state has been proposed to be influenced by electrostatic [10] and magnetic (at least in purple bacteria [11-14]) interactions with the semiquinone-iron complex (see also [1-3]). Changes in these interactions may be involved in the mechanism by which the Q_A state influences the primary radical pair state. Such interactions may also explain the dependence of the lifetime of the reaction centre triplet state on the redox state of Q_A (see [3]). With respect to a possible electrostatic

influence on the triplet lifetime, we mention that a significant influence of an external electric field on the triplet lifetime has been reported in purple bacteria [15]. Finally, based on in vitro work (e.g. [16]), it is unlikely that the triplet lifetime is directly influenced to a large extent by conformational changes associated with the double reduction of Q_A. However, such influences on the rates of formation and decay of the primary radical pair can not be ruled out (see [1-3]).

The reversibility of the Q_A double reduction has also been checked previously [2]. It was found that only in a small part of the reaction centres, reversibility is to the extent that the characteristic (formate-enhanced) $Q_A^-Fe^{2+}$ EPR signal (see [17]) is formed in its original state again, by dithionite addition. Nevertheless, time-resolved fluorescence measurements at ambient redox potentials, indicated a higher degree of reversibility [2]. The observations were explained by the Q_A site being destabilised in most of the reaction centres, not affecting its function at ambient potential, yet resulting in Q_A being more susceptible to double reduction by dithionite [2].

In this work, the reversibility of the Q_A double reduction was investigated in more detail.

Materials and Methods

PSII-enriched thylakoid membrane fragments were prepared from spinach as described earlier [18] using the modifications in Ref. [19]. Samples with doubly reduced Q_A [1,20] were prepared as described in Ref. [2], by incubation at room temperature in the dark, using 20 mM sodium dithionite and 100 μM benzyl viologen. Samples subjected to a complete double reduction and reoxidation cycle, in the following denoted as reversed samples, were prepared from the samples with Q_A doubly reduced as described in Ref. [2], (by washing out the dithionite with argon flushed buffer, followed by reoxidation with 5 mM ferricyanide, which was subsequently removed by washing).

Part of the reversed samples were used for treatment with $FeCl_2$. The samples were diluted in a buffer containing 50 mM Mes (pH 5.5), 300 mM sucrose and 10 mM NaCl, centrifuged and resuspended under argon in the same buffer, which previously had been made anaerobic by flushing with argon. Then, 10 mM $FeCl_2$ was added in near darkness under argon and the sample was incubated under these conditions for approximately two hours at room temperature. The chlorophyll concentration during the incubation was approximately 0.1 mg/ml. After the incubation, the sample was washed twice in the pH 5.5 buffer (argon flushed) and then twice in an (argon flushed) buffer containing 50 mM Mops (pH 7.0), 300 mM sucrose, 1 mM EDTA, 10 mM NaCl and 5 mM $MgCl_2$.

All experiments were done both on a control sample and on a reversed or $FeCl_2$-treated sample and calibrated EPR tubes were used. Samples were kept in the dark or near darkness unless otherwise stated. Before transferring them into the EPR tubes, samples were diluted into the pH 7.0 buffer (see above) to which 200 mM sodium formate had been added and were then concentrated to a chlorophyll concentration of 2 mg/ml, by centrifugation and resuspension in the pH

7.0-formate buffer. The chlorophyll concentrations were measured again at the end of the experiment.

For illumination of the samples at 198 K, the EPR tubes were submerged in a CO_2/ethanol bath. In incubation experiments, a control sample and a reversed or $FeCl_2$-treated sample were treated (frozen, thawed or incubated) pairwise in order to minimise differences in incubation conditions such as incubation-temperature.

EPR spectra were recorded using a Bruker 200 X-band spectrometer fitted with an Oxford Instruments cryostat and temperature control system. In order to record spectra during illumination and for illuminations outside the EPR cavity, an 800 W tungsten projector was used. The light was filtered through 2 cm water and three Calflex (Balzers) heat filters.

Results and Discussion

Samples were treated with dithionite and benzyl viologen to completely doubly reduce all Q_A and then reoxidised by washing them in ferricyanide. After the treatment with ferricyanide, the (reversed) sample was brought back to ambient redox potential by washing it several times in buffer (see Materials and Methods).

At ambient redox potential, no triplet EPR signal was detected in the reversed sample nor in the control sample (not shown). This is what is usually observed in PSII preparations with an intact Q_A present (see [1,21]). It is an indication that Q_A functions normally in the reversed sample, at least at ambient potential. Another indication for a functional Q_A site at ambient potential in reversed samples has come from time resolved fluorescence measurements [2].

Chemical generation of $Q_A^-Fe^{2+}$

Despite the similar behaviour at ambient redox potentials, addition of ascorbate and subsequent incubation clearly showed that there is a difference between the reversed sample and the control sample. This is seen in Fig. 1a. The (small) $Q_A^-Fe^{2+}$ signal that is present under these redox conditions, is not the same size in the two samples, being bigger in the control sample. More significantly, a large triplet signal is seen in the reversed sample, whereas the control sample does not have a detectable triplet signal.

Similar observations were made in the presence of dithionite (Fig. 1b, Table IA). The signal size of the $Q_A^-Fe^{2+}$ signal is smaller in the reversed sample (25-30% of that in the control sample) and the triplet signal is considerably larger in the reversed sample. The size of the triplet signal in the reversed sample, induced by dithionite alone (after 1.5 hr incubation), was further increased by the addition of benzyl viologen, which also resulted in the complete disappearance of the $Q_A^-Fe^{2+}$ signal. In line with Ref. [1], these results indicate that 25-30% of the reaction centres in the reversed sample exhibit a $Q_A^-Fe^{2+}$ signal of normal size and shape, but no triplet signal. Triplet signals can only be

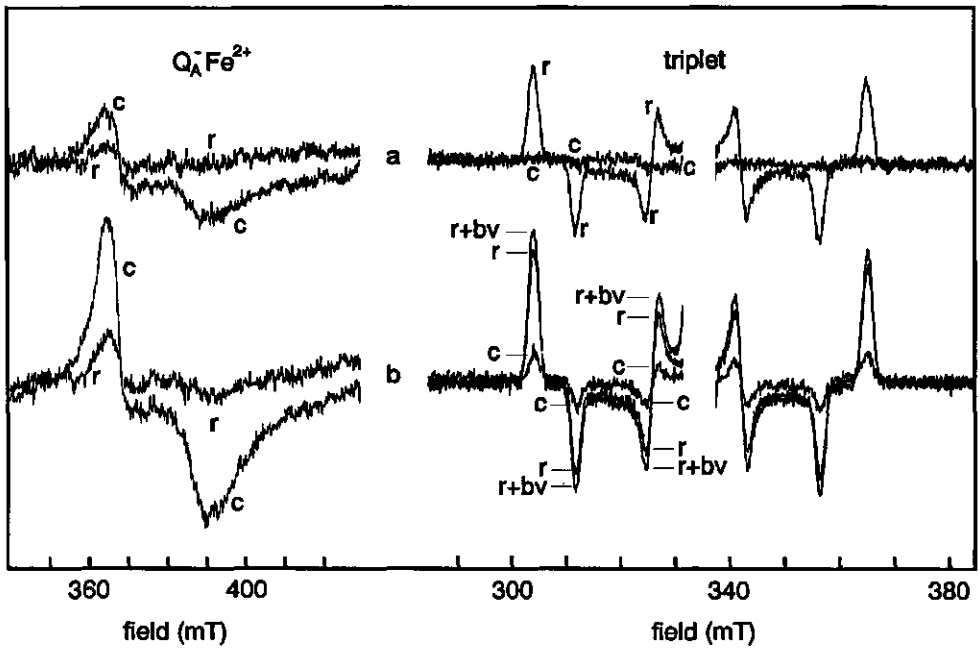

Fig. 1. $Q_A^-Fe^{2+}$ and reaction centre triplet signals from PSII-enriched membranes (2 mg Chl/ml) after different redox treatments (see text for details). The labelling of the traces is as follows: c, control sample; r, reversed sample. (a) Spectra recorded 1 hr after the addition of 10 mM ascorbate; (b) the same samples as in a) after an addition of 20 mM dithionite and an incubation of 1.5 hr (trace "r + bv" is recorded in the reversed sample after the subsequent addition of 100 μM benzyl viologen and an incubation of 2 hr). EPR conditions for the $Q_A^-Fe^{2+}$ spectra: temperature, 4.2 K; microwave power, 32 mW; microwave frequency, 9.44 GHz; modulation amplitude, 25 G. The triplet spectra were recorded under illumination; the EPR conditions were the same as for the $Q_A^-Fe^{2+}$ spectra except that the microwave power was 63 μW.

generated from these reaction centres after double reduction of Q_A, with a concomitant disappearance of the $Q_A^-Fe^{2+}$ signal.

In Ref. [2], an explanation was proposed for the relatively low $Q_A^-Fe^{2+}$ signal and high triplet signal in the presence of dithionite in the reversed sample. The explanation was that a large fraction of the reaction centres in the reversed sample is modified (as a result of the double reduction-reoxidation cycle) to the extent that Q_A is more easily doubly reduced by dithionite [2]. Thus, the high triplet signal in the presence of only ascorbate indicates that Q_A is partly doubly reduced under these conditions in the reversed sample. Ascorbate-induced formation of semiquinone Q_A as a free radical signal at around g = 2 was not observed by EPR, which is consistent with the idea of double reduction by ascorbate.

From the observations under reducing conditions, clearly the reversibility is found to be less than 100 %. Nevertheless, a fraction of the reaction centres (25% -30%) in the reversed samples behaves identically to the control sample: its

$Q_A^-Fe^{2+}$ signal has the usual form [17], it is relatively stable in the presence of dithionite (see Table IA) and it does not give rise to an EPR triplet signal (benzyl viologen addition was needed to reach the maximum triplet amplitude). The latter observation is an indication that the Q_A double reduction-induced increase in triplet lifetime [3] is reversible. This is probably also the case for the other changes in the kinetics of primary reaction centre photochemistry observed upon double reduction of Q_A (see Introduction, [1-3]). The lack of reversibility seems to be attributable to a modification of the properties of the Q_AFe^{2+} acceptor complex as a result of the double reduction-reoxidation cycle. In this respect, we mention that some evidence has been reported [31] for a lowered binding affinity of Q_A after it having been in the doubly reduced state, which is also indicative of modifications at the $Q_A^-Fe^{2+}$ site.

In the present work the percentage of reversibility, as monitored with the dithionite-induced $Q_A^-Fe^{2+}$ formation, is somewhat higher than that in Ref. [2]. It is our experience that the degree of reversibility is dependent on the conditions used for the double reduction, such as the incubation time in the presence of dithionite and benzyl viologen (see also [1,20,22]). Also the conditions during reoxidation may play a role.

Formation of $Q_A^-Fe^{2+}$ by low temperature illumination

The apparently normal functioning of Q_A in reversed samples at ambient redox potentials was further investigated in an experiment in which the formation of the $Q_A^-Fe^{2+}$ state by low temperature photoreduction was checked. Both a control and a reversed sample were illuminated at 200 K for 4 min and Fig. 2 shows the results. The amplitude of the $Q_A^-Fe^{2+}$ signal in the reversed sample was measured to be 25-30% of that of the control sample (see Table IA). This indicates that low temperature charge separation is inhibited in part of the reversed sample. It is supported by the fact that photoinduced EPR signals from the electron donor side such as the S_2 multiline signal, signals from cytochrome *b*-559^+, Chl^+ (reviewed in [23]) and possibly tyr D^+ [24], were smaller than those in the control sample (not shown).

The electron donation rates at low temperature might be different in control and reversed samples due to the different treatments. If electron donation in the reversed sample were slow, the 25-30% difference between control and reversed sample observed after 4 min illumination at 200 K could be due to this instead of being due to modification of the Q_A site. However, we also mea-

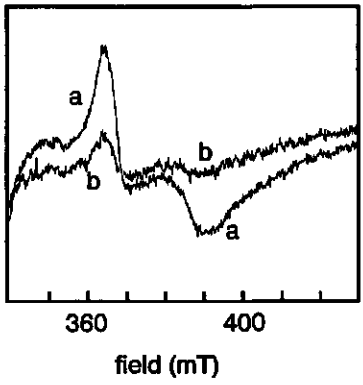

Fig. 2. $Q_A^-Fe^{2+}$ signals recorded after 4 min illumination at 198 K. 0.5 mM PPBQ was added prior to freezing. Spectra before illumination showed no $Q_A^-Fe^{2+}$ signals. (a) Control sample; (b) reversed sample. EPR conditions were as described for Fig. 1.

sured the response to the illumination time at 200 K in both samples and it was found to be similar in the two samples (not shown). Thus, the value of 25-30 % is not thought to be an underestimation due to a slower low temperature electron donation rate in the reversed sample.

The value of 25-30% found in the 200 K illumination experiment is close to the percentage of reversibility as measured by chemical reduction (see above and Table IA). Most likely, the reaction centres incapable of $Q_A^-Fe^{2+}$ formation under illumination at 200 K, are also those which have an increased susceptibility to chemical double reduction of Q_A. Nevertheless, at ambient temperature and redox potential, Q_A seems to be functionally active [2].

Oxidation of the non-heme iron

It is possible, in PSII, to oxidise the non-heme iron to its ferric form (Fe^{3+}) by dark incubation in the presence of ferricyanide (reviewed in [25]). The presence of Fe^{3+} can be detected by EPR as signals at around g = 8 and g = 5.5 (see [23]). Fig. 3a shows the EPR spectrum in this field region for the control sample incubated with ferricyanide. There is indeed a broad signal present at g = 8 and possibly also at around g = 5.5, but they are hard to distinguish from other background signals due to impurities in the sample. Fe^{3+} can be rereduced to Fe^{2+} by illuminating the sample at ambient or cryogenic temperatures and the best way to see the EPR signals from the PSII Fe^{3+} is in a dark-minus-light spectrum, Fig. 3c: two peaks are visible, at g = 8 and g = 5.6 respectively.

In addition to the $Q_A^-Fe^{2+}$ photoreduction experiments, we performed experiments to check whether Fe^{3+} can act as an electron acceptor in the reversed sample. Fig. 3b shows the spectrum from the reversed sample plus ferricyanide, before illumination. A signal at g = 8, similar to that in the control (Fig. 3a) is not seen. There is also no trace of a signal at g = 5.6. As in the control sample, baseline problems are greatly diminished in a dark-minus-light spectrum (Fig. 3d). Consistent with their absence in the spectrum before illumination, no significant signals at g = 8 or g = 5.6 are observed in the dark-minus-light spectrum. Apparently, the extent of iron oxidation is very small in the reversed sample.

The absence of an oxidisable iron in the reversed sample is an observation which may explain the lack of reversibility found in the present work and Ref. [2]. In purple bacteria it is known that if the iron is absent, Q_A may be functionally active but is doubly reduced upon dithionite addition [26]. By analogy, the fact that our reversed PSII samples are more susceptible to double reduction of Q_A upon dithionite or ascorbate addition may be explained by the absence of the iron. Thus the loss of the iron could be the irreversible modification occurring during the double reduction-reoxidation cycle leading to lack of reversibility. Because of the dependence of reversibility after double reduction of Q_A on the incubation time under reducing conditions (see above), the loss of the iron might be described by a relatively slow process which can only take place in the presence of doubly reduced Q_A. The sequence of events

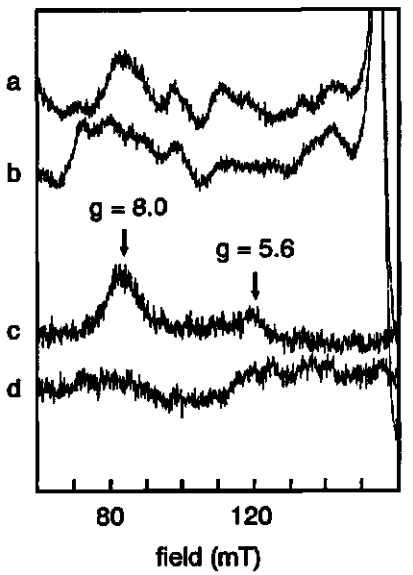

Fig. 3. EPR spectra in the low-field region. The samples were incubated in the presence of 4 mM ferricyanide for approximately 1 hr prior to freezing. (a) Control sample before illumination; (b) reversed sample before illumination; (c) control sample, difference spectrum (before illumination minus after illumination); (d) reversed sample, difference spectrum as in c). EPR conditions were as described for $Q_A^-Fe^{2+}$ spectra (see Fig. 1) except that the modulation amplitude was 32 G.

in the present set of experiments (subsequent double reduction, reoxidation and rereduction treatments) may then be summarised as follows: 1) double reduction (and double protonation [1,2]) of Q_A in an intact PSII membrane sample induced by dithionite and benzyl viologen; 2) loss of the iron from its binding site due to a changed conformation in the presence of doubly reduced Q_A; 3) reoxidation of Q_A induced by ferricyanide, resulting in a functionally active Q_A site at room temperature, but an inhibited low-temperature photoreduction in those reaction centres from which the iron was lost; 4) double reduction of Q_A induced by dithionite or ascorbate (with no need for benzyl viologen to be present), in the reaction centres lacking the iron.

It should be pointed out that based on the above data, we cannot rule out the possibility that the iron in fact remains bound to the PSII reaction centre, but has modified properties giving rise to either a reduced oxidisability or a modified (broader) Fe^{3+} EPR signal, which is more difficult to detect. In any case, a conformational change, occurring upon double reduction (and protonation [1,2]) of Q_A, is most likely the trigger for the changed properties of the iron. To what extent the same conformational change may also be responsible for the changed kinetics of charge separation and lifetime of the primary radical pair [1-3], remains to be clarified.

A simultaneous loss of oxidisability of the iron and the loss of ability to form $Q_A^-Fe^{2+}$ has also been observed in recent photoinhibition-type experiments [27]. This is an indication that also under the particular photoinhibitory conditions used in Ref. [27] (aerobic, both in the presence and absence of an artificial electron acceptor), double reduction of Q_A could be an intermediate step, preceding a modification of the properties of the iron (possibly its loss from the site). It has been suggested before that double reduction of Q_A occurs under photoinhibitory conditions [1] and this has been the subject of several subsequent studies (e.g. [22,28]). It is worth pointing out that the modification (possibly absence) of the iron after double reduction and subsequent reoxidation of Q_A may be related to the block in electron transfer from Q_A to Q_B, observed in some types of photoinhibition experiments (see e.g. [29]).

Table I, the reversibility of the double reduction as measured by the size of the $Q_A^-Fe^{2+}$ signal, induced chemically or photochemically. The ascorbate (asc.) concentration was 10 mM and the dithionite (dith.) concentration was approximately 20 mM.

	A, reversed sample vs. a control sample			B, reversed, $FeCl_2$ treated, sample vs. a control sample		
incubation or illumination conditions	control (rel. units)	reversed sample (rel. units)	reversed sample (% of control)	control (rel. units)	reversed sample (rel. units)	reversed sample (% of control)
1 hr asc. incubation	799	208	26	-	-	-
2.5 min dith. incubation	1773	565	32	-	-	-
4 min dith. incubation	-	-	-	1658	549	33
8.5 min dith. incubation	2021	531	26	-	-	-
0.5 hr dith. incubation	1868	527	28	-	-	-
1 hr dith. incubation	-	-	-	2317	919	40
1.5 hr dith. incubation	1966	512	26	-	-	-
13 min 5 K illumination	600	158	26	-	-	-
4 min 198 K illumination	1232	324	26	-	-	-
8 min 198 K illumination	-	-	-	1363	559	41

Finally, it should be mentioned that loss of the quinone from the Q_A site has been suggested to occur after double reduction of Q_A [1,30,31]. Although in Ref. [31], some evidence is presented that the binding affinity for Q_A can be smaller after it has been in the doubly reduced state (see above), direct evidence for the loss of Q_A from the binding site is lacking. In fact, the fluorescence measurements in Ref. [2] indicate that at least after the treatment used in this reference (dark-incubation with dithionite and benzyl viologen), Q_A is functionally active at ambient redox potential.

Treatment of reversed samples with excess $FeCl_2$

The possibility that the iron leaves its binding site if Q_A is in the doubly reduced state led to the following preliminary experiments, in which we tried to improve reversibility by adding excess $FeCl_2$ to the ferricyanide treated (reversed) sample. The sample (from the same batch of which the results are shown in Figs. 1-3 and Table IA) was incubated in the dark, under argon for 2 hrs in the presence of 10 mM $FeCl_2$ which was subsequently removed by extensive washing (see Materials and Methods for more details).

The degree of reversibility of this sample was tested in the same way as before, by measuring the $Q_A^-Fe^{2+}$ EPR signal in the presence of dithionite or after 198 K illumination and precise comparison to a control sample. The experiment of photoreduction of the preoxidised non-heme iron could not be performed in this sample, because the baseline in the low field region showed large signals from unspecifically bound iron, which could not be removed by the washing.

The results of the $Q_A^-Fe^{2+}$ measurements are summarised in Table IB. It can be seen that the percentage of reversibility increased to approximately 40%. The fact that reversibility is increased by adding excess $FeCl_2$ to the sample supports our suggestion made above, that the iron was initially lost in part of the sample. However, further experiments are needed to fully prove the loss of the iron. If iron loss is indeed occurring after double reduction of Q_A, this would mean that this procedure would constitute a new selective method for removal of the iron from the reaction centre. Furthermore, no attempt has been made to optimise the procedure of $FeCl_2$ treatment. The reversibility of 40% may be further improved by adjusting the conditions (such as incubation time, temperature, pH etc.). Since iron loss possibly occurs in the doubly reduced state of Q_A, a useful approach may be to add the $FeCl_2$ under reducing conditions as well. Finally, based on the present work, procedures may be developed for replacement of the iron by other metals (as has been done in purple bacteria [32]).

References

1 Van Mieghem, F.J.E., Nitschke, W., Mathis, P. and Rutherford, A.W. (1989) Biochim. Biophys. Acta 977, 207-214. Chapter 3 of this work.
2 Van Mieghem, F.J.E., Searle, G.F.W., Rutherford, A.W. and Schaafsma, T.J. (1992) Biochim. Biophys. Acta 1100, 198-206. Chapter 4 of this work.
3 Chapter 8 of this work.
4 Van Gorkom, H.J. (1985) Photosynth. Res. 6, 97-112.
5 Hansson, Ö. and Wydrzynski, T. (1990) Photosynth. Res. 23, 131-162.
6 Renger, G. (1992) in Topics in Photosynthesis Vol 11 (Barber, J., ed.), pp. 45-100, Elsevier, Amsterdam.
7 Budil, D.E. and Thurnauer, M.C. (1991) Biochim. Biophys. Acta 1057, 1- 41.
8 Eckert, H.-J., Renger, G., Bernarding, J., Faust, P., Eichler, H.J. and Salk, J. (1987) Biochim. Biophys. Acta 893, 208-218.
9 Liu, B., Napiwotzki, A., Eckert, H.-J., Eichler, H.J. and Renger, G. (1993) Biochim. Biophys. Acta 1142, 129-138.
10 Schatz, G.H., Brock, H. and Holzwarth, A.R. (1987) Proc. Natl. Acad. Sci. USA 84,

8414-8418.
11 Vidal, M.H., Setif, P. and Mathis, P. (1986) Photosynth. Res. 10, 347- 354.
12 Van Wijk, F.G.H., Gast, P. and Schaafsma, T.J. (1986) Photobiochem. Photobiophys. 11, 95-100.
13 Van Wijk, F.G.H., Gast, P. and Schaafsma, T.J. (1986) FEBS Lett. 206, 238-242.
14 Hore, P.J., Hunter, D.A., Van Wijk, F.G.H., Schaafsma, T.J. and Hoff, A.J. (1988) Biochim. Biophys. Acta 936, 249-258.
15 Franzen, S. (1992) Ph.D. Thesis, Stanford University.
16 Kleibeuker, J.F., Platenkamp, R.J. and Schaafsma, T.J. (1978) Chem. Phys. Lett. 27, 51-64.
17 Vermaas, W.F.J. and Rutherford, A.W. (1984) FEBS Lett. 175, 243-248.
18 Berthold, D.A., Babcock, G.T. and Yocum, C.F. (1981) FEBS Lett. 134, 231-234.
19 Ford, R.C. and Evans, M.C.W. (1983) FEBS Lett 160, 159-164.
20 Rutherford, A.W., Zimmermann, J.L. and Mathis, P. (1984) Advances in Photosynth. Res. (Sybesma C. ed) Vol 1 pp 445-448 Martinus Nijhoff, Dordrecht.
21 Evans, M.C.W., Atkinson, Y.E. and Ford, R.C. (1985) Biochim. Biophys. Acta 806, 247-254.
22 Vass, I., Styring, S., Hundall, T., Koivuniemi, A., Aro, E.-M. and Andersson, B. (1992) Proc. Natl. Acad. Sci. USA 89, 1408-1412.
23 Miller, A.-F. and Brudvig, G.W. (1991) Biochim. Biophys. Acta 1056, 1- 18.
24 Boussac, A. (1993) Pers. Comm.
25 Diner, B.A. and Petrouleas, V. (1987) Biochim. Biophys. Acta 895, 107- 125.
26 Dutton, P.L., Prince, R.C. and Tiede, D.M. (1978) Photochem. Photobiol. 28, 939-949.
27 Gleiter, H.M., Nugent, J.H.A., Haag, E. and Renger, G. (1992) FEBS Lett. 313, 75-79.
28 Vass, I and Styring, S. (1993) Biochemistry 32, 3334-3341.
29 Kirilovski, D., Vernotte, C., Astier, C. and Etienne, A.-L. (1988) Biochim. Biophys. Acta 933, 124-131.
30 Styring, S., Virgin, I., Ehrenberg, A. and Andersson, B. (1990) Biochim. Biophys. Acta 1015, 269-278.
31 Koivuniemi, A., Swiezewska, E., Styring, S., Aro, E.-M. and Andersson, B. (1992) EBEC Short Reports, Vol. 7, p. 6, Elsevier, Amsterdam.
32 Debus, R.J., Feher, G. and Okamura, M.Y. (1986) Biochemistry 25, 2276- 2287.

Chapter 6

A chlorophyll tilted 30° relative to the membrane in the Photosystem II reaction centre

F.J.E. van Mieghem [1,2], K. Satoh [3] and A.W. Rutherford [1]

[1] *Section de Bioénergétique, Département de Biologie Cellulaire et Moléculaire, CE Saclay, Gif-sur-Yvette (France),*
[2] *Department of Molecular Physics, Agricultural University, Wageningen (The Netherlands) and* [3] *Department of Biology, Faculty of Science, Okayama University, Okayama (Japan)*

(Received 24 January 1991)

Key words: Triplet state; EPR; Photosynthesis; Primary electron donor

The orientation properties of the reaction centre triplet in Photosystem II (PS II) were determined. A high triplet yield was generated in PS II membranes by double reduction of the primary quinone electron acceptor Q_A. It is deduced that the triplet state is localised on a chlorophyll, the tetrapyrrolic plane of which is tilted at 30° to the membrane. A similar orientation was found in D1/D2/cyt *b*-559 particles demonstrating that the triplet is confined to the reaction centre. Optical work in the literature has been interpreted as indicating that the triplet is localised on a monomeric chlorophyll and that, in the singlet state, P680 consists of this molecule weakly coupled to a second chlorophyll. The weakness of the coupling, compared to the coupling in the special pair of purple bacteria, allows P680 to be considered as a monomer. Taking the optical data into account, we propose that P680 is a chlorophyll molecule oriented at 30° to the membrane. This result is discussed in terms of the structural analogy between PS II and the reaction centre of purple bacteria. A model is favored in which P680 is a chlorophyll, structurally analogous to one of the monomeric bacteriochlorophylls of the bacterial reaction centre. In addition, the orientation data indicate that this chlorophyll is rotated by 45° in its ring plane compared to the monomeric bacteriochlorophylls in the reaction centre of *Rhodopseudomonas viridis*.

Introduction

The reaction centre of purple bacteria consists of three subunits, H, L and M. The primary photochemical reactions take place in the L and M subunits that form a heterodimer. They bind several pigments: four bacteriochlorophylls, two bacteriopheophytins, two quinones and additionally one iron atom. Most species also bind a carotenoid molecule. The crystal structure of the reaction centre from *Rhodopseudomonas viridis* and *Rhodobacter sphaeroides* have been resolved and an almost symmetrical distribution of these components over the L M heterodimer was shown (reviewed in Refs. 1, 2).

After excitation of the reaction centre with light, a radical pair is formed within a few picoseconds: the positive charge is distributed over a pair of bacteriochlorophylls known as the special pair and the negative charge is located on a bacteriopheophytin on the L side of the reaction centre. In reaction centres where the quinone acceptor Q_A is present, electron transfer from the bacteriopheophytin anion to Q_A occurs in 200 ps. When this electron transfer step is blocked, spin dephasing and then charge recombination of the radical pair can occur, transiently forming a triplet state on the special pair of bacteriochlorophylls (reviewed in Ref. 3).

The special pair is located on the symmetry axis of the reaction centre; the two bacteriochlorophylls have their ring planes almost parallel to this symmetry axis, which means that they are perpendicular to the membrane. There are two monomeric bacteriochlorophylls that are located between the special pair and the

Abbreviations: Q_A, the first quinone electron acceptor; PS II, Photosystem II; P680, the primary electron donor in PS II; PS I, Photosystem I; Chl, chlorophyll; Bchl, bacteriochlorophyll.

Correspondence: A.W. Rutherford, Section de Bioénergétique, Département de Biologie Cellulaire et Moléculaire, CE Saclay, 91191 Gif-sur-Yvette Cedex, France.

bacteriopheophytins, on each side of the symmetry axis. From its position, it seems likely that the monomer on the L side is involved in the electron transfer [1,2]; whether or not it acts as a true electron acceptor is still under debate [4,5].

On the basis of spectroscopic data, there are thought to be many similarities in structure and function between purple bacteria and PS II (reviewed in Refs. 6–8). Based on the similarities of amino acid sequences between D_1 and D_2 in PS II and the L and M subunits in bacteria, a specific folding model for the PS II reaction centre was proposed [9–11]. The proposal that D_1 and D_2 make up the reaction centre was supported by some biochemical evidence (e.g. [12]), but was established by the isolation of a PS II reaction centre core made up of only D_1, D_2, cytochrome *b*-559 [13]. The validity of the folding model was established by site-directed mutagenesis experiments [14,15].

From amino acid sequence comparisons it is clear that the histidines that are the axial ligands to the bacteriochlorophylls of the special pair in purple bacteria, are conserved in PS II [9,10]. It thus seems probable that there is at least a structural equivalent of the bacterial special pair in PS II. It is not clear, however, whether structural equivalents of the monomeric bacteriochlorophylls exist in PS II. In purple bacteria these have histidine residues as axial ligands, each of which is located at the end of a helix that is parallel to the membrane (the so called CD helix) [1], but these histidines are absent in PS II [9,10]. However, in *Rb. capsulatus*, these histidines have been replaced by several other amino acids using site-directed mutagenesis. A preliminary analysis of these mutants indicated that axial histidines are not required for binding of the monomeric bacteriochlorophylls to the reaction centre (reviewed in Ref. 16). Therefore, the fact that histidines in the predicted CD helix of PS II are absent, does not argue against the presence in PS II of monomeric chlorophylls, which are structurally analogous to those in the bacterial reaction centre. Moreover, the existence of a monomeric chlorophyll on the active side of the reaction centre might be predicted on theoretical grounds, based on the rate of electron transfer [17].

From orientation studies of the PS II triplet EPR signal, it was concluded that the triplet at liquid helium temperatures is localised on a chlorophyll molecule, the ring plane of which is oriented approximately parallel to the membrane [18,19]. This is one of the most striking spectroscopic differences between PS II and purple bacterial reaction centres, since, in the latter, the triplet resides on the pair of bacteriochlorophylls which are perpendicular to the membrane [20,21]. Also, in all other types of photosynthetic reaction centres, PS I, green sulphur bacteria and heliobacteria, the triplet is localised on (bacterio)chlorophylls which are perpendicular to the membrane plane, as in purple bacteria [22–24]. It was possible to interpret the orientation data on the triplet of PS II in the context of a strict structural analogy between PS II and purple bacteria by assuming that, in PS II, the triplet is localised on a structural equivalent of one of the monomeric bacteriochlorophylls. In this model the triplet was envisaged either (1) as being transferred from P680 to this chlorophyll monomer [6] or (2) the monomer could be P680 itself [25].

The original orientation experiments were done with preparations in which Q_A was prereduced to block further electron transfer after charge separation [18,19]. It is now known, however, that the presence of Q_A^- almost completely suppresses triplet formation in PS II [26]. By doubly reducing Q_A, the triplet yield can be increased drastically. This effect was attributed to a low yield of the primary radical pair when Q_A^- is present, due to a repulsive coulombic interaction between this radical pair and Q_A^- [26] (see also Refs. 27, 28). When Q_A is doubly reduced, it presumably loses its negative charge by protonation, resulting in an increase of the triplet yield. Similarly, complete removal of Q_A results in a high triplet yield as seen in the D_1/D_2/cyt *b*-559 preparation [29]. Since the conditions under which the triplet can be generated are better understood, we are now able to make oriented PS II samples having triplet signals with a much greater intensity than in earlier work. Two types of preparations with increased triplet yield were used: PS II membranes with Q_A doubly reduced [26] and a reaction centre preparation with Q_A absent [13]. Thus, we were able to obtain much more precise orientation data on the reaction centre triplet.

Materials and Methods

PS II-enriched thylakoid membrane fragments were prepared from spinach as described earlier [30] using the modifications in Ref. 31. In order to doubly reduce Q_A, the membranes were maintained in the dark for several hours at a redox potential of approx. −400 mV, under argon, in the presence of approx. 2 mM sodium dithionite [26]. In addition, 5 mM Mops (pH 7.0), 1 mM EDTA and 50 μM benzyl viologen [26] were present. The samples were then spread under argon onto mylar sheets and dried in an 80% humidity, argon atmosphere in the dark at 4°C, for approx. 24 h [32]. D_1/D_2/cyt *b*-559 particles [13] were resuspended in water, directly spread onto mylar sheets and dried in the same way as the membranes, except that a pyrogallol oxygen trap was present in the drying vessel.

Several of the mylar sheets were put into EPR tubes and a 70% glycerol solution containing approx. 100 mM sodium dithionite and 200 mM glycine (pH 10) was added. In some experiments 150 mM Mops (pH

7.0) was used instead of 200 mM glycine. After 5 min dark incubation, the samples were frozen and spectra were recorded at different orientations of the mylar sheets relative to the EPR magnetic field [32]. For the D_1/D_2/cyt *b*-559 particles data were recorded first in the absence of dithionite. Under these conditions, identical data for triplet orientation were recorded but in addition, data on oxidised cytochrome *b*-559 were also obtained.

EPR spectra were recorded using a Bruker 200 X-band spectrometer fitted with an Oxford Instruments cryostat and temperature control system. In order to record spectra during illumination an 800 W tungsten projector was used. Illumination was performed through the cavity window with the light beam perpendicular to the magnetic field. Infrared radiation was diminished by using a 2 cm water filter and three calflex (Balzers) heat filters.

Results

Oriented PS II membranes with Q_A doubly reduced

It is possible to doubly reduce Q_A in PS II membranes by incubating them under strongly reducing conditions (see Materials and Methods for details). The samples, pretreated in this way, were oriented on mylar strips as described in Materials and Methods. The triplet state can be detected under illumination at liquid helium temperature with EPR [33]. A very intense triplet EPR signal was observed as in Ref. 26. The triplet spectra (Fig. 1a) showed an AEEAAE polarisation pattern and *D* and *E* values of 0.0286

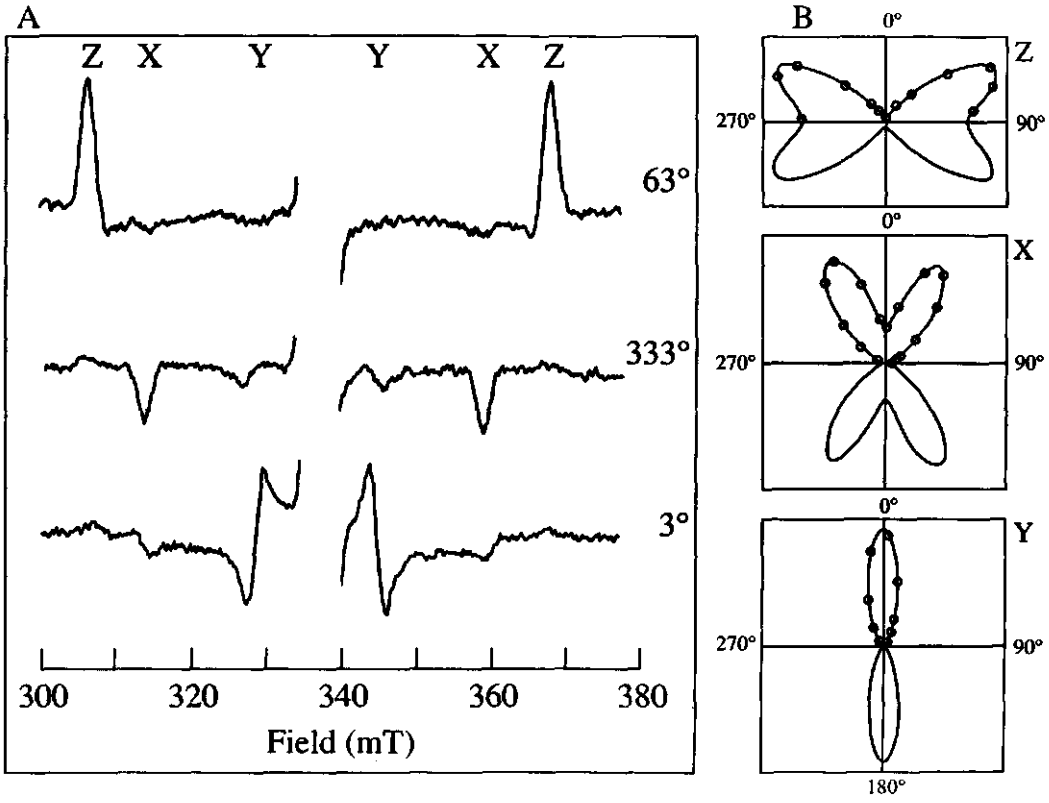

Fig. 1. (A) Orientation dependence of the light-induced PS II reaction centre triplet EPR signal in PS II membranes with Q_A doubly reduced; the sample was reduced with sodium dithionite (see Materials and Methods for details on sample preparation). The figure shows spectra recorded close to the orientation maximum for each of the triplet peaks; the angle between the magnetic field and the plane of the mylar sheets is indicated for each spectrum. The spectra were recorded during illumination with the following instrument settings: temperature, 4.4 K; modulation amplitude, 25 G; gain, $1 \cdot 10^5$; microwave power, 35 dB (63 μW); microwave frequency, 9.434 GHz. (B) Normalised polar plots of the orientation dependence of the Z, X and Y triplet peaks, obtained under the conditions outlined under A.

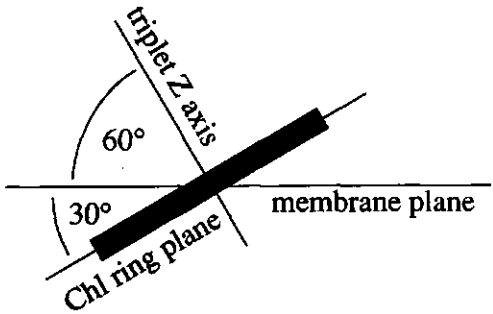

Fig. 2. A schematic drawing (side view) showing the orientation of the chlorophyll on which the triplet state is localised in PS II. The triplet Z axis makes an angle of 60° with the membrane plane, as reported in this work, and is perpendicular to the ring plane of the chlorophyll [36]. The ring plane, therefore, is oriented at 30° with respect to the membrane.

cm^{-1} and 0.0044 cm^{-1} respectively. These are characteristics of the reaction centre triplet of PS II [33,34]. When the angle between the mylar strips and the magnetic field was varied, the amplitudes of the triplet peaks showed a marked orientation dependence. This is shown as polar plots in Fig. 1b.

The triplet Z, X and Y peaks showed maxima at angles of 63°, 30° and 0°, respectively between the plane of the mylar strips and the magnetic field. The orientation dependence of the Z peaks was slightly less well resolved and this may be due to a specific increase in light penetration of the sample when the beam was parallel to the mylar strips (i.e., when the strips were 90° to the magnetic field). This would result in a distortion of the orientation dependence due to an increased Z peak signal amplitude at this orientation. The other peaks are essentially unaffected since they have almost zero intensity at this orientation.

It is also possible to calculate the orientation maximum of the Z peaks from those of the X and Y peaks, using the relationship [35]:

$$\sum_i \cos^2(90° - \alpha_i) = 1 \qquad (1)$$

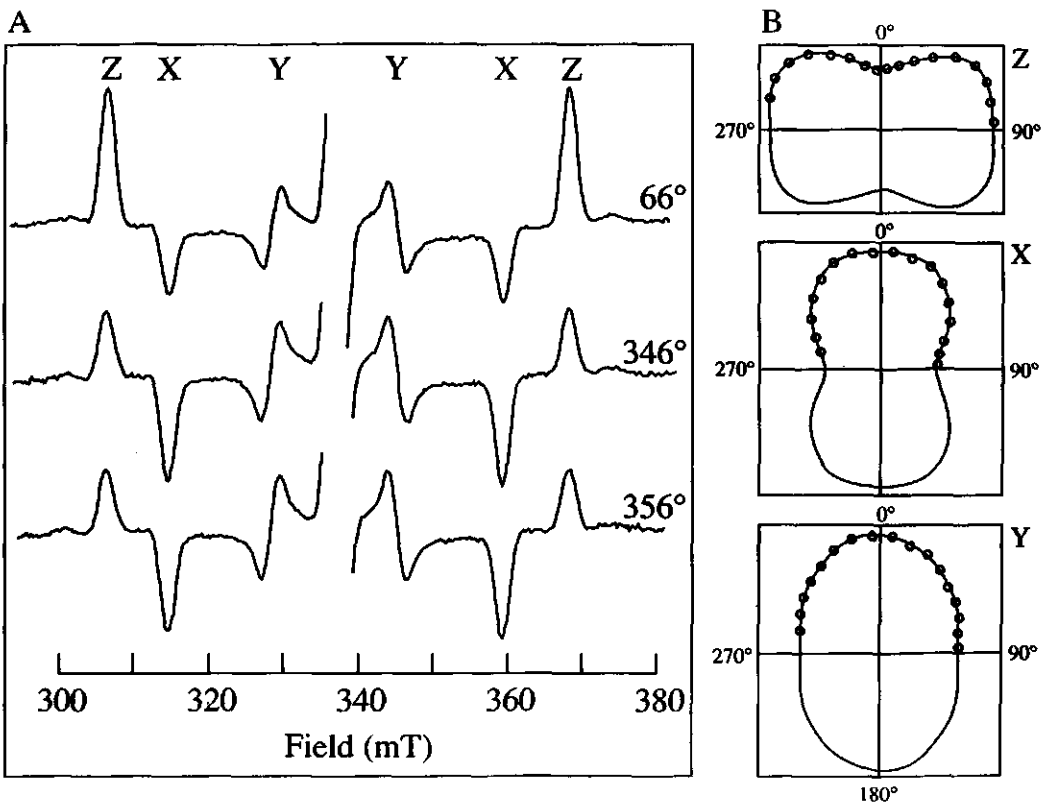

Fig. 3. (A) Orientation dependence of the light-induced PS II reaction centre triplet EPR signal in D_1/D_2/cyt *b*-559 particles. Sample conditions and instrument settings were as described in the legend to Fig. 1, except that the gain was $5 \cdot 10^4$. (B) Normalised polar plots of the three triplet peaks from D_1/D_2/cyt *b*-559 particles.

(where α_i is the orientation maximum for respectively the Z, X and Y peak). This yields an angle of 60°, which we take as a more accurate value (±3°, estimated error). We conclude that the angles of the triplet Z, X and Y axes with the plane of the thylakoid membrane are respectively 60°, 30° and 0°.

The triplet axis system of chlorophylls in vitro has previously been determined [36]. It was found that the triplet Z axis is perpendicular to the ring plane for all types of chlorophylls. Furthermore, we assume that the triplet is entirely located on a single chlorophyll, based on the monomeric *D* value [33,34], the triplet minus singlet spectrum [29,34,37,38] and the weakness of the coupling between the pigments in the PS II reaction centre [38–40]. Thus, we deduce that the ring plane of this chlorophyll is tilted at an angle of 30° relative to the plane of the membrane (see Fig. 2).

Oriented D_1/D_2/cyt b-559 particles

Due to the absence of Q_A in these particles, the triplet yield is high without preincubation under reducing conditions [29,41] (see Ref. 26). The samples were oriented on mylar strips in the same way as the PS II membranes (see above) and EPR spectra of the triplet state were taken during illumination at liquid helium temperature. Essentially the same spectral features as in PS II membranes were observed (Fig. 3a). Fig. 3b shows polar plots of the Z, X and Y peaks of the triplet in oriented D_1/D_2/cyt *b*-559 particles. Due to the fact that the particles were extracted from the membrane, the samples showed a less defined orientation dependence compared to PS II membranes. The orientation dependence of EPR signals from the oxidised cytochrome *b*-559 in these samples (not shown) was as in PS II membranes [18], confirming that the particles were oriented with the symmetry axis of the reaction centre perpendicular to the mylar plane. Despite the lower quality of the data, it is still observable that the orientation maximum for the Z peak deviates 20°–30° from 90°. This is consistent with the triplet residing on a chlorophyll molecule that is tilted approx. 30° out of the plane of the mylar, as found for oriented membranes.

Discussion

The data presented here confirm the earlier observations [18,19] that the reaction centre triplet of PS II has a different orientation compared to all other photosynthetic reaction centres. An orientation parallel to the membrane was reported for the ring plane of the chlorophyll on which the triplet was located, but the signal-to-noise in the earlier work was insufficient to allow this interpretation to be very precise. In the present study, the pretreatment of the sample allowed the triplet yield to increase by orders of magnitude. The signal to noise is correspondingly improved and it is now clear that the ring plane of the chlorophyll on which the reaction centre triplet is localised is tilted 30° out of the membrane plane.

The observation that the orientation dependence of the triplet in the isolated PS II reaction centre (D_1/D_2/cyt *b*-559) is the same as that in the unfractionated membranes, is a clear indication that the triplet resides on the same reaction centre chlorophyll molecule in both preparations. Furthermore, it is evident that the components involved in the primary reactions in the D_1/D_2/cyt *b*-559 preparation [13] are relatively intact.

In other types of photosynthetic reaction centres, the triplet state is localised on the primary electron donor. The triplet minus singlet spectrum [29,34,37,38], indicates that this is also the case in PS II. It was argued in Refs. 34, 37 and 38 that P680 comprises two excitonically coupled chlorophylls in the singlet state, but that the triplet was localised on only one of the chlorophylls (for a recent review of spectroscopy on P680 see Ref. 42). However, it is important to note here that all of the estimations in the literature for possible excitonic coupling between PS II reaction centre pigments (e.g., 40 cm^{-1} [38], 142 cm^{-1} [39] or 110 cm^{-1} [40]) are low compared to estimations for the coupling within the bacterial special pair (in the range of 600–1500 cm^{-1} [43,44]). In addition, the absence of a significant Stark effect, in contrast to the situation in purple bacteria [45,46], indicates that there are no contributions of charge transfer-states to the excited state [45]. Compared to the situation in the purple bacterial centre, these observations can be taken as indicating that all the pigments in the PS II reaction centre are essentially monomeric. Thus, P680 can be considered as a monomer, although weakly coupled with one or more nearby chromophores. The close resemblance between the $P680^+$ minus P680 spectrum and the ^{3}P680 minus P680 spectrum [38] suggests that the triplet state and the positive charge are both localised on the same chlorophyll. If this is the case, this chlorophyll can be considered to be P680 and from the present work, it is oriented at 30° with respect to the membrane plane.

How then should this result be considered in light of the expected structural analogy between PS II and the purple bacterial reaction centre? If, as seems appropriate, we attempt to apply the analogy as strictly as possible, further useful insights on the nature of P680 can be gained. In the following we discuss two different models for the organisation of the P680 region in PS II, in which a major criterion is the maintenance of the structural analogy.

In the first model, two chlorophylls, which are structural analogues to the bacteriochlorophyll special pair, are present in PS II (as suggested by their conserved

histidines), but one of these is oriented at 30° rather than 90° to the membrane plane. Such an arrangement could result in a weaker coupling between the two chlorophylls, giving rise to essentially monomeric properties. However, different tilts of the chromophores of the PS II reaction centre, compared to their purple bacterial counterparts, inevitably imply differences in the protein folding. This seems unlikely in the region where the bacterial special pair is bound, because there, the homology between D_1 and D_2 and the L and M subunits is rather high.

In an alternative model, which was suggested earlier [25], P680 is a chlorophyll molecule structurally equivalent to one of the bacteriochlorophyll monomers of the bacterial reaction centre; two chlorophylls, which are structural analogues to the bacterial special pair, are present in PS II, but they are not the primary electron donor. This model is attractive since a 30° tilt of P680, apparent from the present work, is exactly that seen for the bacteriochlorophyll monomers [1] (see Table I). It is envisaged that the organisation of the chromophores (their positions and the tilts of their ring planes) and the folding of the protein in PS II are essentially the same as in the purple bacterial reaction centre, although different functional roles for some of the chromophores are imagined.

Table I shows orientation data for the monomeric bacteriochlorophylls, taken from the crystal structure of *Rps. viridis* [1], compared to orientation data for the chlorophyll on which the triplet is localised in PS II. It can be deduced that the triplet X and Y axes are rotated * approx. 45° clockwise or 135° counterclockwise within the ring plane, when compared to the directions of the optical transition moments of the bacterial monomers (for chlorophylls, the X and Y triplet axes correspond to the Q_x and Q_y transitions respectively [36]). The most straightforward interpretation for this is that a structural difference is present, involving a rotation of the chlorophyll ring in PS II compared to purple bacteria, while maintaining the 30° tilt of the ring plane. Such a rotational difference is not in contradiction with a close structural analogy between PS II and the purple bacterial reaction centre since it is not likely to have a large impact on the protein folding. It would only require replacement of amino acids in PS II that have close interactions with the chlorophyll and possibly slight modifications due to the phytyl chain taking a different position in the protein compared to purple bacteria. The proposed in-plane rotation could contribute to the functional differences proposed in this model for this chlorophyll, compared to its bacterial counterpart.

* When observing the reaction centre from the donor side.

TABLE I

Orientation of optical axes (Rps. viridis, monomeric bacteriochlorophylls) and triplet axes (PS II) with respect to the membrane

	X-axis	Y-axis	XY-plane
Rps. viridis, optical axes of the monomeric Bchls [a]			
L side	19°	21°	32°
M side	22°	23°	28°
PS II, triplet axes	30°	0°	30°

[a] From Ref. 1.

In order to explain the singlet minus triplet spectrum [29,34,37,38] in line with this model, we consider excitonic coupling to occur between a chlorophyll monomer (structurally analogous to one of the bacteriochlorophyll monomers of the bacterial reaction centre) and one or both of the chlorophylls which are structurally analogous to the constituents of the bacterial special pair. Couplings of 40 cm^{-1} [38], 142 cm^{-1} [39] or 110 cm^{-1} [40] are indeed in the range of the weak couplings which were calculated previously for the interaction of the bacteriochlorophylls of the special pair with the monomeric bacteriochlorophylls in the purple bacterial reaction centre [43,44]. The estimations of the magnitude of the coupling in the PS II reaction centre would also imply that there is only a small interaction in PS II between the structural equivalents of the bacterial special pair. This could occur even if the relative position and tilts of the ring planes are similar in both reaction centres [39] (see also Ref. 47) and thus would not involve major changes of the protein folding. However, the requirement for the structural analogue of the bacterial special pair to be decoupled in PS II in this model, is an ad hoc hypothesis which weakens the model somewhat.

In conclusion, of the two models discussed we favour the second, in which P680 is a chlorophyll molecule which is a structural analogue of one of the monomeric bacteriochlorophylls, because this more closely maintains in PS II the basic structural motif of the bacterial reaction centre.

Acknowledgements

We would like to thank R.E. Blankenship, J. Breton, P. Mathis, T. Mattioli, W. Nitschke, G.F.W. Searle, W.F.J. Vermaas, M.H. Vos and in particular T.J. Schaafsma for useful discussions. Thanks also to G. Renger for sending us a reprint of unpublished work. F.v.M. is supported by the EEC (SCIENCE N.P. Programme) and A.W.R. is suported by the CNRS (URA 1290).

References

1 Deisenhofer, J., Epp, O., Miki, K., Huber, R. and Michel, H. (1985) Nature (London) 318, 618–624.
2 Allen, J.P., Feher, J., Yeates, T.O., Komiya, H. and Rees, D.C. (1987) Proc. Natl. Acad. Sci. USA 84, 5730–5734.
3 Parson, W.W. and Ke, B. (1982) in Photosynthesis: energy conversion by plants and bacteria (Govindjee, ed.), pp. 331–385, Academic Press, New York.
4 Fleming, G.R., Martin, J.-L. and Breton, J. (1988) Nature (London) 333, 190–192.
5 Holzapfel, W., Finkele, U., Kaiser, W., Oesterhelt, D., Scheer, H., Stilz, H.U. and Zinth, W. (1990) Proc. Natl. Acad. Sci. USA 87, 5168–5172.
6 Rutherford, A.W. (1986) Biochem. Soc. Trans. 14, 15–17.
7 Rutherford, A.W. (1987) in Progress in Photosynth. Res. (Biggins, J., ed.), Vol. 1, pp. 277–283 Martinus Nijhoff, Dordrecht.
8 Mathis, P. and Rutherford, A.W. (1987) in New Comprehensive Biochemistry: Photosynthesis (Amesz, J., ed.), pp. 63–96, Elsevier, Amsterdam.
9 Trebst, A. (1986) Z. Naturforsch. 41c, 240–245.
10 Michel, H. and Deisenhofer, J. (1988) Biochemistry 27, 1–7.
11 Barber, J. and Marder, J.B. (1986) in Biotechnology and Genetic Engineering Reviews (Russel, M., ed.), Vol. 4, pp. 355–405, Intercept, Newcastle upon Tyne.
12 Metz, J.G., Bricker, T.M. and Seibert, M. (1985) FEBS Lett. 185, 191–196.
13 Nanba, O. and Satoh, K. (1987) Proc. Natl. Acad. Sci. USA 84, 109–112.
14 Debus, R.J., Barry, B.A., Babcock, G.T. and McIntosh, L. (1988) Proc. Natl. Acad. Sci. USA 86, 427–430.
15 Vermaas, W.F.J., Rutherford, A.W. and Hansson, Ö. (1988) Proc. Natl. Acad. Sci. USA 85, 8477–8481.
16 Coleman, W.J. and Youvan, D.C. (1990) Annu. Rev. Biophys. Biophys. Chem. 19, 333–367.
17 Moser, C.C., Keske, J.M., Warncke, K. and Dutton, P.L. (1991) Biophys. J. 59, 521a.
18 Rutherford, A.W. (1985) Biochim. Biophys. Acta 807, 189–201.
19 Rutherford, A.W. and Acker, S. (1986) Biophys. J. 49, 101–102.
20 Hales, B.J. and Gupta, A.D. (1979) Biochim. Biophys. Acta 548, 276–286.
21 Tiede, D.M. and Dutton, P.L. (1981) Biochim. Biophys. Acta 637, 278–290.
22 Rutherford, A.W. and Sétif, P. (1990) Biochim. Biophys. Acta 1019, 128–132.
23 Nitschke, W., Feiler, U. and Rutherford, A.W. (1990) Biochemistry 29, 3834–3842.
24 Nitschke, W., Sétif, P., Liebl, U., Feiler, U. and Rutherford, A.W. (1990) Biochemistry 29, 11079–11088.
25 Rutherford, A.W. (1988) in Light-Energy Transduction in Photosynthesis: Higher Plant and Bacterial Models (Stevens, S.E. and Bryant, D.A., eds.), pp. 163–177, The American Society of Plant Physiologists, Rockville.
26 Van Mieghem, F.J.E., Nitschke, W., Mathis, P. and Rutherford, A.W. (1989) Biochim. Biophys. Acta 977, 207–214.
27 Schatz, G.H., Brock, H. and Holzwarth, A.R. (1988) Biophys. J. 54, 397–405.
28 Schlodder, E. and Brettel, K. (1988) Biochim. Biophys. Acta 933, 22–34.
29 Takahashi, Y., Hansson, O., Mathis, P. and Satoh, K (1987) Biochim. Biophys. Acta 893, 49–59.
30 Berthold, D.A., Babcock, G.T. and Yocum, C.F. (1981) FEBS Lett. 134, 231–234.
31 Ford, R.C. and Evans, M.C.W. (1983) FEBS Lett. 160, 159–164.
32 Blasie, J.K., Erecinska, M., Samuels, S. and Leigh, J.S. (1978) Biochim. Biophys. Acta 501, 33–52.
33 Rutherford, A.W., Paterson, D.R. and Mullet, J.E. (1981) Biochim. Biophys. Acta 635, 205–214.
34 Den Blanken, H.J., Hoff, A.J. Jongenelis, A.P.J.M. and Diner, B.A. (1983) FEBS Lett. 157, 21–27.
35 Prince, R.C., Crowder, M.S. and Bearden, A. (1980) Biochim. Biophys. Acta 592, 323–337.
36 Thurnauer, M.C. and Norris, J.R. (1977) Chem. Phys. Lett. 47, 100–105.
37 Durrant, J.R., Giorgi, L.B., Barber, J., Klug, D.R. and Porter, G. (1990) Biochim. Biophys. Acta 1017, 167–175.
38 Van Kan, P.J.M., Otte, S.C.M., Kleinherenbrink, F.A.M., Nieveen, M.C., Aartsma, T.J. and Van Gorkom, H.J. (1990) Biochim. Biophys. Acta 1020, 146–152.
39 Tetenkin, V.L., Gulyaev, B.A., Seibert, M. and Rubin, A.B. (1989) FEBS Lett. 250, 459–463.
40 Braun, P., Greenberg, P.M. and Scherz, A. (1990) Biochemistry 29, 10376–10387.
41 Okamura, M.Y., Satoh, K., Isaacson, M.A. and Feher, G. (1987) in Progress in Photosynthesis Research (Biggins, J., ed.), Vol. 1, pp. 379–381, Martinus Nijhoff, Dordrecht.
42 Renger, G. (1991) in Topics in Photosynthesis (Barber, J., ed.), Vol. 11, Elsevier, Amsterdam, in press.
43 Knapp, E.W., Fischer, S.F., Zinth, W., Sander, M., Kaiser, W., Deisenhofer, J. and Michel, H. (1985) Proc. Natl. Acad. Sci. USA 82, 8463–8467.
44 Scherer, P.O.J. and Fischer, S.F. (1987) Biochim. Biophys. Acta 891, 157–164.
45 Lösche, M., Feher, G. and Okamura, M.Y. (1988) in The Photosynthetic Bacterial Reaction Center Structure and Dynamics (Breton, J. and Verméglio, A., eds.), pp. 151–164, Plenum Press, New York.
46 Lösche, M., Satoh, K., Feher, G. and Okamura, M.Y. (1988) Biophys. J. 53, 270a.
47 Pearlstein, R.M. (1982) in Photosynthesis: Energy Conversion by Plants and Bacteria (Govindjee, ed.), pp. 293–330, Academic Press, New York.

Chapter 7

Transient EPR spectroscopy of Photosystem II reaction centre photochemistry with nanosecond time resolution

F.J.E. van Mieghem [a,b], C.H. Bock [c], A.W. Rutherford [a] and D. Stehlik [c]

[a] *Section de Bioénergétique, CNRS URA1290, Département de Biologie Cellulaire et Moléculaire, CE Saclay, Gif-sur-Yvette (France),* [b] *Department of Molecular Physics, Agricultural University, Wageningen (Netherlands) and* [c] *Fachbereich Physik, Freie Universität Berlin, Berlin, (Germany).*

Key words: Chlorophyll; Photosynthesis; Primary electron donor; Radical pair state; Triplet state

The formation of the reaction centre triplet of Photosystem II (PSII) in oriented PSII membranes from spinach has been measured using time-resolved EPR at 4.2 K. This triplet state has its Z axis oriented at an angle of 60° with respect to the membrane as observed in EPR measurements under continuous illumination (Van Mieghem, F.J.E., Satoh, K. and Rutherford, A.W. (1991) Biochim. Biophys. Acta 1058, 379-385). We found that the triplet state with the 60° oriented Z axis is formed on an estimated time scale of 300 - 400 ns following a laser flash, significantly slower than the instrument response-time. Apart from the contributions from this (reaction centre) triplet state, we also found short-lived signal components with instrument-limited risetime and decaying within a microsecond. The time-resolved spectrum of the shortlived contributions does not fit with that of a reaction centre triplet; its exact origin remains unclear at present, but it is probably not related to the primary charge separation in the reaction centre.

Introduction

In the photosystem II (PSII) reaction centre, a (primary) radical pair is formed following the electron transfer from a chlorophyll *a* electron donor, P680, to a pheophytin (see [1,2] for reviews). If subsequent electron transfer to the (quinone) electron acceptor Q_A is blocked, charge recombination can result in the formation of the reaction centre triplet state [3].
From EPR measurements on oriented PSII samples it was concluded that the reaction centre triplet is located on a chlorophyll which is tilted 30° to the membrane plane [4] (see also [5,6]). This finding indicates a difference between

Abbreviations: Chl, chlorophyll; EDTA, ethylenediaminetetraacetate; Mops, 4-morpholinepropanesulphonic acid; P680, the primary electron donor in Photosystem II; PSII, Photosystem II; Q_A, the first quinone electron acceptor.

Correspondence: A.W. Rutherford, Section de Bioénergétique, CNRS URA1290, Département de Biologie Cellulaire et Moléculaire, CE Saclay, 91191, Gif-sur-Yvette Cedex, France.

PSII and reaction centres of purple bacteria (and also other types of photosynthetic reaction centres [7-9]), in which the triplet is located on chlorophylls oriented with their ring planes perpendicular to the membrane plane [10,11]. This difference between purple bacterial reaction centres and PSII as regards their triplet orientation has been discussed in detail: it can be fitted with models [4,12,13] involving a high structural analogy between the two types of reaction centres, as has been proposed on the basis of spectroscopic similarities (reviewed in [12-15]), and biochemical similarities (reviewed in [16-18], see also [19]). Thus, as a possible explanation for the triplet orientation in PSII, it has been proposed that the PSII triplet is formed by charge recombination on P680, oriented perpendicular to the membrane, followed by rapid transfer to a 30° oriented chlorophyll [12]. Note that the reaction centre of purple bacteria contains bacteriochlorophylls, oriented with their ring planes at 30° to the membrane [20,21]. In an alternative explanation, P680 itself was thought to be or to contain a 30° oriented chlorophyll [4-6,13].

The decay of the primary radical pair in PSII has been measured by optical spectroscopy at temperatures of 20 K and lower and lifetimes in the range of 100 ns to 300 ns have been reported [22-25]. This is within the time resolution, accessible to modern transient EPR techniques (see [26] for a review). Thus, the decay of the radical pair, the rise of the reaction centre triplet and a possible triplet transfer process as proposed in Ref. [12] are in principle measurable by transient EPR. In this work, we performed such measurements on oriented PSII membranes, in particular with the aim of looking for the triplet transfer proposed in Ref. [12].

Materials and Methods

PSII-enriched thylakoid membrane fragments were prepared as described earlier [27] using the modifications in Ref. [28]. Oriented samples with Q_A doubly reduced were prepared as described in Ref. [4] (see also [29]), by dark incubation at low redox potential (approximately -400 mV) in the presence of benzyl viologen, transfer to mylar strips followed by slow drying and subsequent submersion of the strips in a dithionite/glycerol solution in the EPR tube. A different (redox) type of oriented samples was also prepared, by drying on mylar of unreduced sample and subsequent submersion of the mylar in a solution containing 70% glycerol, approximately 100 mM sodium dithionite, 150 mM Mops (pH 7.0) and 2 mM EDTA, 5 min dark incubation and freezing. Despite the milder reduction treatment, this sample showed a significant reaction centre triplet signal [3] under continuous illumination, which is indicative of double reduction of Q_A [30]. This might be due to an increased susceptibility of Q_A to double reduction (see [30,31]) in dried samples, as compared to samples in suspension. By comparing the triplet amplitude under continuous illumination to that in (oriented) samples with all Q_A doubly reduced, the fraction of doubly reduced Q_A in the milder treated sample is estimated to be of the order of 50%.

Steady state EPR spectra were recorded using a Bruker 200 X-band spectrometer fitted with an Oxford Instruments cryostat and temperature control

system. To record spectra during illumination, an 800 W tungsten projector was used. Infrared radiation was diminished by using a 2 cm water filter and three Calflex (Balzers) heat filters.

Transient flash-induced EPR signals were measured using the experimental X-band set-up described in detail in Ref. [26]. Transients were recorded until 4 μs after the laser flash with a 10 ns sampling time. The repetition rate of the laser pulses (532 nm, pulse energies up to 15 mJ) was approximately 10 Hz. The instrument response time was determined to be approximately 100 ns by measuring the rise of the reaction centre triplet signal in a prereduced *Rb. sphaeroides* R-26 chromatophore sample.

Results and Discussion

PSII membranes were treated with dithionite and benzyl viologen in order to doubly reduce Q_A, which results in an overall slow-down of photochemical processes in the reaction centre [25]. The membranes were oriented parallel to strips of mylar and time-resolved EPR measurements were performed. A set of data was recorded for which the microwave absorption or emission was measured as a function of both time (after a laser flash) and magnetic field strength. In addition, the orientation of the membranes relative to the magnetic field was varied.

Fig. 1 shows some of the transient signals, taken at different field positions and orientation angles Θ (the angle between the magnetic field direction and the plane of the membranes). A general observation was that at two magnetic field positions, which were at equal distance from the g = 2 field position (325.5 mT under our conditions), the same transients were found, but with opposite amplitude. In Fig. 1, only transients of the low field part of the spectrum are shown. In several traces of Fig. 1, both positive and negative contributions are present and therefore they must be the composite of at least two transients: a fast one, being observed at short times after the flash, and a slower transient, remaining after the fast one has decayed. In Fig. 1a, Θ = 0° and in Fig. 1b, Θ = 0° and Θ = 45°, the fast transient seems to dominate the signal: a rise on a timescale of approximately 100 ns is seen and a decay back to zero in several hundreds of nanoseconds (estimated lifetime 600 - 700 ns). In the same way, the rise and the decay of the slow transient can be estimated from Fig. 1a, Θ = 90° and Fig. 1d, Θ = 0°: 300 - 400 ns and a few microseconds respectively. The observed risetime of 300 - 400 ns is significantly longer than the 100 ns instrumental response-time (see Materials and Methods).

Spectra, associated with the slow transient, were obtained by signal integration in the time interval 1 - 2 μs after the flash (digital boxcar spectrum) and also by fitting of the transients with appropriate rise and decay times. Fig. 2 shows spectra at three characteristic orientations, obtained by fitting. These were similar to boxcar spectra (not shown). The spectra have the characteristics of reaction centre triplet spectra (see [32] for a review and for a comparison of shapes of triplet spectra obtained using direct detection and using field modulation). The $|D|$ and $|E|$ values (0.029 cm^{-1} and 0.0044 cm^{-1}, respectively)

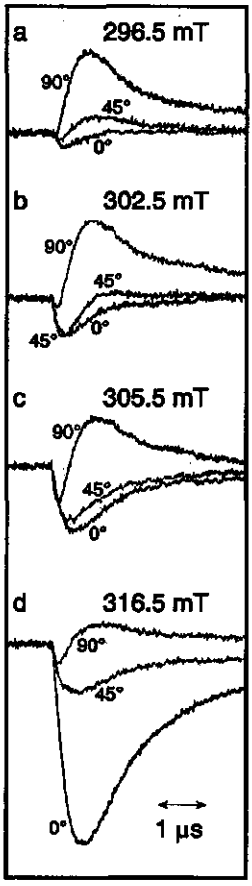

Fig. 1. Transient flash-induced EPR signals from oriented PSII membranes with Q_A doubly reduced. The angle between the magnetic field and the plane of the mylar sheets with oriented sample and the magnetic field strengths are indicated in the figure. Positive signals indicate absorption, negative signals emission of microwaves. Each trace is the average of 1024 measurements. Laser-induced background signals were suppressed by subtracting off-resonance transients. Instrument settings were as follows: temperature, 4.2 K; microwave power, 10 mW; microwave frequency, 9.12 GHz; laser energy, 15 mJ per pulse.

and orientation dependence were similar to those of the reaction centre triplet of PSII, as measured under continuous illumination [3,4]. Thus, the slow transient is attributed to the reaction centre triplet and we conclude that the rise time of the reaction centre triplet is in the 300 - 400 ns time range.

Considering the fact that the decay of the primary radical pair is slowed down in a magnetic field [33,34], the triplet risetime of 300 - 400 ns agrees reasonably well with the decay of the primary radical pair, which has recently been measured optically in the same type of sample (components of approximately 70 ns and 300 ns were found [25]).

Measurements on samples prepared under milder reducing conditions, in which a significant fraction of the reaction centres had singly reduced Q_A (approximately 50%, see Materials and Methods), were also performed. A somewhat faster rise of the reaction centre triplet was observed in these measurements as compared to samples with all Q_A doubly reduced (not shown), which is once more in line with the optical measurements in Ref. [25] (in this reference, the decay of the primary radical pair was found to be faster in samples with Q_A singly reduced as compared to samples with Q_A doubly reduced).

The observed decaytimes of the slow transient (see Fig. 1 for samples with all Q_A doubly reduced), were shorter than those measured optically: in the samples with all Q_A doubly reduced the triplet lifetime has been measured to be 1 - 10 ms [25,30] (see also [24,35-37]), whereas here, a decay on a microsecond timescale is measured. This is due to spin-lattice relaxation and microwave-induced nutation modulation of the transient EPR signals (see [26]). Due to the strong influence of these effects on the decaytime of the signals, a direct comparison of triplet decaytimes between samples with varying amounts of doubly reduced Q_A, as done in the optical work [25], is not possible with the present data.

From an inspection of several transients as shown in Fig. 1, some general features of the spectrum associated with the fast transient appear to be as

follows. It has a negative (emissive) amplitude on the low field side of the g = 2 position and a positive (absorptive) amplitude on the high field side, the separation of extremes (from now on called "splitting") being of the order of 45 mT. The amplitude is somewhat dependent on the orientation of the membranes in the magnetic field. At the field position 305.5 mT (Fig. 1c), the fast transient shows the largest negative amplitude in the trace recorded at an orientation of 90°; at 302.5 mT (Fig. 1b), it is the trace taken at 45° and at 296.5 mT (Fig. 1a) it is the trace at 0°. Thus, the splitting seems to increase when the orientation of the membranes is changed from perpendicular to parallel to the magnetic field.

For the assignment of the fast transient, we consider the following possibilities.

1) It has been proposed that the reaction centre triplet of PSII is formed on the primary donor, which is oriented perpendicular to the membrane (in analogy to the known purple bacterial reaction centre structure), and then rapidly moves to a chlorophyll oriented at 30° to the membrane [12] (see Introduction). In the following, we consider the possibility that the fast transient, found in the present work, arises from such a short-lived triplet on the primary donor, existing prior to the triplet with millisecond lifetime.

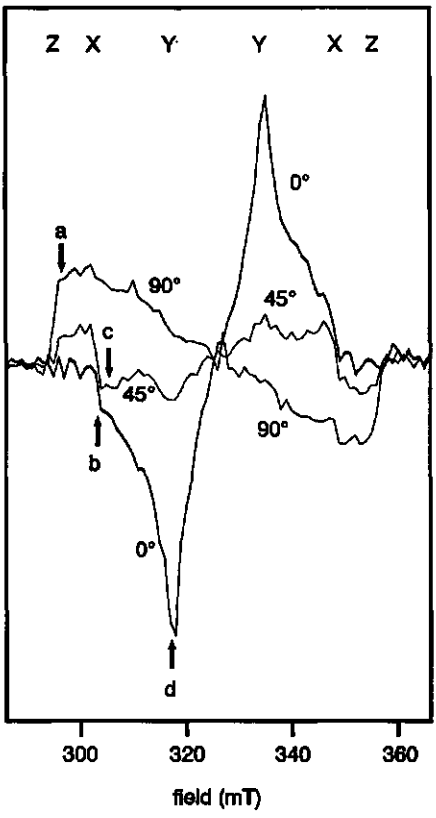

Fig. 2. Spectra obtained from measurements similar to those in Fig. 1. The spectrum was obtained by fitting of the transients (averages of 256 measurements) with two decay components and one rise component, with fixed lifetimes (of 2 μs, 600 ns and 300 ns, respectively), imposing equal amplitudes on the 300 ns rise and 2 μs decay. This amplitude was plotted as a function of the magnetic field in the figure. Labels a) to d) indicate the magnetic field values used in Fig. 1 a-d respectively. Instrument conditions and sample conditions were as in Fig. 1, except that the laser energy was 12.5 mJ per pulse.

The short-lived triplet would be expected to have the characteristics of a chlorophyll reaction centre triplet, formed via a charge separated state, therefore having an AEEAAE polarisation pattern of the Z, X and Y low field- and the Y, X and Z high field transitions respectively (A = absorptive; E = emissive, see [32] for a review). Thus, if the fast transient arose from a reaction centre triplet on the primary donor, it should have a positive amplitude at the position of its low field Z peak and a negative amplitude at the position of its high field Z peak. In addition,

the orientation dependence should be like that in purple bacteria (in which the triplet is localised on the primary donor, oriented perpendicular to the membrane [10,11]). This means that the Z peaks are expected to be maximal when the membranes are oriented parallel to the magnetic field (Θ = 0°). In Fig. 1 (the low field side of the g = 2 position) it can be seen that the fast transient is never positive at an angle Θ = 0°. Thus, it can be ruled out that the fast transient arises from an AEEAAE polarised reaction centre triplet localised on a chlorophyll which is oriented perpendicular to the membrane. Also an EAAEEA polarisation pattern (if D is negative, see [32]) does not seem applicable to the fast transient, because it is in fact never positive in any of the transients at field positions below 325.5 mT (g = 2).

We stress that the present data do not rule out the hypothesis [12] that triplet transfer from the primary donor to a 30° oriented chlorophyll occurs in PSII. A decay of the primary radical pair and rise of the reaction centre triplet on similar timescales (see above, comparing the results in Ref. [25] with those in the present work) leaves the possibility open that a very fast triplet transfer occurs, too fast to be detectable. In any case, the fast transient which we do detect, is not related to the triplet transfer proposed in Ref. [12] as outlined above.

2) It is possible that the fast transient arises from an independently photoexcited component (e.g. a carotenoid or chlorophyll triplet state), not being related to the primary charge separation in the reaction centre. Transients, similar to the fast transient in Fig. 1 were also found in oriented D_1D_2 particles (not shown), which indicates that there is at least a partial contribution from such components in the reaction centre.

3) The possibility that the fast transient arises from the primary radical pair. This possibility seems unlikely for the following reasons. Firstly, the decay kinetics of the fast transient appear to be longer (600 - 700 ns) than the rise kinetics of the reaction centre triplet (300 - 400 ns). Secondly, the global shape of the spectrum of the fast transient (see above) is not compatible with that of a radical pair: for a splitting of 45 mT, the radical pair is not expected to be significantly polarised (see [38]); the amplitude of the spectrum of the fast transient is probably too large for an unpolarised radical pair (using the polarised reaction centre triplet spectrum as a standard). In addition, a splitting of 45 mT is unexpectedly large for a radical pair (compare e.g. with Ref. [38]).

In summary, the spectrum of the fast transient most likely arises from transient states not specific for reaction centre photochemistry (possibility 2). The spectrum of the slow transient is attributed to the reaction centre triplet of which the risetime is estimated to be 300 - 400 ns. Finally, we did not obtain evidence for the intermediate triplet state proposed in Ref. [19].

Acknowledgements

We would like to thank K. Brettel and T.J. Schaafsma for useful discussions. We also thank A.J. van der Est and I. Sieckmann for help with measurements and data processing. F.v.M. is supported by the EEC (SCIENCE Programme) and A.W.R. is supported by the CNRS (URA 1290).

References

1 Van Gorkom, H.J. (1985) Photosynth. Res. 6, 97-112.
2 Renger, G. in Topics in Photosynthesis Vol. 11 (Barber, J., ed.), pp. 45-100, Elsevier, Amsterdam.
3 Rutherford, A.W., Paterson, D.R. and Mullet, J.E. (1981) Biochim. Biophys. Acta 635, 205-214.
4 Van Mieghem, F.J.E., Satoh, K. and Rutherford, A.W. (1991) Biochim. Biophys. Acta 1058, 379-385.
5 Rutherford, A.W. (1985) Biochim. Biophys. Acta 807, 189-201.
6 Rutherford, A.W. and Acker, S. (1986) Biophys. J. 49, 101-102.
7 Rutherford, A.W. and Sétif, P. (1990) Biochim. Biophys. Acta 1019, 128-132.
8 Nitschke, W., Feiler, U. and Rutherford, A.W. (1990) Biochemistry 29, 3834-3842.
9 Nitschke, W., Sétif, P., Liebl, U., Feiler, U. and Rutherford, A.W. (1990) Biochemistry 29, 11079-11088.
10 Hales, B.J. and Gupta, A.D. (1979) Biochim. Biophys. Acta 548, 276-286.
11 Tiede, D.M. and Dutton, P.L. (1981) Biochim. Biophys. Acta 637, 278-290.
12 Rutherford, A.W. (1986) Biochem. Soc. Trans. 14, 15-17.
13 Mathis, P. and Rutherford, A.W. (1987) in New Comprehensive Biochemistry: Photosynthesis (Amesz, J. ed.), pp. 63-96 Elsevier, Amsterdam.
14 Rutherford, A.W. (1987) in Prog. in Photosynth. Res. (Biggins, J., ed.) Vol 1, pp. 277-283 Martinus Nijhoff, Dordrecht.
15 Rutherford, A.W. (1988) in Light-Energy Transduction in Photosynthesis: Higher Plant and Bacterial Models (Stevens, S.E. and Bryant, D.A., eds.), pp. 163-177, The American Society of Plant Physiologists, Rockville.
16 Trebst, A. (1986) Z. Naturforsch 41c, 240-245.
17 Michel, H. and Deisenhofer, J. (1988) Biochemistry 27, 1-7.
18 Barber, J. and Marder, J.B. (1986) in Biotechnology and Genetic Engineering Reviews (Russel, M., ed.) Vol. 4, pp. 355-405, Intercept, Newcastle upon Tyne.
19 Nanba, O. and Satoh, K. (1987) Proc. Natl Acad Sci USA 84, 109-112.
20 Deisenhofer, J., Epp O., Miki K., Huber R. and Michel H. (1985) Nature (London) 318, 618-624.
21 Allen, J.P., Feher, J., Yeates, T.O., Komiya, H. and Rees, D.C. (1987) Proc. Natl. Acad. Sci. USA 84, 5730-5734.
22 Takahashi, Y., Hansson, Ö., Mathis, P. and Satoh, K. (1987) Biochim. Biophys. Acta 893, 49-59.
23 Schlodder, E. and Brettel, K. (1990) in Current Research in Photosynthesis (Baltscheffsky, M., ed.), Vol I, pp.447-450.
24 Van Kan, P.J.M., Otte, S.C.M., Kleinherenbrink, F.A.M., Nieveen, M.C., Aartsma, T.J. and Van Gorkom, H.J. (1990) Biochim. Biophys. Acta 1020, 146-152.
25 Van Mieghem, F.J.E. (1994) Ph.D. Thesis, Agricultural University, Wageningen.
26 Stehlik, D., Bock, C.H. and Thurnauer, M.C. (1990) in Advanced EPR in Biology and Biochemistry (Hoff, A.J., ed.) pp. 371-404, Elsevier, Amsterdam.
27 Berthold, D.A., Babcock, G.T. and Yocum, C.F. (1981) FEBS Lett. 134, 231-234.
28 Ford, R.C. and Evans, M.C.W. (1983) FEBS Lett. 160, 159-164.
29 Blasie, J.K., Erecinska, M., Samuels, S. and Leigh, J.S. (1978) Biochim. Biophys. Acta 501, 33-52.
30 Van Mieghem, F.J.E., Nitschke, W., Mathis, P. and Rutherford, A.W. (1989) Biochim. Biophys. Acta 977, 207-214.

31 Van Mieghem, F.J.E., Searle, G.F.W., Rutherford, A.W. and Schaafsma, T.J. (1992) Biochim. Biophys. Acta 1100, 198-206.
32 D.E. Budil and M.C. Thurnauer, Biochim. Biophys. Acta 1057 (1991) 1.
33 Hansson, Ö., Mathis, P. and Satoh, K. (1990) in Current Research in Photosynthesis, (Baltscheffsky, M., ed.), Vol. I, pp. 439-442, Kluwer, Dordrecht.
34 Gilbert, M., Rousseau, G., Richter, M., Ogrodnik, A., Volk, M. and Michel-Beyerle, M.E. (1993) Biophys. J. 64, A132.
35 Den Blanken, H.J., Hoff, A.J. Jongenelis, A.P.J.M. and Diner, B.A. (1983) FEBS lett. 157, 21-27.
36 Rutherford, A.W., Satoh, K. and Mathis, P. (1983) Biophys. J. 41, 40a.
37 Searle, G.F.W., Telfer, A., Barber, J. and Schaafsma, T.J. (1990) Biochim. Biophys. Acta 1016, 235-243.
38 Stehlik, D., Bock, C.H. and Petersen, J. (1989) J. Phys. Chem. 93, 1612-1619.

Chapter 8

Primary reactions at 20 K in Photosystem II in relation to the redox state of Q_A: kinetics and absorbance difference spectra around 680 nm

The decay kinetics of the primary radical pair P^+Ph^- in photosystem II (PSII) samples (PSII-enriched membranes from spinach) with Q_A doubly reduced have been measured at 20 K by flash absorption spectroscopy in the 680 nm region. A high radical pair yield was found and the decay could be described with two lifetimes of 70 ns and 290 ns. When Q_A is singly reduced, approximately the same amount of radical pair is formed but the decay kinetics are faster: lifetimes of 25 ns and 130 ns were found. When Q_A is doubly reduced, the decay of the reaction centre triplet can be described with lifetimes of 1.5 ms and 4.5 ms. In the presence of singly reduced Q_A, these kinetics are replaced by microsecond kinetics of similar amplitude (lifetimes of 2.5 μs and 20 μs), attributed to the same triplet. Thus, quite unexpectedly, previous EPR triplet data (Van Mieghem, F.J.E., Nitschke, W., Mathis, P. and Rutherford, A.W. (1989) Biochim. Biophys. Acta 977, 207-214.) are now most likely explained by a dramatic difference in the triplet lifetimes instead of being explained (as proposed previously in this reference) by an influence of Q_A on the yield of charge separation, the lifetime of the primary radical pair or the rate of triplet formation. The origin of the short triplet lifetime in the presence of singly reduced Q_A remains unclear.

The absorbance difference spectra attributed to the formation of the primary radical pair and the reaction centre triplet are not greatly influenced by the redox state of Q_A (singly or doubly reduced). However, the spectra are considerably different from equivalent spectra obtained from D_1D_2 preparations. This indicates that one should take care with the interpretation of data obtained from D_1D_2 preparations. On the basis of the difference spectra in the present work it cannot be ruled out that the primary donor in PSII is analogous to that in purple bacteria, the triplet being rapidly transferred to a PSII-analogue of one of the monomeric bacteriochlorophylls of the purple bacterial reaction centre.

1. Introduction

In the photosynthetic reaction centre of purple bacteria, the primary radical pair P^+BPh^- is formed after the light-induced electron transfer from a pair of bacteriochlorophylls (the primary donor P) to a bacteriopheophytin (BPh), (see [1,2] for reviews). The electron is subsequently transferred to a quinone molecule (Q_A), giving rise to the secondary radical pair $P^+Q_A^-$. If Q_A is prereduced or absent, charge recombination in the pair P^+BPh^- can result in the formation of a triplet state on P (see [3] for a recent review on the triplet state of (bacterio)-chlorophylls in vitro and in vivo). All of these reactions can occur both at physiological and at cryogenic temperatures.

In the reaction centre of photosystem II (PSII), similar photochemistry is thought to take place (see [4-9] for reviews on electron transfer processes in

PSII). There are also thought to be structural similarities between the reaction centres of purple bacteria and PSII (reviewed in [5-7]).

Significant differences between PSII and purple bacteria have been reported as well. An example can be found in Ref. [10]: no triplet could be detected in spinach PSII membranes by EPR if Q_A was prereduced to the semiquinone form; it was only observable after double reduction of Q_A. An explanation was favoured in which the low triplet yield reflected a low yield of charge separation and possibly a short lifetime of the primary radical pair [10]. The need for an accurate test of this explanation has become clear from flash absorbance data which indicated that in PSII from Synechococcus at 77 K, in the presence of singly reduced Q_A, charge separation does occur with high yield [11]. In the present work then we have performed nanosecond flash absorbance spectroscopy using samples and conditions (i.e. low temperatures) which were comparable to those in the EPR work [10].

Other discrepancies which have been proposed to be present between the reaction centres of purple bacteria and PSII, concern the structure of P and its surroundings; (see [9] for a recent review). Optical difference spectra of primary photochemistry in isolated reaction centre preparations (D_1D_2 preparations), obtained by (flash) absorbance spectroscopy or ADMR have recently been used in the analysis of the structure of P (e.g. [12-18]). Here we present optical difference spectra obtained at 20 K from spinach PSII membranes.

2. Materials and Methods

2.1. *Sample preparation*

PSII-enriched thylakoid membrane fragments were prepared from spinach as described earlier [19] using the modifications in Ref. [20] and stored in the dark at -80° C until use. Samples with doubly reduced Q_A were prepared as described in Ref. [21], by incubation at room temperature in the dark, using 40 mM sodium dithionite and 100 μM benzyl viologen. These samples were stored under argon and at -80° C in the dark.

For (transient) absorbance measurements, samples were brought into a buffer containing 60% glycerol, 20 mM Mops (pH 7.0), 10 mM NaCl, 5 mM $MgCl_2$ and 125 mM sucrose and, depending on the type of sample, 20 mM dithionite (Q_A singly reduced), 40 mM dithionite (Q_A doubly reduced) or 1 mM ferricyanide (Q_A oxidised). The sample with singly reduced Q_A was prepared by mixing sample from a concentrated stock solution, still at ambient redox potential, with the dithionite-containing buffer under argon, transferring it under argon into the cuvette, letting it incubate in the dark under argon for approximately 5 min and then inserting it (sealed) in near darkness into the already cold optical cryostat. For the sample with doubly reduced Q_A, sample from the already doubly reduced stock (see above) was used; in this case the sample was not incubated, but immediately cooled down in the cryostat. The sample for the measurement under oxidising conditions came from the stock at ambient potential. After the addition of ferricyanide, it was inserted into the uncooled

cryostat and incubated for approximately 1 hr in the cryostat in the dark before the cryostat was cooled to 20 K.

2.2. *Instruments*

EPR spectra were recorded using a Bruker 200 X-band spectrometer fitted with an Oxford Instruments cryostat and temperature control system. In order to record spectra during illumination, an 800 W tungsten projector was used. The light was filtered through 2 cm water and three Calflex (Balzers) heat filters.

Flash absorbance spectroscopy in the 680 nm region was carried out at 20 K in an optical cryostat cooled with helium gas. The sample (approximately 0.01 mg Chl/ml) was in a plastic cuvette with optical paths of 10 mm for the measuring light and 4 mm for the excitation light; the temperature of the sample was measured by a temperature sensor close to the cuvette.

The sample was excited at 532 nm using a frequency doubled Nd:YAG laser (Quantel) with a pulse width at half-maximum amplitude of 300 ps and pulse energies up to 20 mJ at a repetition rate of 5 Hz. The exciting beam was expanded resulting in a cross Section at the position of the sample of 2 cm^2.

As measuring light source, CW laserdiodes (Toshiba TOLD 9140 and 9215) were used, fixed in a temperature regulated holder. The emission wavelength of the laser diode was varied by changing its temperature. The wavelength of the measuring light was controlled with a monochromator, which had been calibrated using the 632.8 nm line of a He - Ne laser. The measuring light was focussed through the cuvette and through interference and cut-off filters (to reduce fluorescence contributions) on a photodiode (FND 100 from EG&G), the output of which was amplified (using an IV72A amplifier from the Hahn - Meitner Institut, Berlin) and measured with a transient digitizer (DSA 602A with plug-in 11A72, from Tektronix). The electronic bandwidth of the detection system was 500 Hz - 100 MHz. In order to minimise actinic effects, the measuring light was pulsed, using the combination of a chopper and a shutter. The pulse duration thus obtained was 70 μs and the repetition rate was 5 Hz. In order to correct for the fact that the pulses were not completely squarely shaped, a measurement without excitation was subtracted from an absorbance change measurement. At short timescales of 1.5 μs duration and less, the measurement without excitation yielded a virtual straight line with a slope of less than 0.1%.

For measurements on a millisecond timescale, continuous measuring light was used, but it was attenuated by a factor of approximately 10^4 as compared to the nanosecond measurement. The output of the photodiode in a 100 kΩ load resistance was amplified by a Tektronix AM 502 amplifier. The electronic bandwidth of the detection system was DC - 10 kHz.

For the low temperature flash absorbance experiments in the 500 nm region, a plexiglass cuvette with a thickness of 2.7 mm was used, placed at an angle of 45° with respect to the mutually perpendicular exciting and measuring light beams. The sample concentration was approximately 0.1 mg Chl/ml. Excitation was at 600 nm with a pulse width at half-maximum amplitude of 7 ns and pulse energies up to 3 mJ and a repetition rate of 2 Hz, using a dye laser with

rhodamine 600, pumped by a frequency doubled Nd:YAG laser (YG 780C from Quantel). A tungsten halogen lamp was used as the measuring light source which passed through a shutter with an opening time of 15 ms. Interference filters before and after the sample were used for selecting the measuring wavelength. A photodiode (S 3204-05 from Hamamatsu) was used for detection. The electronic bandwidth of the detection system was varied according to the timescale of the measurement by appropriate choice of the load resistance of the photodiode and the bandwidth of the amplifier (Tektronix AM 502). The fastest possible response time was determined to be 200 ns by measuring the time response of light scattering from the laser pulses.

Exponential fitting procedures were performed using a computer program employing the Marquardt method.

2.3. *Correction for light-induced signal loss*

When repeated measurements were performed on the same sample, it was observed that the amplitude of the absorbance changes irreversibly decreased. This is explained by low quantum yield photoaccumulation of Ph^- under reducing conditions and of Q_A^- under oxidising conditions, due to the measuring and excitation light (see [6]). The loss was kept as low as possible by illuminating the sample only during the measurement.

The light-induced loss of signal was relatively fast at the beginning of a series of measurements (each consisting of typically 128 or 256 laser flashes) on a fresh sample. To minimise the influence of the irreversible loss on the shape of absorbance difference spectra, the only data used were those which were obtained after the fast initial signal loss had occurred. The following slower decrease was taken as being monoexponential, dependent on the number of measurements. The rate of this monoexponential signal loss was estimated by measuring the absorbance change at some wavelengths several times during the course of the measurements and comparing them. This rate was then used to correct for the loss of signal during the series of measurements from which difference spectra were to be derived. Under reducing conditions, the loss was estimated to be of the order of 0.003 % per laser flash, whereas under oxidising conditions it was estimated to be approximately 0.01 %. After the correction of a difference spectrum for the (assumed) monoexponential loss during the measurements, it was scaled to the very first measurement made. Despite the latter correction, an overall underestimation of the amplitude of the spectrum remains, due to exposure of the sample to light before the first measurement (e.g. during the alignment of the optics).

2.4. *Flattening correction*

Particle flattening is the effect that in a suspension of pigment-containing particles, the absorbance is lower than in the hypothetical case that all pigments are homogeneously distributed (i.e. as in solution). This is due to the fact that in a particle, pigments can be shielded from the measuring light by others. The

effect is therefore most pronounced at the absorbance maxima of the pigments.

In order to correct the amplitude of the absorbance changes measured for particle flattening (originally described by Duysens [22], see e.g. also [23,24]), we followed the procedure described recently in Ref. [25].

2.4.1. *The low temperature absorption spectrum*

To calculate the flattening correction factor at a certain wavelength, one firstly needs the absorption at this wavelength, corrected for light scattering [22]. Since our time resolved absorbance measurements were performed at 20 K, at several wavelengths, we had to determine the scatter corrected absorbance spectrum of the sample at this temperature. This was done with a Cary 2300 UV-VIS-NIR spectrophotometer (Varian) equipped with the same cryostat and temperature control unit as those used in the time resolved measurements. The monochromator of the spectrophotometer was calibrated using its autocalibration function and it was also checked using a didymium filter and interference filters. The latter were in turn calibrated with the same monochromator as used in the time-resolved experiments in the 680 nm region (see above). Spectra were recorded in the range 500 nm - 800 nm, with the following instrument settings: wavelength interval, 1 nm; spectral bandwidth, 1 nm; time constant, 0.5 s; scan rate, 1 nm/s. Furthermore, the beam size-reduction (to 1/3) facility was used. The cuvette thickness was 2.7 mm. The sample was in the absence of dithionite and ferricyanide.

The spectrum, corrected for scattering was obtained using the equation [26]:

$$E' = E(\gamma_1) - A[E(\gamma_2) - E(\gamma_1)] \qquad (1)$$

where

$$A = \{E(\gamma_1)/[E(\gamma_2) - E(\gamma_1)]\}_{\lambda=\lambda 0} \qquad (2)$$

E' is the absorbance after correction for scattering, $E(\gamma_1)$ is the absorbance of the sample with a diffusing plate mounted approximately 1 mm behind the sample and $E(\gamma_2)$ is the absorbance of the sample in the absence of a diffusing plate. Both $E(\gamma_1)$ and $E(\gamma_2)$ were determined by subtraction of a measurement on a cuvette, filled with buffer from a measurement on a cuvette filled with sample plus buffer. The wavelength independent factor A was determined at room temperature, in the absence of the cryostat, using the same relative positions of cuvette and diffusing plate as at low temperature. This was done at 735 nm, a wavelength (λ_0) at which the sample has negligible absorbance (see [25]).

The spectrum, corrected in the way described above, did not have exactly zero amplitude at 735 nm, but a value of 0.03. This is most likely due to some lack of reproducibility in placing the sample in the cryostat in the measurements at low temperature, influencing mainly the level of the baseline in the spectrum: repeating a measurement at slightly different sample positions showed that there was some variation in the level of the baseline of the spectrum. This phenome-

non is also expected to introduce an uncertainty in the value for A. We stress that the relative amplitude of absorbance peaks was much less affected by the sample position (varying only a few percent).

The baseline error (0.03 at 735 nm) was suppressed to some extent by subtraction of a sufficient percentage of baseline to yield a value of zero at 735 nm, but this does not decrease the error in the factor A. Thus, we estimate the relative error in the corrected spectrum to be approximately 10%, mainly due to the uncertainty in the factor A. Fig. 1a shows the scatter-corrected absorbance spectrum at 20 K. The curve corresponding to the term $A[E(\gamma_2) - E(\gamma_1)]$ from equation (1) (Fig. 1b) has a shape similar to that in Ref. [25].

2.4.2. *Brief theoretical description of the flattening effect for spherical particles*

The flattening correction factor F for the absorbance of a suspension is defined as [22]:

$$F = E_s/E' \tag{3}$$

where E_s is the absorbance which the suspension would have if no flattening were occurring; E' is known from the absorbance spectrum corrected for scattering. From E', the average transmittance of a particle T_p can be determined using the equation [22]:

$$E' = (p/2.303)[1 - T_p] \tag{4}$$

where p is a parameter dependent on the particle size (but not on the wavelength) and proportional to the sample concentration, which can be determined as described in Ref. [24] (see below). T_p is related to E_s via a (wavelength dependent) parameter α_p (proportional to the optical density for a thin beam passing through the centre of the particle, see [22]):

$$T_p = 2[1 - (1 + \alpha_p) \exp(-\alpha_p)]/\alpha_p^2 \tag{5}$$

$$E_s = (2/3)[p/2.303] \alpha_p \tag{6}$$

Equations 3 - 6 can be used to plot the relation between T_p and F by calculating both of them at different values of α_p (Fig. 2a, see also [23-25]). Thus, F can be determined graphically from T_p, which in turn can be calculated from E', if p is known (equation 4).

Also the flattening factor for small absorbance changes (see [23]), F_Δ, can be determined in a graphical way. An equation for F_Δ as a function of T_p can be obtained by differentiating equations 4 and 6 with respect to α_p:

$$F_\Delta = (dE_s/d\alpha_p)/(dE'/d\alpha_p) \tag{7}$$

In Fig. 2b, F_Δ is plotted as a function of T_p (see also [23-25]).

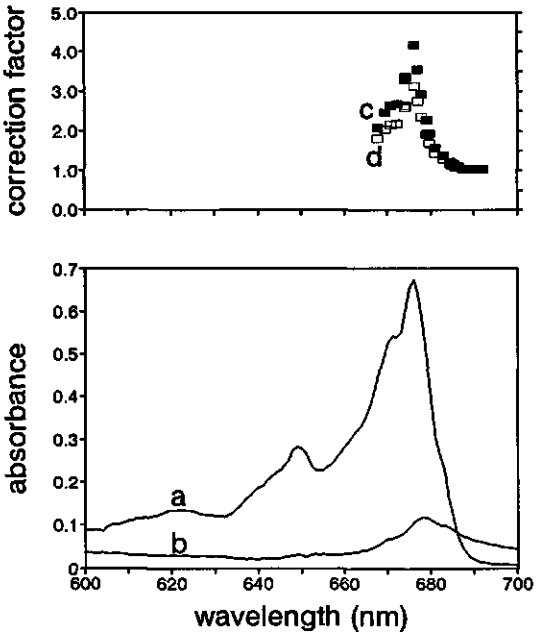

Fig. 1. (a) Absorption spectrum of PSII-enriched membranes (0.05 mg Chl/ml) at 20 K, corrected for scattering. The cuvette thickness was 2.7 mm (see the text for more details). (b) The scatter correction function used to obtain the spectrum in (a) (see text). (c) *Filled squares:* flattening correction factors used in the present work for samples with Q_A singly reduced and oxidised. (d) Squares: flattening factors used for samples with Q_A doubly reduced.

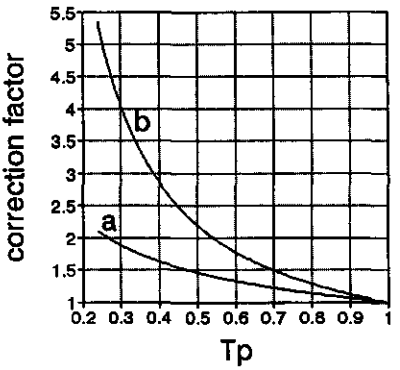

Fig. 2. Flattening correction factors as functions of the average particle transmission, see text for details. (a) The flattening correction factor for the absorbance. (b) The flattening correction factor for small absorbance changes.

2.4.3. *Determination of the flattening correction factors*

It was assumed that the particles are spherical. The parameter p (see preceding Section) was determined at room temperature as in Ref. [24], by measuring the (scatter corrected) absorbance of the sample in buffer and ethanol in a peak at 435 nm (the peak is at the same wavelength under both conditions). For these measurements, the Cary spectrophotometer was equipped with its cuvette holder, which allowed good reproducibility of sample positioning. Correction for scattering was done using the same procedure as described above [26].

It was found that the value of p in samples, treated with dithionite and benzyl viologen (for measurements under conditions of doubly reduced Q_A) was greater (1.1 for a chlorophyll concentration of 5 μg/ml) than that of samples which had not been treated in this way (used for measurements under conditions of Q_A oxidised and singly reduced; a value of 0.9 was found for a chlorophyll concentration of 5 μg/ml in these samples). This means (see [22]) that the particle size was smaller in the dithionite/benzyl viologen-treated samples. Consequently, two sets of (wavelength dependent) flattening correction factors for absorbance changes were derived, using equation 4 and Fig. 2b. Fig. 1c shows the correction factors used for the measurements on samples with Q_A singly

reduced and oxidised; Fig. 1d shows these factors for the measurements on samples with Q_A doubly reduced. The 10% error in the scatter corrected low temperature absorbance spectrum introduces an uncertainty in the flattening correction. Thus, the error in the absorbance difference spectra from samples with Q_A doubly reduced is estimated to be maximal (approximately 15%) at 676 nm (the wavelength where the correction factor was the largest, see Fig. 1d). The error in the difference spectra from samples with Q_A singly reduced or oxidised is larger (estimated to be 30 % at 676 nm) due to the larger flattening correction (see Fig. 1c).

3. Results

3.1. *Experiments under reducing conditions*

PSII-enriched membranes with Q_A in the doubly reduced state [10] were prepared by incubation with dithionite and benzyl viologen, as described in Materials and Methods. At different times during the incubation, the proportion of reaction centres with doubly reduced Q_A was determined by EPR (see [10]). The formate-enhanced $Q_A^-Fe^{2+}$ signal [27] was maximal at the start of the incubation and decreased beyond detection after an incubation time of approximately 1.5 hours at room temperature. During this incubation time, the amplitude of the light-inducible reaction centre triplet signal, measured under continuous illumination by EPR (see [28]), increased by a factor of approximately 10, in agreement with results in Refs. [10,21]. It was proposed in these references that the triplet yield is negligible if Q_A is singly reduced and close to 100% if it is doubly reduced.

Samples with singly reduced Q_A were prepared by addition of dithionite without benzyl viologen (see Materials and Methods for more details). A small triplet signal (approximately 10% of that in samples with Q_A doubly reduced) was seen in these samples by EPR. This can be explained by a fraction of reaction centres (approximately 10%) being more susceptible to double reduction, not requiring the presence of the mediator benzyl viologen (see [21]).

3.1.1 *Flash-induced absorbance changes in the 680 nm region*

Flash-induced absorbance changes were measured at 20 K in samples with Q_A in the doubly reduced state. The wavelength of the measuring light was varied in approximately 1 nm steps, in the range of 668 nm to 693 nm. For comparison, samples with Q_A singly reduced were also measured at a number of wavelengths. In Fig. 3, nanosecond absorbance changes (after a virtually saturating laser flash with an energy of approximately 1.5 mJ) are shown for both types of samples, at three characteristic wavelengths.

The least complicated traces are those at 676 nm (Fig. 3b): in both types of sample, an almost instantaneous bleaching is seen (on this timescale), which then decays back to a level slightly above zero in hundreds of nanoseconds. Clearly, this decay is faster in the sample with Q_A singly reduced (trace 2).

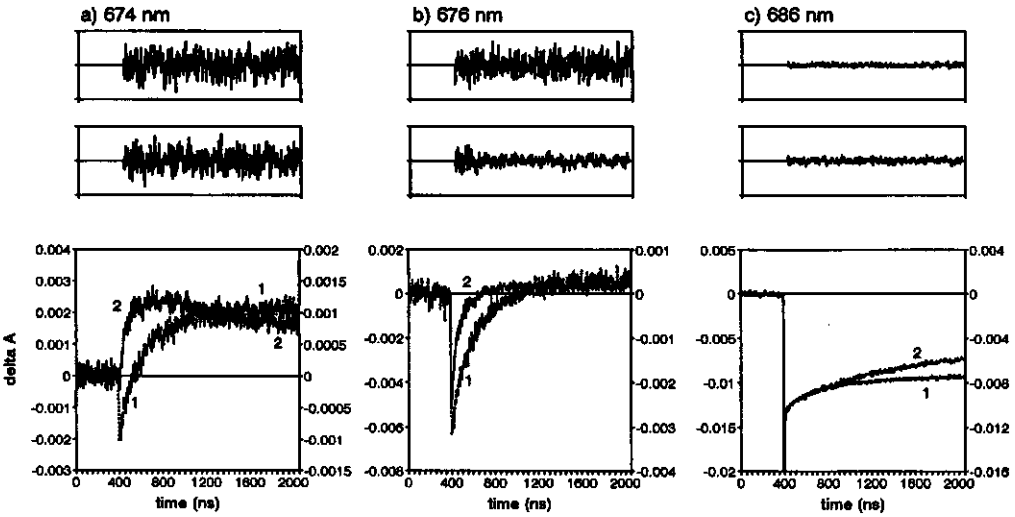

Fig. 3. Absorbance changes in PSII-enriched membranes at 20 K. Difference curves with the fits in table II are also shown (upper traces). The labeling is as follows: (1) samples with Q_A doubly reduced (0.013 mg Chl/ml); (2) samples with Q_A singly reduced (0.011 mg Chl/ml). Note that the traces are scaled differently: the left-hand Y-axis is for samples with Q_A doubly reduced (traces 1); the right-hand Y-axis is for samples with Q_A singly reduced (traces 2).

Satisfactory fits were obtained with two decay components plus a constant (see Table I). In the sample with Q_A singly reduced, approx. equal contributions of a 25 ns and a 130 ns component were found. In the doubly reduced sample, the decay is dominated by a component of 290 ns (approx. 70%); the second component was found to be approx. 70 ns (30%).

The fitting of exponential lifetimes and relative amplitudes in the present work enables a more quantitative description of the kinetics. We stress that with the present signal to noise ratio, this description is approximate. With a higher signal to noise ratio, kinetics might appear to contain more components than found in our fits or to be governed by a distribution of lifetimes.

Kinetics, similar to those found at 676 nm are also seen at 674 nm (Fig. 3a). At this wavelength, the initial bleaching changes into a distinct positive signal. Again, this change is clearly faster in the sample with Q_A singly reduced (trace 2). In the sample with Q_A doubly reduced (trace 1), the positive signal is essentially constant at the end of the time scale, whereas in the singly reduced sample (trace 2) it slowly starts to decay, already after approximately 1 μs.

At 686 nm (Fig. 3c), a slow decay similar to that found at 674 nm is seen for the singly reduced sample (trace 2) and a essentially constant signal (at the end of the timescale) when Q_A is doubly reduced (trace 1), but their amplitudes are opposite to those at 674 nm. Fast kinetics as seen at 674 nm and 676 nm, although less well-resolved, seem also to be present. A clear difference in these kinetics between singly and doubly reduced samples, as seen at the other two wavelengths, is not obvious at 686 nm. The period starting at the moment of the

Table I, results of fits. Traces were fitted to a multi-exponential decay function. In some cases, a non-decaying component (C) was included in the fit. Lifetimes are given and amplitudes are given in percentage of the total initial amplitude.

State of Q_A	Wavelength (nm)	Timewindow used	Components		C
singly reduced	676	8 ns - 850 ns	26 ns (54%)	130 ns (52%)	(-6%)
doubly reduced	676	8 ns - 1.6 μs	72 ns (32%)	290 ns (77%)	(-10%)
singly reduced	686	850 ns - 55 μs	2.6 μs (57%)	20 μs (36%)	(7%)
doubly reduced	686	110 μs - 8 ms	1.4 ms (57%)	4.5 ms (43%)	

flash until a few nanoseconds afterwards, is marked by a large spike in both types of sample, which is not completely shown in Fig. 3c. Subtraction of the fluorescence contribution (recorded without measuring light) removed most of it, but not all. We assume that the remaining part reflects bleaching and stimulated emission due to singlet excited chlorophylls. In the present work, we will not further analyse these very fast kinetics.

The slow decay as seen in samples with Q_A singly reduced at 674 and 686 nm (Fig. 3a,c; traces labeled 2), was further investigated on a microsecond timescale. The result at 686 nm is shown in Fig. 4b. At least two components were needed for a good fit of the decay (see Table I), one with a lifetime of approximately 2.5 μs (approximately 60 %), the other with a lifetime of 20 μs (approximately 40 %).

The non-decaying component as detected on the nanosecond timescale in samples with doubly reduced Q_A in Fig. 3, was further investigated on a ms timescale, at the same wavelengths as in the nanosecond experiment. In Fig. 4a, the result at 686 nm is shown. The kinetics at the other wavelengths were similar to the one shown in Fig. 4a. It can be seen that the amplitude corresponds to that of the nondecaying component in Fig. 3c.

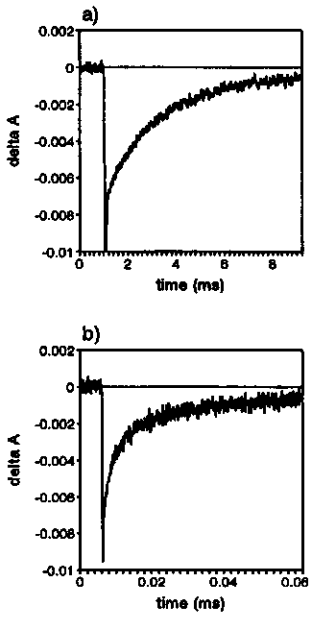

Fig. 4. Absorbance changes at 686 nm in PSII-enriched membranes (20 K). (a) Samples with Q_A doubly reduced, 0.013 mg Chl/ml; (b) Samples with Q_A singly reduced, 0.011 mg Chl/ml.

TABLE II, comparison of fits at various wavelengths. For samples with Q_A doubly reduced (A), traces were fitted to the equation:

$$A(t) = \alpha_1 \exp(-t/\tau_1) + \alpha_2 \exp(-t/\tau_2) + C \quad (8)$$

where A(t) is the absorbance change at time t after the flash, α_i is the relative amplitude of component i, given in percents of the total initial amplitude and τ_i its lifetime. C is a non-decaying component. For samples with Q_A singly reduced, traces were fitted either (B) to the equation:

$$A(t) = \alpha_1 \exp(-t/\tau_1) + \alpha_2 \exp(-t/\tau_2) + \alpha_3 \exp(-t/\tau_3) + C \quad (9)$$

or (C) to the equation:

$$A(t) = \alpha_1 \exp(-t/\tau_1) + C \quad (10)$$

A. Q_A doubly reduced

Wavelength (nm)	Timewindow used	Components 1 72 ns, fixed	2 290 ns, fixed	α_1/α_2	C
674	24 ns - 1.7 μs	57%	141%	0.4	(-98%)
676	24 ns - 1.7 μs	32%	78%	0.4	(-10%)
686	24 ns - 1.7 μs	6%	20%	0.3	(74%)

B. Q_A singly reduced

Wavelength (nm)	Timewindow used	Components 1 26 ns, fixed	2 130 ns, fixed	α_1/α_2	3	C
674	24 ns - 1.6 μs	174%	193%	0.9	1.0 μs (-159%)	(-109%)
676	24 ns - 1.6 μs	51%	57%	0.9	560 ns (-1%)	(-6%)
686	24 ns - 1.6 μs	5%	5%	1.0	1.1 μs (47%)	(43%)

This was also the case for the other wavelengths investigated. The decay could be described by two components of approximately 1.5 ms and 4.5 ms respectively (see Table I).

In order to extract difference spectra of the states and kinetics involved in the absorbance changes observed between 667 nm and 693 nm, we proceeded as follows.

First we checked whether the absorbance changes can be described by the

Table II *(continued)*

C. Q_A singly reduced

Wavelength (nm)	Timewindow used	Components 1	C
674	850 ns - 6.5 μs	3.0 μs (70%)	(30%)
686	850 ns - 6.5 μs	2.6 μs (68%)	(32%)

same kinetic compounds at various wavelengths. 1) we tested whether the traces at 674 nm and 686 nm (Figs. 3a and c) could be fitted with the same rate constants as found at 676 nm (72 ns and 290 ns for Q_A doubly reduced; 26 ns and 130 ns for Q_A singly reduced, Table I). Therefore these rate constants were fixed during the fitting procedure. The first 25 ns after the flash were not included in the fit to eliminate fast contributions, e.g. from singlet excited states. The results are shown in Table IIA (Q_A doubly reduced) and IIB (Q_A singly reduced). The difference curves between experiments and fits are shown in the upper traces of Fig. 3 and indeed, it can be seen that the traces can be fitted well with these rate constants. In addition, the ratio between the amplitudes of the two fast components was similar at the three wavelengths (Table IIA,B). 2) For samples with singly reduced Q_A, kinetics were compared by fitting also on a longer (microsecond) timescale. The result is shown in Table IIC. It can be seen that the kinetics are similar also on this timescale.

Two difference spectra were constructed for each type of sample. Fig. 5a shows difference spectra associated with the formation of the first detectable state, existing a few nanoseconds after the flash, not taking into account the fast contributions attributed to singlet excited states. Filled circles represent data from samples with Q_A singly reduced; circles are data from samples with Q_A doubly reduced. Fig. 5b shows difference spectra associated with the state which decays with microsecond (Q_A singly reduced) or millisecond (Q_A doubly reduced) kinetics. Filled circles are data from samples with Q_A singly reduced; circles are data from samples with Q_A doubly reduced. More details on the procedures and corrections used to derive these difference spectra are given in the Materials and Methods Section and the figure legends to Fig. 5

Both in Fig. 5a and Fig. 5b, it is seen that the difference spectra from samples with Q_A singly reduced are very similar to those from samples with Q_A doubly reduced. This indicates that the same states are involved in both types of sample, but with different kinetics.

Our assignment of the difference spectra and kinetics of samples with Q_A doubly reduced (Fig. 5a and b, circles, and Table I) is as follows. The difference spectrum associated with the millisecond decay (Fig. 5b, circles) is attributed to the reaction centre triplet state (i.e. it is the triplet minus singlet spectrum), which has been reported to have such a lifetime [29,30] (see also [10]). The

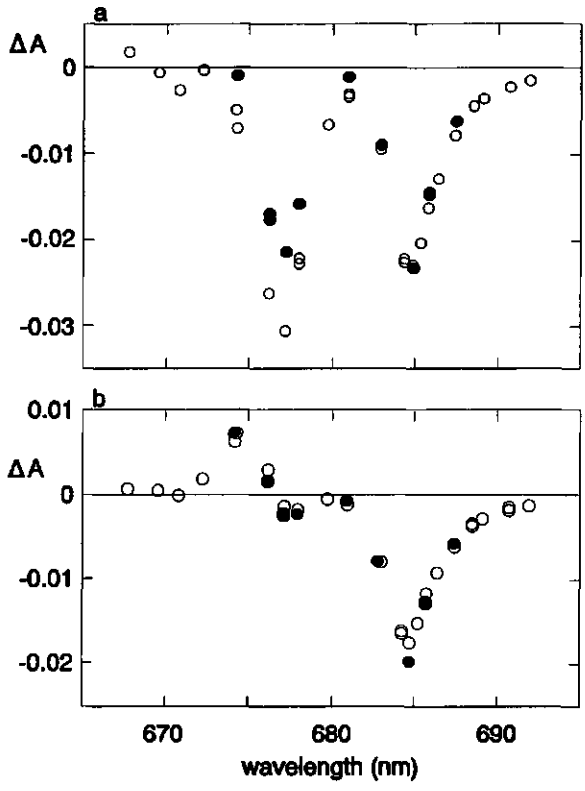

Fig. 5. Difference spectra obtained from the absorbance changes measured between 667 nm and 693 nm, some of which were shown in fig. 3. The data are corrected for light-induced signal loss and particle flattening (see Materials and Methods) and normalised to a concentration of 0.013 mg Chl/ml. Circles represent data from samples with Q_A doubly reduced; filled circles represent data from samples with Q_A singly reduced. (a) Spectra of the absorbance changes present immediately after the flash, obtained by back extrapolation of the traces to the moment of the flash, ignoring the first data points after the flash (to avoid fast contributions from singlet excited states). (b) Spectra of the millisecond (Q_A doubly reduced) and microsecond (Q_A singly reduced) decays. For the case of doubly reduced Q_A (circles), it was obtained by measuring the (on the timescale of fig 3) non-decaying component. For the spectrum from samples with Q_A singly reduced (filled circles), the amplitude of the microsecond decay was obtained by fitting.

kinetics described by the lifetimes of 72 ns and 290 ns (Table I) are attributed to the decay of the primary radical pair state and the rise of the reaction centre triplet state. They correspond well to those previously measured in PSII, for the decay of the primary radical pair (time-resolved absorbance measurements [15,31,32]), for delayed fluorescence [33,34] and for the risetime of the reaction centre triplet (time-resolved EPR [35]). Thus, the difference spectrum of the initial state (Fig. 5a, circles) is attributed to the primary radical pair state P^+Ph^- (i.e. it is the P^+Ph^- minus PPh spectrum).

In line with the similarity between the difference spectra obtained from samples with Q_A singly and doubly reduced (see above), the assignments for samples with Q_A singly reduced are analogous to those for samples with Q_A doubly reduced: the difference spectrum associated with the microsecond decay (Fig. 5b, filled circles) is attributed to the triplet minus singlet spectrum; the 26 ns/130 ns kinetics are attributed to the decay of the primary radical pair and the rise of the triplet; the difference spectrum of the initial state (Fig. 5a, filled circles) is attributed to the P^+Ph^- minus PPh spectrum.

This assignment is summarised in Table III. It can be seen that both the primary radical pair state and the triplet are significantly shorterlived when Q_A is singly reduced, as compared to the doubly reduced state. With respect to the

short triplet lifetime when Q_A is singly reduced, we recall that under those conditions, in Ref. [10], a microsecond decay component was seen at 820 nm, although it was not assigned to the triplet state at that time. We also mention that in time-resolved EPR measurements [35], the triplet risetime was found to increase upon double reduction of Q_A.

Finally, we mention that the shapes of kinetic traces as shown in Figs. 3 and 4 were independent of the degree of saturation of the exciting laser flashes (up to an energy of approximately 2 mJ per pulse). An estimation of the effective absorbance cross-section at 532 nm (see [36]) from the saturation behaviour of the absorbance changes, yielded a value of approximately 20 $Å^2$. This is consistent with the absorption changes arising from a reaction centre surrounded by a few hundred antenna chlorophylls (the effective absorbance cross-section of chlorophyll *a* and *b* at 532 nm can be estimated to be approximately 0.1 $Å^2$ (see [37]).

3.1.2. *Flash-induced absorbance changes in the 520 nm region*

A possible explanation for the shorter lifetime of the reaction centre triplet in reaction centres with singly reduced Q_A could be that it is quenched by a carotenoid molecule, involving triplet transfer. This would give rise to a carotenoid triplet state. Indeed, the reaction centre of PSII has been reported to contain one or two carotenoid molecules (reviewed in [38]). Quenching of the reaction centre triplet by a specific carotenoid is known to occur in some types of carotenoid-containing purple bacterial reaction centres at temperatures above 35 K (see [39] for a review). In an attempt to check whether the reaction centre triplet in PSII is quenched by carotenoid when Q_A is singly reduced, preliminary experiments were performed in the 500-550 nm region, where the formation of carotenoid triplets can be seen as a strong absorbance increase (see [31]).

Fig. 6 shows absorbance changes on a microsecond time scale at 520 nm for both types of sample, at similar excitation conditions, scaled to the same sample concentration and corrected for particle flattening. In the singly reduced sample (Fig. 6a), an initial absorbance increase is seen, which decays in tens of microseconds. Both its kinetics and its spectrum (maximum at 520 nm, not shown) corresponded to those of a carotenoid triplet (see [31]). In the doubly reduced sample (Fig. 6b), a similar kinetic component is present, indicative of carotenoid triplet states. However, there is an additional nondecaying phase present. We attribute it to the (chlorophyll) reaction centre triplet, which is known to absorb in the same wavelength region [31]. Measurements on a longer timescale (not shown) indeed revealed a decay on a millisecond timescale, similar to that measured at 686 nm, which is indicative of the reaction centre triplet in doubly reduced samples (see Section 3.1.1 and Refs. [10,29,30]). Also the fact that a nondecaying phase is absent when Q_A is singly reduced corresponds to the observations at 686 nm, at which wavelength virtually no phase with millisecond decay was found in this type of sample. Nevertheless, we do expect the (chlorophyll) reaction centre triplet to contribute to the kinetics at 520 nm, but with

the faster decay components, found in the singly reduced sample: approximately 2.5 μs and 20 μs. However, these are in fact not very different from the carotenoid triplet decay time (see [31]) and this probably makes it indistinguishable from carotenoid triplets (in terms of decay characteristics).

The carotenoid triplet found in the sample with Q_A doubly reduced, most likely arises from the antenna. The same amount might be expected when Q_A is singly reduced, however, the signal is larger in Fig. 6a (singly reduced Q_A). The additional signal (as compared to the doubly reduced sample) could arise from a carotenoid reaction centre triplet, formed after triplet transfer from the chlorophyll reaction centre triplet. According to the difference in signal size between traces of Fig. 6a and b, the contribution of a possible reaction centre carotenoid triplet can not be much larger in amplitude than that of the non decaying phase in Fig. 6b. However, in this wavelength region, the differential extinction coefficient of triplet carotenoid formation is thought to be at least six times that of triplet chlorophyll formation (see [31]). Hence, the additional amount of carotenoid triplet when Q_A is singly reduced, seems to be well below the amount of reaction centre triplet in the sample with Q_A doubly reduced.

In fact, an explanation for the different carotenoid triplet amplitudes in samples with Q_A singly and doubly reduced can also be found in differences in the amount of excited states in the antenna. In Ref. [40], a close correlation was demonstrated, at room temperature, between the fluorescence intensity (a measure of the amount of excited states) and the amount of carotenoid triplet formed. The fluorescence yield (at room temperature) has indeed been shown to be lower if Q_A is doubly reduced [21].

Comparative experiments at higher time resolution (200 ns response time, see Materials and Methods) were also carried out. If a carotenoid triplet is generated by quenching of the chlorophyll reaction centre triplet when Q_A is singly reduced, the fast kinetics at 520 nm are expected to be different compared to samples with QA doubly reduced (rise kinetics on a microsecond time scale might be expected if Q_A is singly reduced). However, no significant differences in the rise kinetics were found (not shown). They appeared to be instrument-limited in both types of sample. Blocking the primary reaction centre photochemistry (including reaction centre triplet formation) in the sample with Q_A singly reduced by photoreduction of Ph (reviewed in [6]), did not result in significantly changed rise kinetics either.

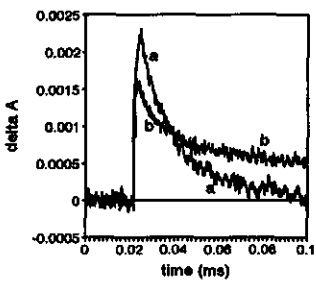

Fig. 6. Absorbance changes at 520 nm in PSII-enriched membranes (0.09 mg Chl/ml) at 20 K, corrected for particle flattening. (a) Samples with Q_A singly reduced; (b) samples with Q_A doubly reduced.

In summary, there is no convincing evidence from these measurements that the short lifetime of the reaction centre triplet in samples with QA singly reduced is due to quenching by carotenoid. Based on the extinction coefficients in Ref. [31], we consider such a quench-

ing mechanism as rather unlikely.

3.2. *Measurements under oxidising conditions*

In order to obtain the low-temperature difference spectrum associated with $P^+Q_A^-$ formation (the $P^+Q_A^-$ minus PQ_A spectrum), absorbance changes were measured on a millisecond timescale, under oxidising conditions (see Materials and Methods for details on the sample conditions). Fig. 7 shows some characteristic traces, taken at 677 nm, 681 nm and 685 nm. The decay with an estimated half-time of 3 ms corresponds to that found earlier at low temperature for the charge recombination of $P^+Q_A^-$ (see [41] and references cited therein). Fig. 8, trace c shows the difference spectrum of the absorbance change after correction for particle flattening and light-induced signal loss (see Materials and Methods). The resolution of two negative peaks (at 676 nm and 685 nm) and one positive peak (at 681 nm) was not reported in earlier work [42,43] with lower spectral resolution. Our spectrum is similar to that recently obtained at 77 K from Synechococcus [44].

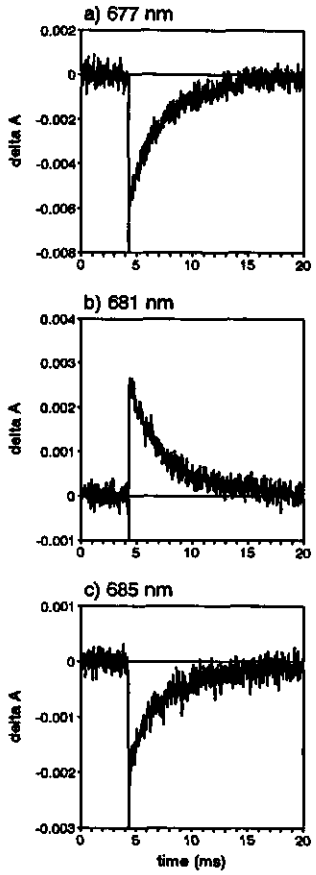

Fig. 7. Absorbance changes in PSII-enriched membranes with Q_A oxidised (0.012 mg Chl/ml) at 20 K.

4. Discussion

4.1. *Kinetics*

As shown in the results Section, it is possible to ascribe the absorbance changes in the 680 nm region, in samples with Q_A singly or doubly reduced, to two sequential states, the first formed within a few nanoseconds, the second formed from the first, on a slower timescale (hundreds of nanoseconds). The first state is attributed to the primary radical pair, the second to the reaction centre triplet state. This assignment is summarised in Table III.

4.1.1. *Formation of the primary radical pair*

From the amplitudes of the P^+Ph^- minus PPh spectra in Fig. 5a, it appears that the amount of radical pair a few nanoseconds after a flash, is similar in samples with Q_A singly and doubly reduced. Thus, the suggestion made in Ref. [10] that at low temperature, the yield of radical pair formation is much lower if Q_A is singly reduced than when it is doubly reduced, is ruled out.

The fact that the amplitudes of the P^+Ph^- minus PPh spectra are similar does not necessarily mean that the rate constant of charge separation is similar in the two types of sample: the yield of the primary radical pair would be close to 100 %, independent of the rate of charge separation, if other decay pathways from the excited state were much slower. In addition, the amount of radical pair measured after the flash rises to maximum within a few nanoseconds, before a decay (hundreds of nanoseconds) can become important. Therefore, possible variations (dependent on the Q_A redox state) in the risetime of the radical pair will not influence the maximum in the amount of radical pair measured. Thus, from our measurements we have no information on the risetime. Such information may be obtained by directly measuring the rise of the radical pair state or the decay of the excited state. For such measurements a higher time resolution than that used here is required.

4.1.2. *Decay of the primary radical pair; formation of the reaction centre triplet state*

Different kinetics are observed for the decay of the primary radical pair state and the rise of the reaction centre triplet state, when comparing samples with Q_A singly and doubly reduced. They are slower in samples with Q_A doubly reduced (see Table III). The radical pair decay is expected to depend on the rate constants of charge recombination to triplet and singlet states of P (see [45-47] for recent reviews on these reactions and singlet-triplet conversion in the radical pair state). One or more of these recombination processes must be slowed down upon double reduction of Q_A.

Results from fluorescence and absorbance measurements at ambient temperature have been explained by an electrostatic influence of the negative charge in the Q_A^- state on the kinetics of charge separation [48]. It has been proposed that in the doubly reduced state, this charge is neutralised due to protonation and in this way, the higher rate of charge separation could be explained [21]. Such an electrostatic influence could also cause charge recombination rates to singlet and triplet states of P to be slower in samples with Q_A doubly reduced as compared to singly reduced (see [21,49] for indications at room temperature). Thus, electrostatics may explain the difference in radical pair decay time observed here at low temperature.

Table III, summary of the assignments

state of Q_A	decay time of the primary radical pair	decay time of the reaction centre triplet
singly reduced	26 ns / 130 ns	2.6 µs / 20 µs
doubly reduced	72 ns / 290 ns	1.4 ms / 4.5 ms

It should be pointed out that conformational effects, in relation to the Q_A redox state might influence the charge recombination rate as well. There are indeed some indications that conformational changes occur upon double reduction of Q_A [50]. In addition, magnetic interactions of the semiquinone-iron com-

plex with the radical pair state (e.g., these interactions may transmit the magnetic relaxation from the iron) can influence the process of singlet-triplet conversion in the radical pair state. Such influences from the semiquinone-iron on the radical pair state have for example been proposed in Refs. [51-54] for purple bacteria, to explain changes observed in the properties of the triplet in relation to the state of the semiquinone-iron complex.

4.1.3. *The yield and the decay of the reaction centre triplet state*

In the assignment summarised in Table III, the (chlorophyll) reaction centre triplet state decays on a millisecond timescale in samples with Q_A doubly reduced, whereas in samples with singly reduced Q_A, a much faster decay is observed, on a timescale of several microseconds (Table I). From the amplitudes of the T-S spectrum (Fig. 5b), it can be concluded that the yield of formation of the triplet state is similar in both types of sample. Thus the low amplitude of the reaction centre triplet in samples with Q_A singly reduced, as monitored by EPR under continuous illumination, is not due to a low yield of triplet formation as suggested before [10], but due to a shortened triplet lifetime.

The question remains why the lifetime of the reaction centre triplet state is short when Q_A is singly reduced. Quenching by carotenoid is probably not the reason (see Section 3.1.2). Explanations may be found in a magnetic interaction of the triplet state with the semiquinone-iron complex. This would be surprising in view of the large distance of the latter from the primary donor site.

We mention that significant differences in reaction centre triplet lifetimes have been found in purple bacteria, when samples with singly and doubly reduced QA were compared [51,55,56]; however, these differences were absent at cryogenic temperatures [55] and the effect was not as dramatic as that observed here. Also a significant influence of an external electric field on the triplet lifetime has been reported in purple bacteria [57].

Clearly, further work (e.g. studies of the dependence of the radical pair and triplet kinetics on temperature and the presence of a magnetic or an electric field) is required for a better understanding of the phenomena observed in the present work.

4.2. *The difference spectra in the 680 nm region*

4.2.1. *The bleached areas*

The area under the triplet minus singlet curve in Fig. 8a is estimated to be approximately four times smaller than that of the P^+Ph^- minus PPh spectrum, Fig. 8b (note that both are measured from the same kinetic traces, in the same sample, which reduces the possible error in this comparison). After correction of this factor for the yield of triplet formation from the radical pair, it may help to decide whether the positive charge in the P^+ state is localised on a single chlorophyll or delocalised over two chlorophylls. For the situation in which both

the positive charge and the triplet are localised on a single chlorophyll and being formed with the same yield, one would expect a factor of approximately 1.4 (reduction of pheophytin *a* in vitro, results in a loss of oscillator strength in the Q_Y region which is approximately 0.4 times the loss associated with triplet or cation formation on a chlorophyll *a* molecule, see [58-60]). This factor would be larger (theoretically 2.4) if the positive charge of P^+ were delocalised over two chlorophylls on an optical timescale (the triplet being localised on one chlorophyll, see Section 4.2.2.).

The yields of triplet and radical pair formation at 20 K were estimated from measurements at 820 nm (samples with Q_A doubly reduced). The absorbance change due to triplet formation was measured using an excitation energy, which was close to saturating for the contributions from the primary radical pair. The absorbance change due to triplet formation was corrected for a small contribution from antenna chlorophyll triplets as determined by comparison of radical pair and triplet contributions at lower and higher excitation energies. The triplet yield thus found was 50 %, using an extinction coefficient of 3800 M^{-1} cm^{-1} (see [31]) and assuming that there are 220 - 230 chlorophylls per reaction centre in our preparation. The radical pair yield was estimated to be close to 100 % under the same excitation conditions using an extinction coefficient at 820 nm of 12400 M^{-1} cm^{-1} (see [31]). Thus, the factor between the areas under the difference spectra for radical pair and triplet formation, corrected for the relative yields, is estimated to be approximately 2. This is almost midway between the values expected for a localised and a delocalised cation (1.4 and 2.4, respectively, see above).

We also compared the areas of the P^+Ph^- minus PPh and $P^+Q_A^-$ minus PQ_A spectra (Fig. 8b and c) to that of chlorophyll *a* in vitro in the Q_Y region (see e.g. Ref. [61] for in vitro spectra). We assumed that there were 220-230 chlorophylls per reaction centre. Thus a bleaching area per reaction centre corresponding to the oscillator strength of 2.2 Chl *a* was found in the P^+Ph^- minus PPh spectrum, which gives approximately 1.8 Chl *a* per reaction centre after subtraction of the contribution due to bleaching of pheophytin *a* (0.4, see [59,60]). A value of 1.0 bleached Chl *a* per reaction centre was found for the $P^+Q_A^-$ minus PQ_A spectrum (Q_A is not thought to contribute to the absorbance in the red region). This large difference may be due to inaccuracies in the flattening correction and the correction for light-induced signal loss during the acquisition of the difference spectra (see Materials and Methods).

In summary, with the present accuracy, the comparisons of the bleached areas do not yield an unambiguous conclusion with respect to the question of a monomeric or dimeric cation. Improved precision (e.g. by reducing particle size and therewith the uncertainty due to the flattening correction) may allow a clear conclusion in the future.

4.2.2. *The triplet minus singlet spectrum*

Of the difference spectra obtained in the present work (Fig. 8), the triplet minus singlet (T-S) spectrum is probably the easiest to interpret, because

electrochromic bandshifts can be assumed to be absent. The main features of the spectrum are a bleaching near 685 nm and an absorbance increase near 675 nm, the latter being relatively smaller in amplitude. In addition, a small trough around 678 nm and a small peak around 680 nm seem to be present.

The monomeric zero-field splitting parameters, D and E [28,29], and also LD-ADMR data [17] indicate that the triplet state is localised on a single chlorophyll (at least on an EPR time-scale). A dimeric triplet, delocalised over two parallel chlorophylls with parallel optical transition moments cannot strictly be ruled out on the basis of the D and E values and Ref. [17]; however, given the fact that no strong excitonic couplings are observed in the PSII reaction centre (see [15,62,63]), we think that the latter possibility is rather unlikely.

The fact that there is a positive band in the T-S spectrum (at 675 nm, Fig. 8a), shows that in the singlet state, the chlorophyll on which the triplet is localised is coupled to at least one other pigment. This can be understood in the following way: upon triplet formation the excitonic coupling is broken and those pigments which were involved in the coupling change their absorption maximum, giving rise to bandshift-like features in the T-S spectrum.

The T-S spectrum is the resultant of such bandshifts and the bleaching of the chlorophyll on which the triplet is localised (in the Q_Y region, the triplet state of chlorophyll *a* absorbs much less than the singlet state, see Ref. [58]). From the wavelength of maximum bleaching in Fig. 8a, this chlorophyll is thought to absorb significantly at 685 nm.

The small features at 678 nm and 680 nm are indications that more than one absorption band is shifted upon triplet formation. This indicates that the coupling involves more than two pigments (including the pigment on which the triplet is localised).

For a comparison of the low temperature T-S spectrum obtained by us with those from the literature, we will focus on Refs. [15-17]. Refs. [18,29] are less suited, because the spectra in these Refs. were detected at only one microwave frequency. This represents a (rather arbitrary) selection of one population of reaction centres from a heterogeneous group (as argued in Refs. [17,29]).

In Refs. [15-17], D_1D_2 preparations were used. Comparing the spectra from these Refs. (summarised in [17]) to those from PSII membranes (Fig. 8a), it is seen that the general shapes are similar. The main difference is found in the wavelength of maximum bleaching (685 nm in membrane preparations, 680 nm in D_1D_2 preparations); in addition, the bleaching band is broader in D_1D_2 preparations. The positive band is relatively smaller in amplitude and is slightly shifted to the blue in D_1D_2 preparations, but this is possibly due to it being closer to the bleaching band and to the greater broadness of the bleaching band. The broadening indicates that the D_1D_2 preparation is more heterogeneous in terms of pigment-pigment and pigment-protein interactions (see e.g. [16,17]). In fact, one of the T-S spectra in Ref. [17] (the one recorded at 715 MHz) is more similar to that in membranes (Fig. 8a). Possibly, a fraction of the reaction centres in the D_1D_2 preparation has properties similar to those in membranes. The shift of the bleaching band towards the positive band in the D_1D_2 preparation, could be explained by a smaller excitonic coupling or by a different

environmental shift.

4.2.3. *Comparison of the $P^+Q_A^-$ minus PQ_A difference spectrum with the T-S spectrum*

Absorbance difference measurements at room temperature and also low temperature measurements on D_1D_2 preparations have always yielded bleaching maxima at 680 nm both upon triplet formation and upon P^+ formation (see e.g. [14-17,31,64]). Therefore, it has often been assumed that the triplet and positive charge (in the P^+ state) are localised on the same pigment. However, here we show (Fig. 8a,c) that at low temperature in a PSII membrane preparation, the bleaching maxima are at completely different wavelengths (see also [44]): in the $P^+Q_A^-$ minus PQ_A spectrum, the main bleaching is at around 676 nm, whereas in the T-S spectrum it is at 685 nm. At room temperature this difference may be masked due to band broadening. Knowing the low temperature data (Fig. 8a,c and Ref. [44]) it is much less certain that the triplet and the positive charge are localised on the same pigment. This is only possible if the $P^+Q_A^-$ minus PQ_A spectrum is the result of a (strong) electrochromic redshift centred around 680 nm superimposed over a bleaching near 685 nm (due to the disappearance of P absorption). Such a redshift would give a positive contribution above 680 nm and partly compensate the bleaching of P near 685 nm, explaining the relatively small bleaching at 685 nm in the $P^+Q_A^-$ minus PQ_A spectrum; the negative band

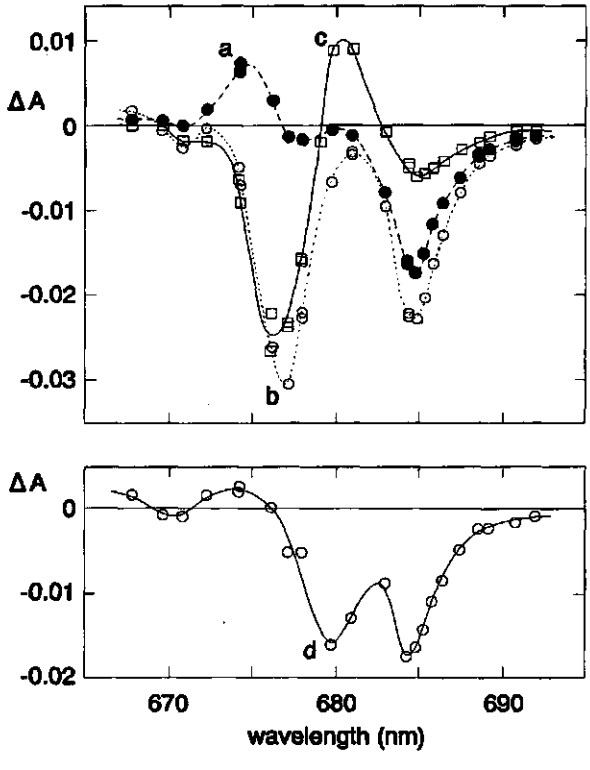

Fig. 8. Absorbance difference spectra from PSII-enriched membranes, corrected for light-induced signal loss and particle flattening (see Materials and Methods) and normalised to a chlorophyll concentration of 0.013 mg/ml. (a) Broken line, filled circles: the triplet minus singlet spectrum from samples with Q_A doubly reduced (the data points are identical to those in Fig. 5b (circles). (b) Dotted line, circles: the P^+Ph^- minus PPh spectrum from samples with Q_A doubly reduced (the data points are identical to those in Fig. 5a (circles). (c) Solid line, squares: the $P^+Q_A^-$ minus PQ_A spectrum, obtained from the absorbance changes measured in samples with Q_A oxidised, some of which were shown in Fig. 7. The initial amplitude (without taking into account the initial spike from singlet excited state contributions) is plotted. (d) Difference between (b) and (c), corresponding to the Ph^-Q_A minus PhQ_A^- spectrum.

of the redshift would be at around 676 nm.

Localisation of the triplet and the positive charge on different pigments is possible if the triplet moves to the other chlorophyll after being formed by charge recombination on P (see [5]). From the kinetics presented in Section 3, there is no evidence for such a triplet transfer but it may be too fast to be detectable (see also [35]). In summary, the question where exactly P absorbs at low temperature and whether or not the triplet is localised on P, remains open.

4.2.4. *Comparison of the P^+Ph^- minus PPh spectrum with the $P^+Q_A^-$ minus PQ_A spectrum*

Comparison of the P^+Ph^- minus PPh and the $P^+Q_A^-$ minus PQ_A difference spectra should give an indication of the absorbance spectrum of Ph, although differences in electrochromic bandshifts may complicate the analysis. Figs. 8b,c show that the two spectra have quite similar shapes: in both of them there are negative peaks at around 676 nm and 685 nm and a positive peak at around 681 nm. The main difference between the spectra is seen in the region above 680 nm, where the P^+Ph^- minus PPh spectrum seems to have an additional bleaching, superimposed over the $P^+Q_A^-$ minus PQ_A spectrum. This could be explained by the bleaching of Ph in the P^+Ph^- minus PPh spectrum, with a maximum in the 680-685 nm region. This corresponds to the value of around 685 nm found at room temperature upon illumination in the presence of dithionite in similar preparations (e.g. [43,65], see also [64]). Thus, there does not seem to be a drastic difference between the P^+Ph^- minus PPh and the $P^+Q_A^-$ minus PQ_A difference spectra with regard to the contributions of electrochromic bandshifts. In other words, the P^+ minus P spectrum is not greatly dependent on whether the electron is on Ph or on Q_A. The global spectral similarity between the states P^+Ph^- and $P^+Q_A^-$ is in fact also the case in purple bacteria (see for example [66,67]; see [1,2] for reviews on difference spectra obtained in purple bacteria). It seems that electrochromic bandshifts are relatively insensitive to the exact location of the charged groups as long as the electric field is more or less aligned with the electron transfer chain. In this respect we mention that the $Chl^+Q_A^-$ minus $ChlQ_A$ spectrum, measured by Visser [68] upon stable oxidation of a chlorophyll (donor to P), is rather similar to our $P^+Q_A^-$ minus PQ_A spectrum. This indicates that also upon formation of the state $Chl^+Q_A^-$, a similar bandshift is involved. In addition, the absorption maximum of this oxidisable chlorophyll cannot be very different from that of P.

4.2.5. *Comparison of the P^+Ph^- minus PPh spectrum in PSII membranes with that in D_1D_2 preparations.*

In D_1D_2 particles [15], the P^+Ph^- minus PPh spectrum is quite different from that reported here for PSII membranes (Fig. 8b): we observed two negative peaks at around 677 nm and 685 nm, whereas in the work on the D_1D_2 preparation [15], only one negative peak was found at 680 nm.

From a comparison of the T-S and the P^+Ph^- minus PPh spectra, Ph was

thought to absorb around 676 nm in Ref. [15]: around this wavelength, the P^+Ph^- minus PPh spectrum had a greater bleaching than the T-S spectrum. In our work the difference around 676 nm between T-S and P^+Ph^- minus PPh spectra is much more pronounced, appearing as a separate bleaching band. As outlined in Section 4.2.3, we do not attribute the bleaching at 676 nm to Ph, because it is also present in the $P^+Q_A^-$ minus PQ_A spectrum.

Our explanation of the fact that the P^+Ph^- minus PPh spectrum in PSII membranes is different from that in D_1D_2 preparations is as follows. First we note that in the D_1D_2 preparation used in Ref. [15], the Ph^- minus Ph spectrum obtained by phototrapping has its bleaching at approximately 680 nm [16]. In other work on D_1D_2 preparations including ADMR and holeburning studies, similar pheophytin bleaching spectra have been found [13,17,69]. However, in membranes, the bleaching in the Ph^- minus Ph spectrum is at 685 nm [43,65]. On the basis of differential LD measurements, the Ph^- minus Ph spectrum is in fact thought to be composed of the bleaching due to Ph^- formation and the blueshift of another pigment [13,70]. The Ph bleaching is thought to be close to 680 nm in both D_1D_2 and membrane preparations. The difference in Ph^- minus Ph spectra, comparing D_1D_2 and membrane preparations, is the shift: in D_1D_2 preparations the shift is thought to affect a pigment close to 680 nm [13], whereas in the work on the membrane-type preparation [70], this pigment is thought to be absorbing close to 685 nm. Most likely the same shift is also contributing to P^+Ph^- minus PPh spectra (see [64]). It is clear that for the case of the D_1D_2 preparation, this shift, the bleaching of Ph and a negative peak around 676 nm in the P^+ minus P spectrum will overlap and probably result in a single negative peak at 680 nm, whereas in the case of membrane preparations, the features remain spectrally separated. In addition, a general band-broadening as is indicated by the broadening observed in the T-S spectrum of D_1D_2 preparations (see Section 4.2.1) may contribute to the loss of spectral resolution in the D_1D_2 preparation.

Returning briefly to the LD (Ph^- minus Ph) spectra in Refs. [13,70]: apparently, the pigment affected by the blueshift absorbs at around 680 nm in D_1D_2 preparations [13] and around 685 nm in membrane preparations [70]. This behaviour is identical to that observed for the chlorophyll on which the triplet is localised as outlined in Section 4.2.1 (comparing Fig. 8c to Refs. [15-17]). Thus, it might be that the pigment affected by the blue shift in Ph^- minus Ph spectra [13,64,70] is the same as the chlorophyll on which the triplet is localised (oriented at 30° to the membrane [71]). The LD of the shifted pigment in PSII is in agreement with that of a chlorophyll making a small angle to the membrane [13,70]. In Ref. [64], it was argued that the pigment affected by the blueshift could not be P, because it was also thought to be present under conditions that P is oxidised. As outlined in Section 4.2.3., the triplet is not necessarily localised on P. Finally, we mention that the Ph^-Q_A minus PhQ_A^- spectrum obtained from our data (Fig. 8d) can be interpreted as consisting of a bleaching at 680 nm and a blueshift of a pigment absorbing around 685 nm, which is in agreement with Ref. [70].

4.2.6. *The analogy between the reaction centres of PSII and purple bacteria*

A number of spectroscopic observations, made in D_1D_2 preparations have led to the suggestion that the primary donor of PSII is structurally different from that in purple bacteria (see e.g. [12,17,71,72], reviewed in [9]). In Ref. [71] it was for example proposed that P is a chlorophyll oriented at 30° to the membrane. This proposal was based on low-temperature absorbance difference spectra from a D_1D_2 preparation [15], which indicated that the positive charge and the triplet were localised on the same (30° oriented [71]) chlorophyll. However, in the present work, we show that difference spectra, associated with the primary photochemistry in the D_1D_2 preparation, are considerably different from those of more intact membrane preparations. This indicates that one should take care with the interpretation of data obtained from D_1D_2 preparations. The question now arises whether also data from more intact PSII membrane preparations point to differences between the two types of reaction centres.

In optical difference spectra from purple bacteria associated with P^+ formation, BPh^- formation or Q_A^- formation, blueshifts are always seen of one or both of the monomeric bacteriochlorophylls (see, e.g.[66,67,73,74] and [1,2] for reviews). These are oriented at angles of approximately 30° to the membrane plane [75,76]. It is possible to interpret the spectra in Fig. 8b,c and d in a similar way if a blueshift is assumed to be present around 683 nm. From the T-S spectrum (Fig. 8a), and the orientation of the triplet [71] there is indeed a chlorophyll absorbing around that wavelength, oriented at 30° to the membrane plane (as outlined in Section 4.3.3, the triplet is not necessarily localised on P). The LD of the blueshifted pigment in Ph^- minus Ph spectra has been measured [70] (see also [13]) and it is consistent with an orientation of this pigment of 30°. Thus, the difference spectra in the present work do not rule out a reaction centre structure of PSII similar to that in purple bacteria (with P being equivalent to the special pair of purple bacteria). The triplet state would have to be rapidly transferred from P to an equivalent of one of the monomeric bacteriochlorophylls of the purple bacterial reaction centre (see [5]). Further experiments are needed to obtain more structural information on the PSII reaction centre in order to allow a closer comparison to purple bacteria. For this, measurements on preparations which are as intact as membrane preparations are preferable.

Time-resolved LD measurements as well as (LD)-ADMR, might be possible on the preparation used in the present work. Using these techniques, the orientations of the transition dipole moments of shifted or bleached bands can be measured with respect to the membrane (LD) or with respect to the (known 71]) axes of the triplet state (LD-ADMR). One could for example think of comparing the orientations of the positive band at 675 nm in the T-S spectrum and the bleaching at 676 nm in the P^+ minus P spectrum, to see whether they arise from the same pigment(s). It could also be verified whether the bleaching at 685 nm in the T-S spectrum has the same orientation as the postulated blue shifted band around 683 nm in the $P^+Q_A^-$ minus PQ_A spectrum, which should be the case if both arise from the chlorophyll on which the triplet is localised. In

addition to the orientation information, a better separation of overlapping bands might be achieved using orientation selective techniques such as LD and LD-ADMR.

Another useful preparation for further experiments may be that from Synechococcus [77] which has a smaller antenna size than spinach PSII membranes, and from which results similar to ours have been obtained [44,78].

In general, use of samples with doubly reduced QA may have advantages, because of the slower kinetics, without drastic changes of the spectral properties.

References

1 Parson, W.W. and Ke, B. (1982) in "Photosynthesis: energy conversion by plants and bacteria" (Govindjee ed) pp 331-385 Academic press, New York.
2 Kirmaier, C. and Holten,D. (1987) Photosynth. Res. 13, 225-260.
3 Budil, D.E. and Thurnauer, M.C. (1991) Biochim. Biophys. Acta 1057, 1-41.
4 Van Gorkom H.J. (1985) Photosynth. Res 6 97-112.
5 Rutherford, A.W. (1986) Biochem. Soc. Trans. 14, 15-17.
6 Mathis, P. and Rutherford, A.W. (1987) in "New Comprehensive Biochemistry: Photosynthesis" (J.Amesz ed), pp. 63-96, Elsevier, Amsterdam.
7 Rutherford, A.W. (1988) in Light-Energy Transduction in Photosynthesis: Higher Plant and Bacterial Models (Stevens, S.E. and Bryant, D.A., eds.), pp. 163-177, The American Society of Plant Physiologists, Rockville.
8 Hansson, Ö. and Wydrzynski, T. (1990) Photosynth. Res. 23, 131-162.
9 Renger, G. (1992) in Topics in Photosynthesis Vol 11 (Barber, J., ed.), pp. 45-100, Elsevier, Amsterdam.
10 Van Mieghem, F.J.E., Nitschke, W., Mathis, P. and Rutherford, A.W. (1989) Biochim. Biophys. Acta 977, 207-214. Chapter 3 of this work.
11 Schlodder, E. and Hillmann, B. (1992) in Research in Photosynthesis (Murata, N., ed.), pp. 45-48, Kluwer, Dordrecht.
12 Shuvalov, V.A., Heber, U. and Schreiber, U. (1989) FEBS Lett. 258, 27-31.
13 Breton, J. (1990) in Perspectives in Photosynthesis (Jortner, J. and Pullman, B., eds.), pp. 23-38, Kluwer, Dordrecht.
14 Durrant, J.R., Giorgi, L.B., Barber, J., Klug, D.R. and Porter, G. (1990) Biochim. Biophys. Acta 1017, 167-175.
15 Van Kan, P.J.M., Otte, S.C.M., Kleinherenbrink, F.A.M., Nieveen, M.C., Aartsma, T.J. and Van Gorkom, H.J. (1990) Biochim. Biophys. Acta 1020, 146-152.
16 Otte, S.C.M., Van der Vos, R. and Van Gorkom, H.J. (1992) J. Photochem. Photobiol. B: Biol. 15, 5-14.
17 Van der Vos, R., Van Leeuwen, P.J., Braun, P. and Hoff, A.J. (1993) Biochim. Biophys. Acta 1140, 184-198.
18 Angerhofer, A. Bernlocher, D. and Robert, B. (1993) Z. Phys. Chem. (in press).
19 Berthold, D.A., Babcock, G.T. and Yocum, C.F. (1981) FEBS Lett. 134, 231-234.
20 Ford, R.C. and Evans, M.C.W. (1983) FEBS Lett 160, 159-164.
21 Van Mieghem, F.J.E., Searle, G.F.W., Rutherford, A.W. and Schaafsma, T.J. (1992) Biochim. Biophys. Acta 1100, 198-206. Chapter 4 of this work.
22 Duysens, L.N.M. (1956) Biochim. Biophys. Acta 19, 1-12.
23 Amesz, J. (1964) Ph.D. Thesis, State University of Leiden.
24 Pulles, M.P.J. (1978) Ph.D. Thesis, State University of Leiden.
25 Buser, C.A., Diner, B.A. and Brudvig, G.W. (1992) Biochemistry, 31, 11441-11448.
26 Latimer, P. and Eubanks, C.A.H. (1962) Arch. Biochem. Biophys. 98, 274-285.
27 Vermaas, W.F.J. and Rutherford, A.W. (1984) FEBS Lett. 175, 243-248.
28 Rutherford, A.W., Paterson, D.R. and Mullet, J.E. (1981) Biochim Biophys Acta 635, 205-214.
29 Den Blanken, H.J., Hoff, A.J. Jongenelis, A.P.J.M. and Diner, B.A. (1983) FEBS lett

157, 21-27.
30 Rutherford, A.W., Satoh, K. and Mathis, P. (1983) Biophys J. 41, 40a.
31 Takahashi, Y., Hansson, O., Mathis, P. and Satoh, K. (1987) Biochim Biophys Acta 893, 49-59.
32 Schlodder, E. and Brettel, K. (1990) in Current Research in Photosynthesis (Baltscheffsky, M., ed.), Vol I, pp. 447-450, Kluwer, Dordrecht.
33 Sonneveld, A., Duysens, L.N.M. and Moerdijk, A. (1980) Proc. Natl. Acad. Sci. USA 77, 5889-5893.
34 Schoen, E., Searle, G.F.W. and Schaafsma, T.J. (1993) Pers. Comm.
35 Chapter 7 of this work.
36 Schlodder, E., Brettel, K., Schatz, G.H. and Witt, H.T. (1984) Biochim. Biophys. Acta 765, 178-185.
37 Ley, A.C. and Mauzerall, D.C. (1982) Biochim. Biophys. Acta 680, 95- 106.
38 Cogdell, R. and Malkin, R. (1992) in Topics in Photosynthesis Vol 11 (Barber, J., ed.), pp. 1-16, Elsevier, Amsterdam.
39 Cogdell, R.J. and Frank, H.A. (1987) Biochim. Biophys. Acta 895, 63- 79.
40 Satoh, K. and Mathis, P. (1981) Photobiochem. Photobiophys. 2, 189- 198.
41 Reinman, S. and Mathis, P. (1981) Biochim. Biophys. Acta 635, 249-258.
42 Ke, B. and Dolan, E. (1980) Biochim. Biophys. Acta 590, 401-406.
43 Ke, B., Inoue, H., Babcock, G.T., Fang, Z.-X. and Dolan, E. (Biochim. Biophys. Acta 682, 297-306.
44 Schlodder, E. and Hillmann, B. (1992) IXth International Congress on Photosynthesis, Nagoya, Japan (Poster).
45 Hoff, A.J. (1986) Photochem. Photobiol. 43, 727-745.
46 Lersch, W. and Michel-Beyerle, M.E. (1989) in Advanced EPR in Biology and Biochemistry (Hoff, A.J., ed.), pp. 685-705, Elsevier, Amsterdam.
47 Angerhofer, A. (1991) in The Chlorophylls (Scheer, H., ed.), pp. 945-992, CRC Press, Boca Raton.
48 Schatz, G.H., Brock, H. and Holzwarth, A.R. (1987) Proc. Natl. Acad. Sci. USA 84, 8414-8418.
49 Liu, B., Napiwotzki, A., Eckert, H.-J., Eichler, H.J. and Renger, G. (1993) Biochim. Biophys. Acta 1142, 129-138.
50 Chapter 5 of this work.
51 Vidal, M.H., Setif, P. and Mathis, P. (1986) Photosynth. Res. 10, 347- 354.
52 Van Wijk, F.G.H., Gast, P. and Schaafsma, T.J. (1986) Photobiochem. Photobiophys. 11, 95-100.
53 Van Wijk, F.G.H., Gast, P. and Schaafsma, T.J. (1986) FEBS Lett. 206, 238-242.
54 Hore, P.J., Hunter, D.A., Van Wijk, F.G.H., Schaafsma, T.J. and Hoff, A.J. (1988) Biochim. Biophys. Acta 936, 249-258.
55 Shuvalov, V.A. and Parson, W.W. (1981) Biochim. Biophys. Acta 638, 50- 59.
56 Chidsey, C.E.D., Takiff, L., Goldstein, R.A. and Boxer, S.G. (1985) Proc. Natl. Acad. Sci. USA 82, 6850-6854.
57 Franzen, S. (1992) Ph.D. Thesis, Stanford University.
58 Lindschnitz, H. and Sarkanen, K. (1958) J; Am; Chem. Soc. 80, 4826- 4832.
59 Fujita, I., Davis, M.S. and Fajer, J. (1978) J. Am. Chem. Soc. 100, 6280-6282.
60 Davis, M.S., Forman, A. and Fajer, J. (1979) Proc. Natl. Acad. Sci. USA 76, 4170-4174.
61 Hoff, A.J. and Amesz J. (1991) in The Chlorophylls (Scheer, H., ed.), pp. 723-738, CRC Press, Boca Raton.
62 Tetenkin, V.L., Gulyaev, B.A., Seibert, M. and Rubin, A.B. (1989) FEBS Lett. 250, 459-463.
63 Braun, P., Greenberg, P.M. and Scherz, A. (1990) Biochemistry 29, 10376-10387.
64 Nuijs, A.M., Van Gorkom, H.J., Plijter, J.J. and Duysens, L.N.M. (1986) Biochim. Biophys. Acta 848, 167-175.
65 Klimov, V.V., Klevanik, A.V. and Shuvalov, V.A. (1977) FEBS Lett. 82, 183-186.
66 Rockley, M.G., Windsor, M.W., Cogdell, R.J. and Parson W.W. (1975) Proc. Natl. Acad. Sci. USA 72, 2251-2255.
67 Kirmaier, C., Holten, D. and Parson, W.W. (1985) Biochim. Biophys. Acta 810, 33-48.

68 Visser, J.W.M., Rijgersberg, C.P. and Gast, P. (1977) Biochim. Biophys. Acta 460, 36-46.
69 Tang., D., Jankowiak, R., Yocum, C.F., Seibert, M. and Small, G.J. (1990) J. Phys. Chem. 94, 6519-6522.
70 Ganago, I.B., Klimov, V.V., Ganago, A.O., Shuvalov, V.A. and Erokhin, Y.E. (1982) FEBS Lett. 140, 127-130.
71 Van Mieghem, F.J.E., Satoh, K. and Rutherford, A.W. (1991) Biochim. Biophys. Acta 1058, 379-385. Chapter 6 of this work.
72 Lösche, M., Feher, G. and Okamura, M.Y. (1988) in The Photosynthetic Bacterial Reaction Center Structure and Dynamics (Breton, J. and Verméglio, A., eds.), pp. 151-164, Plenum Press, New York.
73 Zhou, Q., Mattioli, T.A. and Robert, B. (1990) in Reaction Centers of Photosynthetic Bacteria (Michel-Beyerle, M.-E., ed.), pp. 11-18, Springer, Berlin.
74 Mäntele, W., Leonhard, M., Bauscher, M., Nabedryk, E., Breton, J. and Moss, D.A. (1990) in Reaction Centers of Photosynthetic Bacteria (Michel-Beyerle, M.-E., ed.), pp. 31-44, Springer, Berlin.
75 Deisenhofer, J., Epp, O., Miki, K., Huber, R. and Michel, H. (1985) Nature (London) 318, 618-624.
76 Allen, J.P., Feher, J., Yeates, T.O., Komiya, H. and Rees, D.C. (1987) Proc. Natl. Acad. Sci. USA 84, 5730-5734.
77 Dekker, J., Boekema, E.J., Witt, H.T. and Roegner, M. (1988) Biochem. Biophys. Acta 936, 307-318.
78 Hillmann, B., Kamlowski, A., Rutherford, A.W., Schlodder, E. and Brettel, K. (1993) Pers. Comm.

Summary

In this Thesis, a number of spectroscopic measurements are presented on Photosystem II (PSII) preparations from spinach, which provide some new information on the PSII reaction centre structure and function.

The experimental part of this thesis is preceded by a general introduction (Chapter 1) and a brief overview of methods and techniques used (Chapter 2).

In Chapter 3, a low temperature Electron Paramagnetic Resonance (EPR) study on PSII-enriched membranes is presented. The redox dependencies of the light-inducible signals from the spin-polarised reaction centre triplet state and signals from the semiquinone-iron ($Q_A^-Fe^{2+}$) acceptor complex were studied. It was found that the reaction centre triplet signal was only seen after the $Q_A^-Fe^{2+}$ signal had disappeared on double reduction of Q_A.

In Chapter 4, a time-resolved fluorescence study at ambient temperature is presented on samples in which Q_A was oxidised, singly reduced or doubly reduced. Two types of preparations were used: PSII-enriched membranes (with large antenna size) and PSII core complexes (partly stripped of antenna). The results indicated that the effective rate of charge separation was larger when Q_A was oxidised or doubly reduced than when it was singly reduced. In addition, it was found that the lifetime of the primary radical pair state increases when going from the singly reduced state of Q_A to the doubly reduced state. The differences between the two types of preparation and the reversibility of the double reduction of Q_A were also investigated.

In Chapter 5, a more detailed EPR study of the reversibility of the double reduction of Q_A in PSII-enriched membranes is presented. Only a small degree of reversibility was found. In addition, the non-heme iron was found to be irreversibly modified (possibly lost) upon double reduction of Q_A, which may explain the lack of reversibility.

In Chapter 6, the orientation dependence of the reaction centre triplet EPR signal was determined in oriented samples. Both PSII-enriched membranes and D_1D_2 reaction centre preparations were used. The reaction centre triplet state was found to be localised on a reaction centre chlorophyll of which the tetrapyrrolic plane is oriented at 30° to the membrane plane.

In Chapter 7, time-resolved EPR experiments on oriented samples (PSII-enriched membranes) are described. Thus, the risetime of the reaction centre triplet state was estimated to be of the order of 300 - 400 ns.

In Chapter 8, low temperature flash-induced absorbance difference measurements are presented on PSII enriched membranes under several redox conditions, including those having Q_A singly or doubly reduced. These experiments provided an unexpected explanation for the absence of a detectable EPR triplet signal when Q_A is singly reduced (see above): the lifetime is too short to give a measurable signal under continuous illumination. Furthermore, the lifetime of the primary radical pair state was found to increase when going from the singly reduced state of Q_A to the doubly reduced state. Finally, low temperature absorbance difference spectra are presented and analysed. These were found to be significantly different from difference spectra in the literature obtained using

D_1D_2 preparations. It was concluded that presently available D_1D_2 preparations are considerably modified on the donor side compared to PSII-enriched membrane preparations.

Samenvatting

In dit proefschrift worden spectroscopische metingen aan fotosysteem II (PSII) preparaten van spinazie beschreven, die nieuwe informatie over de structuur en het functioneren van het PSII reactiecentrum hebben opgeleverd.

Het experimentele gedeelte van het proefschrift wordt vooraf gegaan door een algemene introductie (hoofdstuk 1) en een overzicht van de gebruikte methoden en technieken (hoofdstuk 2).

Hoofdstuk 3 behandelt electron paramagnetische resonantie (EPR) metingen aan PSII membraanfragmenten bij lage temperaturen. Het ging bij deze metingen om EPR signalen afkomstig van de gepolariseerde triplettoestand van het reactiecentrum dat tijdens belichting wordt gevormd en van het chinon-ijzer acceptorcomplex ($Q_A^-Fe^{2+}$) en de manier waarop deze signalen afhangen van de redoxpotentiaal. Gevonden werd dat het tripletsignaal van het reactiecentrum alleen te zien was als het $Q_A^-Fe^{2+}$ signaal verdwenen was als gevolg van de dubbele reductie van Q_A.

Hoofdstuk 4 behandelt tijdsopgeloste fluorescentiemetingen bij 4° C aan PSII samples met geoxideerd, enkel gereduceerd of dubbel gereduceerd Q_A. Er werden twee soorten PSII preparaat gebruikt: PSII membraanfragmenten (met een groot antennesysteem) en PSII core complexen (met een relatief kleiner antennesysteem). De resultaten van de metingen geven aan dat in samples met Q_A geoxideerd en dubbel gereduceerd de ladingsscheiding sneller verloopt dan in samples met Q_A enkel gereduceerd. Verder zijn er aanwijzingen gevonden dat de levensduur van het primaire radicaalpaar toeneemt als enkel gereduceerd Q_A wordt omgezet in dubbel gereduceerd Q_A. Ook de verschillen tussen de twee soorten preparaat zijn onderzocht en tot slot is de mate van reversibiliteit van de dubbele reductie van Q_A bepaald.

De reversibiliteit van de dubbele reductie van Q_A vormt het hoofdonderwerp van hoofdstuk 5. In deze meer gedetailleerde studie van PSII membraanfragmenten werd evenals in hoofdstuk 4 slechts een geringe reversibiliteit gevonden. Ook bleek na dubbele reductie van Q_A het Fe^{2+} ion irreversibel gemodificeerd te zijn. Zelfs is het mogelijk dat het Fe^{2+} ion na dubbele reductie van Q_A uit het reactiecentrum verdwenen is. Dit verklaart mogelijk waarom de reversibiliteit van de dubbele reductie van Q_A zo gering is.

In hoofdstuk 6 wordt de orientatiegevoeligheid van het EPR signaal afkomstig van de triplettoestand van het reactiecentrum behandeld. Voor deze metingen werden georienteerde samples gebruikt van zowel PSII membraanfragmenten als van een D_1D_2 reactiecentrumpreparaat). De conclusie luidt dat het triplet van het reactiecentrum op een chlorofyl gelocaliseerd is waarvan het tetrapyrroolvlak een hoek van 30° maakt met het membraanvlak en dat dit chlorofyl zich in het reactiecentrum bevindt.

Hoofdstuk 7 rapporteert tijdsopgeloste EPR metingen aan georienteerde PSII membraanfragmenten. Voor de ingroeitijd van het signaal afkomstig van het triplet van het reactiecentrum werd naar schatting 300 - 400 ns gevonden.

Hoofdstuk 8 beschrijft tijdsopgeloste absorptie metingen bij lage temperatuur aan PSII membraanfragmenten. Gemeten werd onder andere aan samples met Q_A

enkel en dubbel gereduceerd. De experimenten gaven een onverwachte verklaring voor de afwezigheid van een detecteerbaar triplet EPR signaal als Q_A enkel gereduceerd is (zie hoofdstuk 3): de levensduur van de triplettoestand van het reactiecentrum is dan te kort om tijdens continue belichting een meetbaar signaal te kunnen geven. Een ander resultaat was dat de levensduur van het primaire radicaalpaar bleek toe te nemen als enkel gereduceerd Q_A werd omgezet in dubbel gereduceerd Q_A. Verder worden in dit hoofdstuk absorptie-verschilspectra gepresenteerd en geanalyseerd. Deze worden onder andere vergeleken met die van D_1D_2 preparaten uit de literatuur. Aanzienlijke verschillen worden geconstateerd en dit leidt tot de conclusie dat, in vergelijking tot PSII membraanfragmenten, de huidige generatie D_1D_2 preparaten een gemodificeerde donorkant heeft.

Curriculum vitae

Frans van Mieghem, geboren op 9 augustus 1965 te Tilburg, studeerde biologie aan de Landbouw Universiteit Wageningen van 1983 tot 1989. Zijn afstudeervakken waren Biochemie, Moleculaire Fysica en Neurochemie; het laatstgenoemde vak werd gevolgd aan de University of Dundee, Department of Biochemistry, in Groot-Brittannië. Zijn praktijktijd bracht hij voor de vakgroep Moleculaire Fysica door in de Service de Biophysique, Département de Biologie, CE Saclay in Frankrijk.

In de laatstgenoemde instelling werd daarna, in de periode 1989-1993, het onderzoek verricht dat tot dit proefschrift leidde.